

Institut für Theoretische Physik  
Fachrichtung Physik  
Fakultät Mathematik und Naturwissenschaften  
der Technischen Universität Dresden

# **QCD Sum Rules for D Mesons in Nuclear Matter**

Diplomarbeit  
zur Erlangung des akademischen Grades  
Diplom-Physiker

vorgelegt von  
Thomas Hilger  
geboren am 29. September 1981 in Eisenhüttenstadt

Dresden 2008



Eingereicht am 18.03.2008

1. Gutachter: Prof. Dr. R. Schmidt
2. Gutachter: Prof. Dr. B. Kämpfer

## Kurzfassung:

Die Methode der QCD Summenregeln wird auf D-Mesonen sowohl im Vakuum als auch bei endlicher Dichte angewendet. Die Operatorprodukt-Entwicklung wird bis zur Massendimension 5 und bis zur 1. Ordnung in der starken Kopplung  $\alpha_s$  durchgeführt. Da durch die schwere Charm-Quarkmasse eine neue Skala eingeführt wird, treten nicht-störungstheoretische Effekte in Form von Infrarotdivergenzen für den Grenzfall einer verschwindenden Down-Quarkmasse auf. Um eine konsistente Separation der störungstheoretischen und nicht-störungstheoretischen Skalen zu gewährleisten, werden physikalische Kondensate anstelle von normalgeordneten Kondensaten eingeführt. Es werden Gleichungen für die Renormierung der Kondensate gegeben, welche für die Aufhebung der Massenlogarithmen bis fixierter Ordnung in  $\alpha_s$  und für endliche Dichten sorgen. Die Schwere-Quark-Massen-Entwicklung wird im selben Zusammenhang nachvollzogen. Die Borel-transformierten Summenregeln werden im Rahmen des "Pol + Kontinuum"-Ansatzes ausgewertet und die Ergebnisse mit der Literatur verglichen. Die Massenaufspaltung in den D-Mesonen-Iso-Doublets kann in diesem Zusammenhang mit ungefähr 32 MeV bestimmt werden, während die Bestimmung der mittleren Massenverschiebung stark von der verwendeten Methode zur Bestimmung des durch den "Pol + Kontinuum"-Ansatz eingeführten Schwellenparameters abhängt.

## Abstract:

The method of QCD sum rules is applied to D mesons in vacuum as well as at finite density. The operator product expansion is performed up to mass dimension 5 and next-to-leading order in the strong coupling  $\alpha_s$ . Because the heavy charm quark mass introduces a new scale, non-perturbative effects emerge as infrared divergences for vanishing down quark mass. In order to ensure a consistent separation of perturbative and non-perturbative scales, physical condensates instead of normal ordered ones are introduced. Equations for the renormalization of condensates, which allow for a cancellation of the mass logarithms at a fixed order in  $\alpha_s$  and for finite densities, are presented. The heavy-quark-mass expansion is reproduced in the same context. The Borel transformed sum rules are analyzed using a "pole + continuum" ansatz and the results are compared to the literature. In this context a mass splitting within the D meson iso-doublets of approximately 32 MeV is determined, while the determination of the shift of the mass centroid strongly depends on the methods used to determine the threshold of the "pole + continuum" ansatz and, therefore, can not be reliably determined within the presented approach.



# Contents

|          |   |           |
|----------|---|-----------|
| <b>1</b> | <b>Introduction</b>                                 | <b>7</b>  |
| <b>2</b> | <b>QCD Sum Rules</b>                                | <b>11</b> |
| 2.1      | Current-Current Correlator                          | 11        |
| 2.2      | Analytic Properties and Dispersion Relations        | 12        |
| 2.2.1    | Analytic Properties                                 | 12        |
| 2.2.2    | Vacuum Dispersion Relations                         | 15        |
| 2.2.3    | In-Medium Dispersion Relations                      | 18        |
| 2.3      | Operator Product Expansion                          | 21        |
| 2.4      | Fock Schwinger Gauge and Background Field Method    | 24        |
| 2.5      | Sum Rules   | 29        |
| 2.6      | Borel Transformed Sum Rules                         | 30        |
| <b>3</b> | <b>Sum Rules for D Mesons</b>                       | <b>37</b> |
| 3.1      | D Mesons  | 37        |
| 3.2      | Operator Product Expansion for the D Meson          | 38        |
| 3.2.1    | Projections   | 41        |
| 3.2.2    | Gluon Condensates from $\Pi_{D^+}^{(0)}$            | 45        |
| 3.2.3    | Quark Condensates from $\Pi_{D^+}^{(2)}$            | 52        |
| 3.2.4    | Physical Condensates and Heavy-Quark Mass Expansion | 55        |
| 3.2.5    | Operator Mixing                                     | 59        |
| 3.3      | Borel transformed Sum Rules for the D Meson         | 63        |
| 3.3.1    | OPE Terms   | 63        |
| 3.3.2    | Comparison with Literature                          | 64        |
| 3.3.3    | Perturbative Term                                   | 67        |
| 3.3.4    | Pole + Continuum Ansatz                             | 67        |
| 3.3.5    | Complete Sum Rules                                  | 69        |
| 3.4      | Numerical Evaluations                               | 73        |
| 3.4.1    | Parameters  | 73        |
| 3.4.2    | Area of Validity of the Sum Rules                   | 73        |
| 3.4.3    | Vacuum Borel Curves                                 | 74        |
| 3.4.4    | In-Medium Borel Curves                              | 78        |
| 3.4.5    | Analyzing the Sum Rules                             | 89        |
| <b>4</b> | <b>Summary and Outlook</b>                          | <b>93</b> |

|          |   |            |
|----------|---|------------|
| <b>A</b> | <b>Brief Survey on Quantum Chromodynamics</b>               | <b>95</b>  |
| <b>B</b> | <b>Bethe-Salpeter Approach</b>                              | <b>99</b>  |
| B.1      | Introduction  | 99         |
| B.2      | Ladder Approximation  | 103        |
| B.3      | Solving the Bethe-Salpeter Equation in Ladder Approximation | 105        |
| B.4      | Decomposition into Spin-Angular Matrices                    | 106        |
| B.5      | Symmetry properties of the partial amplitudes               | 110        |
| B.6      | Decomposition into Hyperspherical Harmonics                 | 110        |
| B.7      | Numerical Evaluations                                       | 121        |
|          | <b>Bibliography</b>   | <b>127</b> |

# 1 Introduction

Many different efforts in many different directions have been made, and are still made, in order to clarify and to understand the origin of the mass of the matter that surrounds us. The most popular one is the search for the Higgs boson, which has been postulated in order to explain the masses of the gauge bosons. Moreover, the interaction of the Higgs boson with the fermion fields within the standard model also gives masses to the quarks and some of the leptons. However, the main contribution to the mass that surrounds us has a different origin. The mass of usual matter resides in nuclei composed of nucleons. Nucleons belong to the hadrons. Hadrons are strongly interacting, subatomic particles which are made up of quarks and gluons. The masses of quarks are more or less well known from several experiments, while gluons are supposed to be massless. But against naive intuition, summing up all constituents masses of a hadron, one can not explain its mass. In contrast, the hadron masses are much larger than the sum of their constituents masses.

Let us consider, for example, the nucleon. In the naive quark model it consists of three light quarks with the sum of their masses being less than 20 MeV, while the nucleon mass is about 938 MeV. Hence, the masses are even of different scales. In this special case, i.e. for nucleons, we might think of nearly massless quarks but still would be surrounded by nucleons having a mass of several hundred MeV. Another example is given by the  $D^\pm$  meson, which consists of a charm quark with the mass being  $m_c = 1.25 \dots 1.45$  GeV, and a down quark, having the mass  $m_d = 4 \dots 8$  MeV. In contrast the mass of the  $D^\pm$  meson is about  $m_{D^\pm} = 1.87$  GeV, which is again larger than the sum of its constituents masses. This mass difference is a direct result of the complicated structure of the strong interaction which binds quarks and gluons into hadrons. The given examples tell us that genuine quark masses, as supposed to be generated by the Higgs mechanism in the electro-weak sector in the standard model, are of minor importance in an explanation of the mass of the matter around us. It is the strong interaction which has to be understood in order to understand our "massive world".

Quantum Chromodynamics (QCD) is the accepted theory which describes the strong interaction at quark level. It is a non-Abelian gauge field theory. (Basic details of QCD which are needed throughout this work are reviewed in appendix A.) One success of QCD is "asymptotic freedom", which means that in scattering experiments at large momentum transfer a projectile, say an electron, being scattered off a proton behaves as being scattered off almost free quarks. QCD entails this feature and tells us that the coupling strength of strong interaction decreases with increasing momentum. This enables one to apply perturbative techniques in the high momentum regime.

On the other side, one can not observe isolated individual quarks. This feature of strong interaction is called confinement. Quarks are always bound into hadrons as color singlets.

Unfortunately, it is not yet clear how confinement is reproduced by QCD. Moreover, because the coupling strength of the strong interaction grows with decreasing momentum (or increasing distance), perturbative techniques are not applicable anymore and one has to look for different methods in order to perform calculations in the low momentum regime.

As hadrons are composite objects consisting of confined quarks and gluons, hadronic properties should be related to the quark and gluon structure of the hadron, thus, to the non-perturbative properties of the theory. Instead of calculating directly hadronic properties from first principles, a tool in order to connect low momentum properties of the hadron to its large momentum structure is provided by the method of QCD sum rules (QSR).

The method is based on dispersion relations, which are used to relate different energy regimes, and introduces phenomenological parameters, called condensates, in order to introduce non-perturbative physics and to understand and to reproduce hadronic properties, e.g. hadron masses. These parameters enter the theory as ground state expectation values of quantum field operators and, hence, are directly connected to the fundamental properties of QCD and its ground state.

Loosely speaking, a condensate can be read as a measure for the probability of a particle being annihilated by a virtual particle from the ground state and therefore creating another real particle somewhere else. A non-vanishing condensate indicates a particle interaction with the ground state. Hence, the hadron appears much heavier than its QCD constituents, because not only interactions among quarks transmitted by gluons or among gluons have to be considered, but also interactions of these particles with the ground state. The hadrons acquire an effective mass by the interaction of their constituents with the ground state of QCD. This can be taken as a very simplified illustration of the mass effects mentioned at the beginning of this chapter. Such a concept might be known from many-particle physics and indeed many concepts, like the Lehmann representation or dispersion relations, are also subject to this field. Furthermore, if we continue in this illustrative language, the probability of a virtual light-quark pair creation from the ground state must be much larger than the probability of a heavy-quark pair creation. Therefore, the mass increase via coupling of a quark to a condensate shall be much lower for a heavy quark than for a light quark. This explains why the mass of the nucleon compared to its constituent quarks is of different scales, while the D meson is only somewhat heavier than its constituents. The charm quark does not contribute to the mass acquirement. Moreover, we see that the appearance of the heavy quark must require a different treatment than the light-quark systems, because it seems to be unaffected by non-perturbative effects.

However, QSR play a twofold role. On the one side, they are used to determine the condensates in order to get valuable information about the structure of QCD and strong interaction. On the other side, they are used to evaluate hadronic properties, like masses, in terms of the condensates.

But QSR enable us to go even further and to look for hadron masses and condensates, when the hadronic system under consideration is embedded in a strongly interacting medium, e.g. an atomic nucleus as displayed in fig. 1.0.1, instead of being considered in vacuum. For such a system, one observes a change of the hadron mass with increasing density, which directly can be translated by QSR to a density dependence of the condensates.



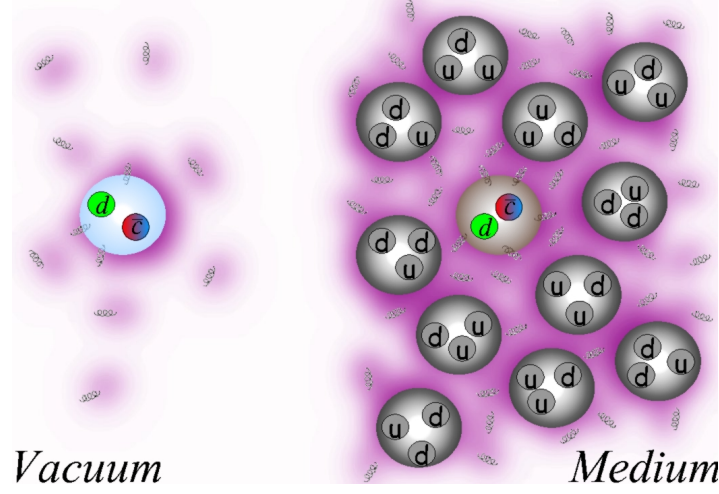


**Figure 1.0.1:** Illustrative picture of a  $D^-$  meson in vacuum and placed in nuclear matter. Gluon lines and "clouds" symbolize the non-perturbative ground state.

The chiral condensate  $\langle \bar{q}q \rangle$ , with  $q$  being a light quark, is connected to the chiral symmetry breaking of the theory. The symmetry is expected to be restored at finite density and temperature, which is signaled by a change of the condensate in nuclear matter.

In view of the planned experiments at FAIR in Darmstadt, where charm-quark systems will be accessible to detailed experimental investigations, it is reasonable to apply QSR to D mesons. The large charm quark mass is expected to amplify the importance of the chiral condensate compared to other condensates. Moreover, due to the new mass scale, new effects concerning a separation of low-momentum and large-momentum physics will show up.

This thesis is organized as follows. In chapter 2 we give a short introduction to the method of QSR. We focus on the aspects that are connected to the D meson and to medium modifications. The starting point is the current-current correlator. Its analytic structure is investigated using a Lehmann representation. Dispersion relations in vacuum and in medium are derived, relating large momenta to low momenta. The operator product expansion is introduced as an asymptotic expansion and the Fock Schwinger gauge is used to introduce the background field method as a tool for calculating an operator product expansion. Finally we give a detailed discussion of Borel transformed sum rules.

In chapter 3, the sum rules for the D meson in vacuum and medium are calculated. Thereby, we discuss the role of the charm-quark mass as a new scale parameter and show that a meaningful operator product expansion automatically leads to the heavy-quark mass expansion. The chapter ends with a detailed analysis of the vacuum and medium sum rules. We also investigate the influence of specific condensates to the results.

Finally, in chapter 4 the main results are collected and reviewed. Possible extensions of the preceding analysis are also presented.

The main subject of this thesis is the investigation of D mesons in vacuum and in nuclear matter within QCD sum rules. There are other approaches to the relativistic bound state. For instance, the Bethe-Salpeter equation is suitable for two-body bound states. A useful formalism is recollected in appendix B; however, the application to heavy quarks bound in mesons is outside of the scope of this thesis.

For a didactic introduction to quantum field theory and renormalization we recommend [Ro69]. Details about dimensional regularization and connected techniques can be found in [It80]. Also, many paragraphs are dealing directly or indirectly with the theory of complex functions, especially Cauchy's theorem plays an important role for dispersion relations, Wick rotation and Laurent expansions, which are presented in according textbooks [Fr95, Ja96]

## 2 QCD Sum Rules

### 2.1 Current-Current Correlator

As known from quantum field theory, n-point functions play an important role in calculating observables. Many quantities can be calculated directly if an appropriate n-point function is known. The main object of investigations within QCD sum rules is the current-current correlation function  $\Pi(q)$  defined as the two-point function

$$\Pi(q) = i \int d^4x e^{iqx} \langle \Omega | T [j(x) j^\dagger(0)] | \Omega \rangle \quad (2.1.1)$$

being the Fourier transform of the expectation value of the time-ordered product of two currents. Here the physical ground state  $|\Omega\rangle$  satisfies

$$\mathcal{H}|\Omega\rangle = E_\Omega|\Omega\rangle, \quad (2.1.2a)$$

$$\langle \Omega | \Omega \rangle = 1, \quad (2.1.2b)$$

$$a^-|\Omega\rangle \neq 0, \quad (2.1.2c)$$

with  $\mathcal{H}$  being the full Hamiltonian of the theory and  $|\Omega\rangle$  being its lowest lying eigenstate. The operator  $a^-$  is an annihilation operator which annihilates the canonical ground state of free particles  $a^-|0\rangle = 0$  used in perturbation theory. The latter one is, in contrast to the physical ground state  $|\Omega\rangle$ , the lowest lying eigenstate of the free Hamiltonian. The state  $|0\rangle$  is often referred to as the vacuum state, but in order to prevent confusions we will only refer to it as perturbative ground state. (2.1.2) reflects the non-perturbative physics of the strong interaction, hence, it is referred to as non-perturbative or physical ground state. We will distinguish between the in-medium ground state, i.e. the non-perturbative ground state when embedded in strongly interacting matter, and the vacuum ground state, i.e. the non-perturbative ground state considered at zero temperature and density. The properties of the physical ground state change when the system is embedded in a strongly interacting medium, instead of being considered in vacuum. Although the vacuum ground state must still be understood as non-perturbative ground state it is defined to satisfy  $E_\Omega = 0$ ; it is Lorentz invariant and invariant under time-reversal and parity transformations. In contrast, the in-medium ground state is only assumed to be invariant under time reversal and parity in its local rest frame. It is not invariant under all Lorentz transformations, but expectation values calculated in this state, e.g. the above current-current correlator  $\Pi(q)$ , transform covariant [Fu92]. As a result of (2.1.2a), the in-medium ground state is not translational invariant but obeys

$$e^{iPx}|\Omega\rangle = e^{ip_\Omega x}|\Omega\rangle, \quad (2.1.3)$$

where  $\mathbf{P}$  is the momentum operator and  $p_\Omega$  the related momentum of the in-medium ground state. The latter one is proportional to the medium four-velocity  $v_\mu$ . Hence, application of the translation operator results in a phase factor.

The current  $j(x)$  in (2.1.1) is a composite operator consisting of field operators in the Heisenberg picture. It has to reflect the quantum numbers of the particle under consideration. The correlator  $\Pi(q)$  can be understood then as a function describing the propagation of a particle from 0 to  $x$ . In the high momentum regime, i.e. at small distances, it must reflect the quark structure of the particle, while at low momentum, i.e. large distances, it is determined by hadronic properties of the respective particle.

If perturbation theory is applicable, i.e. the coupling strength  $g$  is small, (2.1.1) can be calculated by the following expansion [Pa84, Ge51]

$$\Pi(q) = i \int d^4x e^{iqx} \frac{\langle 0 | T \left[ j(x) j^\dagger(0) e^{i \int d^4y \mathcal{L}_{int}^{(0)}(y)} \right] | 0 \rangle}{\langle 0 | T \left[ e^{i \int d^4y \mathcal{L}_{int}^{(0)}(y)} \right] | 0 \rangle}, \quad (2.1.4)$$

where  $\mathcal{L}_{int}^{(0)}(x)$  is the interaction Lagrange density and the superscript (0) indicates that all fields have to be taken as free fields.

The basic idea of QCD sum rules is to connect large-momentum properties of the correlation function to properties in the region of small momenta [Sh78]. Instead of deriving properties of hadrons which are results of the non-perturbative character of the interaction from first principles of the theory, one introduces non-vanishing ground state expectation values of quantum field operators, called condensates, in order to reproduce the hadronic properties of the current-current correlator. In this sense, by introducing condensates, a possibility is offered to implement non-perturbative physics. Either hadronic phenomenology is used to determine the condensates or known condensates are used to predict and to understand hadronic properties. The condensates as expectation values of QCD operators are accessible, e.g. , in lattice QCD.

## 2.2 Analytic Properties and Dispersion Relations

### 2.2.1 Analytic Properties

We will now relate the different energy regimes of the current-current correlator (2.1.1) to each other. Therefore, we study its analytic properties. In doing so we will be able to perform the analytic continuation to complex values of the energy variable  $q_0$ .

Let us start with the Lehmann representation following [Fe71]. We write out the time-ordered product in (2.1.1) explicitly as

$$\Pi(q) = i \int d^4x e^{iqx} \left( \Theta(x_0) \langle \Omega | j(x) j^\dagger(0) | \Omega \rangle + \Theta(-x_0) \langle \Omega | j^\dagger(0) j(x) | \Omega \rangle \right). \quad (2.2.1)$$

The positive sign reflects the bosonic character of the current under consideration.<sup>1</sup> In-

<sup>1</sup>If one would consider fermions instead, e.g. nucleons, there should be a negative sign.

serting a complete set of physical eigenstates

$$\mathbb{1} = \sum_{\alpha} |\alpha\rangle\langle\alpha| \quad (2.2.2)$$

with

$$P|\alpha\rangle = p_{\alpha}|\alpha\rangle, \quad p_{\alpha,0} \geq 0, \quad p_{\alpha}^2 \geq 0, \quad (2.2.3)$$

which means that the momentum lies in the forward light-cone. Extracting the coordinate dependence of the Heisenberg operators using

$$\Psi(x) = e^{iPx}\Psi(0)e^{-iPx}, \quad (2.2.4)$$

we can write

$$\begin{aligned} \Pi(q) = & i \int d^4x e^{iqx} \left( \Theta(x_0) \sum_{\alpha} e^{-i(p_{\alpha}-p_{\Omega})x} |\langle\Omega|j(0)|\alpha\rangle|^2 \right. \\ & \left. + \Theta(-x_0) \sum_{\alpha} e^{i(p_{\alpha}-p_{\Omega})x} |\langle\Omega|j^{\dagger}(0)|\alpha\rangle|^2 \right), \end{aligned} \quad (2.2.5)$$

with  $p_{\Omega}$  being the above defined momentum of the physical ground state,  $P|\Omega\rangle = p_{\Omega}|\Omega\rangle$ . Now we introduce the Fourier representation of the Heaviside function

$$\Theta(x_0) = -\frac{1}{2\pi i} \int_{-\infty}^{\infty} d\omega \frac{e^{-i\omega x_0}}{\omega + i\eta}, \quad (2.2.6)$$

where the limit  $\eta \rightarrow 0$  is understood in order to ensure convergence of the integral. This enables us to perform the space-time integration:

$$\begin{aligned} \Pi(q) = & -\frac{1}{2\pi i} i \int d^4x e^{iqx} \left( \int_{-\infty}^{\infty} d\omega \frac{e^{-i\omega x_0}}{\omega + i\eta} \sum_{\alpha} e^{-i(p_{\alpha}-p_{\Omega})x} |\langle\Omega|j(0)|\alpha\rangle|^2 \right. \\ & \left. + \int_{-\infty}^{\infty} d\omega \frac{e^{i\omega x_0}}{\omega + i\eta} \sum_{\alpha} e^{i(p_{\alpha}-p_{\Omega})x} |\langle\Omega|j^{\dagger}(0)|\alpha\rangle|^2 \right) \\ = & -\sum_{\alpha} \int_{-\infty}^{\infty} d\omega \left( (2\pi)^3 \delta(q_0 - (p_{\alpha,0} - E_{\Omega}) - \omega) \delta^{(3)}(\vec{q} - (\vec{p}_{\alpha} - \vec{p}_{\Omega})) \frac{|\langle\Omega|j(0)|\alpha\rangle|^2}{\omega + i\eta} \right. \\ & \left. + (2\pi)^3 \delta(q_0 + (p_{\alpha,0} - E_{\Omega}) + \omega) \delta^{(3)}(\vec{q} + (\vec{p}_{\alpha} - \vec{p}_{\Omega})) \frac{|\langle\Omega|j^{\dagger}(0)|\alpha\rangle|^2}{\omega + i\eta} \right). \end{aligned} \quad (2.2.7)$$

The Lehmann representation of the current-current correlator therefore reads

$$\begin{aligned} \Pi(q_0, \vec{q}) = & -\sum_{\alpha} (2\pi)^3 \left( \delta^{(3)}(\vec{q} - (\vec{p}_{\alpha} - \vec{p}_{\Omega})) \frac{|\langle\Omega|j(0)|\alpha\rangle|^2}{q_0 - (p_{\alpha,0} - E_{\Omega}) + i\eta} \right. \\ & \left. - \delta^{(3)}(\vec{q} + (\vec{p}_{\alpha} - \vec{p}_{\Omega})) \frac{|\langle\Omega|j^{\dagger}(0)|\alpha\rangle|^2}{q_0 + (p_{\alpha,0} - E_{\Omega}) - i\eta} \right). \end{aligned} \quad (2.2.8)$$

The advantage of this representation is that the whole energy dependence is contained in the denominator. The first term is the particle contribution and gives rise to simple poles below the positive real energy axis at the excitation energies of the particle with quantum numbers encoded in  $j(0)$ .<sup>2</sup> The second term is the antiparticle (hole) contribution, giving rise to simple poles above the negative real energy axis. The nominator of each term is the probability to find the ground state  $|\Omega\rangle$  in the state  $j(0)|\alpha\rangle$  for the first term and in  $j^\dagger(0)|\alpha\rangle$  for the second term. Both are positive, real numbers and are only non-zero when the state  $|\alpha\rangle$  arises from  $|\Omega\rangle$  by adding one particle with the quantum numbers of  $j(x)$  for the first term and by subtracting such a particle, i.e. creating a hole, for the second term. Hence, the poles appear at the excitation energies of a particle (antiparticle) with the quantum numbers encoded in  $j(0)$  ( $j^\dagger(0)$ ).<sup>3</sup> Beside this, the current-current correlation function is analytic everywhere in the complex energy plane except for the real axis.

Before proceeding we will briefly investigate the discontinuities of the current-current correlation function  $\Delta\Pi(s)$  along the real axis with the help of the Lehmann representation (2.2.8). For fixed three-momentum  $\vec{q}$  of the respective particle we define

$$\Delta\Pi(s, \vec{q}) = \frac{1}{2i} \lim_{\epsilon \rightarrow 0} [\Pi(s + i\epsilon, \vec{q}) - \Pi(s - i\epsilon, \vec{q})] , \quad (2.2.9)$$

which corresponds to the discontinuities along the real axis for real energies. Inserting the Lehmann representation we obtain

$$\begin{aligned} \Delta\Pi(q) &= \frac{1}{2i} \lim_{\epsilon \rightarrow 0} [\Pi(q_0 + i\epsilon, \vec{q}) - \Pi(q_0 - i\epsilon, \vec{q})] \\ &= -\frac{(2\pi)^3}{2i} \sum_{\alpha} \lim_{\epsilon \rightarrow 0} \left( \delta^{(3)}(\vec{q} - (\vec{p}_{\alpha} - \vec{p}_{\Omega})) \frac{|\langle \Omega | j(0) | \alpha \rangle|^2}{q_0 - (p_{\alpha,0} - E_{\Omega}) + i\eta + i\epsilon} \right. \\ &\quad - \delta^{(3)}(\vec{q} + (\vec{p}_{\alpha} - \vec{p}_{\Omega})) \frac{|\langle \Omega | j^\dagger(0) | \alpha \rangle|^2}{q_0 + (p_{\alpha,0} - E_{\Omega}) - i\eta + i\epsilon} \\ &\quad - \delta^{(3)}(\vec{q} - (\vec{p}_{\alpha} - \vec{p}_{\Omega})) \frac{|\langle \Omega | j(0) | \alpha \rangle|^2}{q_0 - (p_{\alpha,0} - E_{\Omega}) + i\eta - i\epsilon} \\ &\quad \left. + \delta^{(3)}(\vec{q} + (\vec{p}_{\alpha} - \vec{p}_{\Omega})) \frac{|\langle \Omega | j^\dagger(0) | \alpha \rangle|^2}{q_0 + (p_{\alpha,0} - E_{\Omega}) - i\eta - i\epsilon} \right) \\ &= -\frac{(2\pi)^3}{2i} \sum_{\alpha} \lim_{\epsilon \rightarrow 0} \left( \delta^{(3)}(\vec{q} - (\vec{p}_{\alpha} - \vec{p}_{\Omega})) \frac{-2i\epsilon |\langle \Omega | j(0) | \alpha \rangle|^2}{(q_0 - (p_{\alpha,0} - E_{\Omega}) + i\eta)^2 + \epsilon^2} \right. \\ &\quad \left. - \delta^{(3)}(\vec{q} + (\vec{p}_{\alpha} - \vec{p}_{\Omega})) \frac{-2i\epsilon |\langle \Omega | j^\dagger(0) | \alpha \rangle|^2}{(q_0 + (p_{\alpha,0} - E_{\Omega}) - i\eta)^2 + \epsilon^2} \right) . \end{aligned} \quad (2.2.10)$$

<sup>2</sup>We omit the chemical potential  $\mu$  here. A non-vanishing chemical potential would lead to poles above the real axis for  $q_0 < \mu$ , and below for  $q_0 > \mu$ . For a detailed discussion see [Fe71].

<sup>3</sup>Actually we have to introduce the chemical potential of the ground state in (2.2.8) in order to understand that the poles are located at the exact excitation energies. But, for now it is sufficient to understand that the poles are located at the real axis.

Using a representation of Dirac's  $\delta$  distribution in the form of Lorentz curves

$$\delta(x) = \frac{1}{\pi} \frac{\epsilon}{x^2 + \epsilon^2}, \quad (2.2.11)$$

where the limit  $\epsilon \rightarrow 0$  is to be understood, we arrive at

$$\begin{aligned} \Delta\Pi(q) = (2\pi)^3 \pi \sum_{\alpha} & \left( \delta^{(4)}(q - (p_{\alpha} - p_{\Omega})) |\langle \Omega | j(0) | \alpha \rangle|^2 \right. \\ & \left. - \delta^{(4)}(q + (p_{\alpha} - p_{\Omega})) \left| \langle \Omega | j^{\dagger}(0) | \alpha \rangle \right|^2 \right), \end{aligned} \quad (2.2.12)$$

where we omitted the  $\eta$  prescription, which is understood to be absorbed in  $q_0$ . We note here that, by the last equation, the discontinuities along the real axis, defined in this way, are real.

Let us now return to the current-current correlation function  $\Pi(q)$  itself. Due to Lorentz covariance of the current-current correlator and by the Theorem of Hall and Wightman (cf. for example [Ro69])  $\Pi(q)$  (and also  $\Delta\Pi(q)$ ) is merely a function of all possible scalar products of the Lorentz vectors it depends on, i.e.  $q$  for the vacuum case and  $q$  and  $v$ , for the in-medium case, where  $v$  stands for the medium four-velocity. If we consider vacuum sum rules,  $\Pi(q)$  therefore only depends on  $q^2$ ,  $\Pi(q) = \Pi(q^2)$ . Asking for the analytic structure of  $\Pi(q^2)$  in the complex  $q^2$  plane, we recall that  $|\alpha\rangle$  is a physical state satisfying (2.2.3) with real momentum. By the occurrence of the  $\delta$  distribution and due to the vanishing four-momentum of the vacuum ground state, i.e.  $p_{\Omega} = 0$ , we see that  $q^2 < 0$  requires  $q_0^2 \neq p_0^2$ . Hence,  $\Pi(q^2)$  has poles only on the positive real axis, i.e. for  $q^2 \geq 0$ .

However, considering in-medium sum rules, the ground state also depends on the medium four-velocity  $v_{\mu}$ . Hence one has  $\Pi(q) = \Pi(q, v) = \Pi(q^2, v^2, qv)$ . For fixed medium velocity the current-current correlation function remains a function of  $q_0$  and  $\vec{q}$ , and we can not make further restrictions to the pole structure. Thus,  $\Pi(q)$  is analytic in the complex energy plane apart from the real  $q_0$ -axis.

In the following subsections we relate the values of the current-current correlation function for complex values of  $q_0$  (or  $q^2$ ) to its values at the real axis (positive real axis), i.e. to its pole structure and hence, due to (2.2.8), to the excitation energies of the considered particle. This enables us to relate large momentum properties, determined by the quark structure, to hadronic observables. Due to the additional dependence of the current-current correlation function on the medium velocity these relations differ in vacuum and medium.

## 2.2.2 Vacuum Dispersion Relations

By the analytic structure of the correlation function, Cauchy's theorem enables us to give an integral representation for it, called dispersion relation [Fu92, Su61]. Therefore, we use the analyticity of  $\Pi(q^2)$  for the vacuum case in the area surrounded by the contour exhibited in the left diagram of fig. 2.2.1.

For  $q^2$  off the positive real axis,  $q^2 \notin \mathbb{R}^+ \cup 0$ , one gets the identity

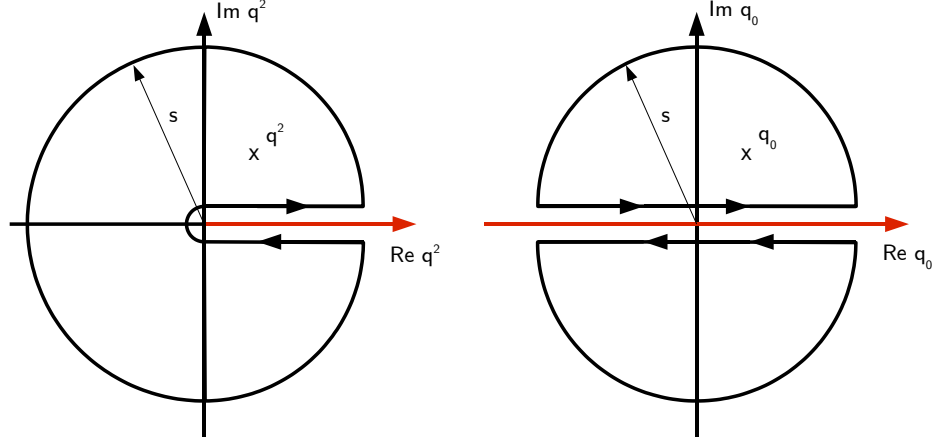


**Figure 2.2.1:** Integration contours  $\Gamma$  in the complex  $q^2$ -plane in the left panel and in the complex  $q_0$ -plane in the right panel. The parallel integration paths tend to the real axis (but do not coincide with it), while the outer circle or half-circles tend to infinity.

$$\Pi(q^2) = \frac{1}{2\pi i} \int_{\Gamma} \frac{\Pi(s)}{s - q^2} ds \quad (2.2.13)$$

$$\begin{aligned} &= \frac{1}{2\pi i} \int_0^{+\infty} \frac{\Pi(s + i\epsilon)}{s - q^2} ds + \frac{1}{2\pi i} \int_{+\infty}^0 \frac{\Pi(s - i\epsilon)}{s - q^2} ds \\ &+ \frac{1}{2\pi i} \oint_{\epsilon} \frac{\Pi(s)}{s - q^2} ds + \frac{1}{2\pi i} \oint_{\infty} \frac{\Pi(s)}{s - q^2} ds, \end{aligned} \quad (2.2.14)$$

where the last integral is for the integration over the outer circle for the radius tending to infinity, and the third is for integration on the semicircle at the origin. As the distance of the poles to the real axis emerges from the  $\eta$ -prescription for the Heaviside function, where the limit  $\eta \rightarrow 0$  is understood, we also understand the limit  $\epsilon \rightarrow 0$  for the integrals above. Thus, the integral over the semicircle becomes zero.

One can now show that the contribution of the integral over the infinitely large circle is a finite polynomial in  $q^2$  if and only if  $|\Pi(q^2)| \leq |q^2|^N$  for  $|q^2| \rightarrow \infty$ , where  $N \in \mathbb{N}$  is a finite and fixed number [Su61]. Because  $|q^2| < |s|$ , if  $s$  goes along the outer circle, one can write

$$\frac{1}{s - q^2} = \sum_{n=0}^{\infty} \frac{1}{s} \left( \frac{q^2}{s} \right)^n. \quad (2.2.15)$$

By making use of the boundary condition for  $\Pi(q^2)$  the integral over the outer circle reads

$$\begin{aligned} \frac{1}{2\pi i} \oint_{\infty} \frac{\Pi(s)}{s - q^2} ds &= \sum_{n=0}^{\infty} \frac{(q^2)^n}{2\pi i} \oint_{\infty} \frac{\Pi(s)}{s^{n+1}} ds = \sum_{n=0}^{\infty} \frac{(q^2)^n}{2\pi i} \oint_0^{2\pi} \frac{\Pi(s)}{s^n} d\phi \\ &= \sum_{n=0}^N \frac{(q^2)^n}{2\pi i} \oint_0^{2\pi} \frac{\Pi(s)}{s^n} d\phi = \sum_{n=0}^N a_n (q^2)^n \end{aligned} \quad (2.2.16)$$



which is a finite polynomial in  $q^2$ . This polynomial is not equal to the so-called subtractions, which we will introduce later. The exact dispersion relation in vacuum then reads

$$\Pi(q^2) = \frac{1}{\pi} \int_0^\infty \frac{\Delta\Pi^{vac}(s)}{s - q^2} ds + \sum_{n=0}^N a_n q_0^n \quad (2.2.17)$$

with  $\Delta\Pi^{vac}$  being defined analogue to (2.2.9) as

$$\Delta\Pi^{vac}(q^2) = \frac{1}{2i} \lim_{\epsilon \rightarrow 0} [\Pi(q^2 + i\epsilon) - \Pi(q^2 - i\epsilon)] , \quad (2.2.18)$$

which is a real function. From this we see: If  $\Pi(q^2)$  does not vanish fast enough when  $|q^2|$  approaches infinity, the boundary condition is essential and adequate that we can eliminate the contribution of the infinite circle by subtracting a finite polynomial in  $q^2$ . It is important to note that the coefficients  $a_n$  are not proportional to the derivatives of  $\Pi(q^2)$  for  $q^2 = 0$  even if  $\Pi(q^2)$  is analytic in an open circle around the origin (unless the circle is the infinite circle itself, which would require infinite excitation energies in (2.2.8)). Because of the pole structure along the real axis, the current-current correlation function is not analytic inside the infinite circle and Cauchy's theorem is therefore not applicable to the integral over the infinite circle. Instead, in [Su61], the authors show that the contribution from the infinite circle can be expressed by the boundary values of  $\Pi(q^2)$  along the real axis.

However, there are several methods to get rid of the polynomial contributions. One possibility is to take the  $N + 1$ -st derivative of (2.2.17). The polynomial vanishes and one gets

$$\left(\frac{d}{dq^2}\right)^{N+1} \Pi(q^2) = \frac{(N+1)!}{\pi} \int_0^\infty \frac{\Delta\Pi^{vac}(s)}{(s - q^2)^{N+2}} ds . \quad (2.2.19)$$

Of course, we also could have done this right at the beginning in (2.2.13) and by the boundary condition the integral over the outer circle would vanish. This method is called the method of power moments  $M_n(q^2)$ , and the  $n$ th moment is given by

$$M_n(q^2) = \frac{1}{n!} \left(\frac{d}{dq^2}\right)^n \Pi(q^2) . \quad (2.2.20)$$

We mention this method just for completeness. It will not be considered anymore throughout this thesis.

However, if  $\Pi(q^2)$  is also analytic in an open (finite) circle around the origin we can give a dispersion relation which is free from the polynomial contribution of the infinite circle. In this case the lower bound for the integration along the positive real axis effectively starts from a lower boundary threshold  $s_0$ ,<sup>4</sup> because then the integrations above and below the positive real axis cancel each other up to the threshold due to analyticity. The dispersion relation then can be obtained from (2.2.13) by subtracting a polynomial of degree  $N - 1$ ,

<sup>4</sup> $s_0$  corresponds to the lowest-lying excitation energy.

with coefficients  $\propto \Pi^{(n)}(0)$ . Here the derivatives are solely calculated from (2.2.13), which means that we use the contour given in the left panel of fig. 2.2.1.

In order to clarify the difference between the subtractions and the polynomial coefficients  $a_n$  in (2.2.17), we emphasize that the derivatives  $\Pi^{(n)}(0)$  used as coefficients for the subtractions are not calculated from an integral over the infinite circle, in contrast to the polynomial coefficients  $a_n$ , i.e.

$$\Pi(q^2) - \sum_{n=0}^{N-1} \frac{\Pi^{(n)}(0)}{n!} (q^2)^n = \frac{1}{2\pi i} \int_{\Gamma} \frac{\Pi(s)}{s - q^2} ds - \sum_{n=0}^{N-1} \frac{(q^2)^n}{2\pi i} \int_{\Gamma} \frac{\Pi(s)}{s^{n+1}} ds. \quad (2.2.21)$$

Again by using the standard expression for geometric series

$$\frac{1}{s - q^2} - \sum_{n=0}^{N-1} \frac{(q^2)^n}{s^{n+1}} = \sum_{n=N}^{\infty} \frac{1}{s} \left( \frac{q^2}{s} \right)^n = \frac{1}{s} \left( \frac{q^2}{s} \right)^N \sum_{n=0}^{\infty} \left( \frac{q^2}{s} \right)^n = \left( \frac{q^2}{s} \right)^N \frac{1}{s - q^2}, \quad (2.2.22)$$

one ends up with

$$\Pi(q^2) - \sum_{n=0}^{N-1} \frac{\Pi^{(n)}(0)}{n!} (q^2)^n = \frac{1}{2\pi i} \int_{\Gamma} \left( \frac{q^2}{s} \right)^N \frac{\Pi(s)}{s - q^2} ds. \quad (2.2.23)$$

By the boundary condition of the current-current correlation function the integral over the infinite circle vanishes now:

$$\frac{1}{2\pi i} \oint_{\infty} \left( \frac{q^2}{s} \right)^N \frac{\Pi(s)}{s - q^2} ds = \sum_{n=0}^{\infty} \frac{(q^2)^{n+N}}{2\pi i} \oint_{\infty} \frac{\Pi(s)}{s^{N+n+1}} ds = 0. \quad (2.2.24)$$

The  $N - 1$  times subtracted dispersion relation in vacuum finally reads

$$\begin{aligned} \Pi(q^2) - \sum_{n=0}^{N-1} \frac{\Pi^{(n)}(0)}{n!} (q^2)^n &= \frac{1}{\pi} \int_0^{\infty} \left( \frac{q^2}{s} \right)^N \frac{\Delta\Pi^{vac}(s)}{s - q^2} ds \\ &= \frac{1}{\pi} \int_{s_0}^{\infty} \left( \frac{q^2}{s} \right)^N \frac{\Delta\Pi^{vac}(s)}{s - q^2} ds. \end{aligned} \quad (2.2.25)$$

Now, the coefficients of the polynomial are well known functions. Additionally one could also take the  $N$ th derivative of (2.2.25) to get also rid of these polynomials.

### 2.2.3 In-Medium Dispersion Relations

For the in-medium case we can proceed in a similar way as in the previous subsection, but with the difference that we now work in the complex  $q_0$  plane and not in the complex  $q^2$  plane and explicitly exclude the entire real axis. Using the integration contour given in the right panel of fig. 2.2.1 and the analyticity of  $\Pi(q_0, \vec{q})$  in the area surrounded by the

integration contour, we can write for fixed  $\vec{q}$

$$\begin{aligned}\Pi(q_0, \vec{q}) &= \frac{1}{2\pi i} \int_{\Gamma} \frac{\Pi(s, \vec{q})}{s - q_0} ds \\ &= \frac{1}{2\pi i} \int_{-\infty}^{+\infty} \frac{\Pi(s + i\epsilon, \vec{q})}{s - q_0} ds + \frac{1}{2\pi i} \int_{+\infty}^{-\infty} \frac{\Pi(s - i\epsilon, \vec{q})}{s - q_0} ds \\ &\quad + \frac{1}{2\pi i} \oint_{\infty} \frac{\Pi(s, \vec{q})}{s - q_0} ds.\end{aligned}\tag{2.2.26}$$

Following the same arguments as for the vacuum case we can note the exact dispersion relation for the in-medium case as

$$\Pi(q_0, \vec{q}) = \frac{1}{\pi} \int_{-\infty}^{+\infty} \frac{\Delta\Pi(s, \vec{q})}{s - q_0} ds + \sum_{n=0}^N a_n q_0^n,\tag{2.2.27}$$

where the polynomial again corresponds to the contribution of the infinite circle and  $\Delta\Pi(s, \vec{q})$  is defined in (2.2.9). If  $\Pi(q_0, \vec{q})$  is analytic in an open (finite) area at the origin, the integration along the cuts at the real axis effectively starts from thresholds  $s_0^+, s_0^-$ .<sup>5</sup> In this case one can again arrive at a subtracted dispersion relation which is free from polynomial contributions arising from the integral over the infinite circle. Similar to the vacuum case we get

$$\begin{aligned}\Pi(q_0, \vec{q}) - \sum_{n=0}^{N-1} \frac{\Pi^{(n)}(q_0=0, \vec{q})}{n!} q_0^n &= \frac{1}{2\pi i} \int_{\Gamma} \Pi(s, \vec{q}) \left( \sum_{n=0}^{\infty} - \sum_{n=0}^{N-1} \right) \left( \frac{q_0}{s} \right)^n \frac{1}{s} ds \\ &= \frac{1}{2\pi i} \int_{\Gamma} \left( \frac{q_0}{s} \right)^N \frac{\Pi(s, \vec{q})}{s - q_0} ds.\end{aligned}\tag{2.2.28}$$

The integral over the infinite circle again vanishes due to the boundary condition, giving the  $N - 1$  times subtracted dispersion relation in  $q_0$

$$\begin{aligned}\Pi(q_0, \vec{q}) - \sum_{n=0}^{N-1} \frac{\Pi^{(n)}(0, \vec{q})}{n!} (q_0)^n &= \frac{1}{\pi} \int_{-\infty}^{+\infty} \left( \frac{q_0}{s} \right)^N \frac{\Delta\Pi(s, \vec{q})}{s - q_0} ds \\ &= \frac{1}{\pi} \int_{s_0^+}^{+\infty} \left( \frac{q_0}{s} \right)^N \frac{\Delta\Pi(s, \vec{q})}{s - q_0} ds + \frac{1}{\pi} \int_{-\infty}^{s_0^-} \left( \frac{q_0}{s} \right)^N \frac{\Delta\Pi(s, \vec{q})}{s - q_0} ds.\end{aligned}\tag{2.2.29}$$

For purposes which will become evident later on, we are more likely to work with a dispersion relation in  $q_0^2$  rather than a dispersion relation in  $q_0$ . Therefore we split the current-current correlation function  $\Pi(q_0, \vec{q})$  into a part that is even ( $e$ ) in  $q_0$  and a part that is odd ( $o$ ) in  $q_0$

$$\begin{aligned}\Pi(q_0, \vec{q}) &= \frac{1}{2} (\Pi(q_0, \vec{q}) + \Pi(-q_0, \vec{q})) + \frac{1}{2} (\Pi(q_0, \vec{q}) - \Pi(-q_0, \vec{q})) \\ &= \Pi^e(q_0, \vec{q}) + q_0 \Pi^o(q_0, \vec{q}),\end{aligned}\tag{2.2.30}$$

---

<sup>5</sup>This corresponds to an energy gap between the lowest-lying particle state and the lowest-lying antiparticle excitation.

where the energy factor in front of  $\Pi^o(q_0, \vec{q})$  is just convention. By the above definition we only assume certain reflection symmetries for the even and odd parts of the correlation function

$$\Pi^e(q_0, \vec{q}) = \frac{1}{2} (\Pi(q_0, \vec{q}) + \Pi(-q_0, \vec{q})) = \Pi^e(-q_0, \vec{q}), \quad (2.2.31)$$

$$\Pi^o(q_0, \vec{q}) = \frac{1}{2q_0} (\Pi(q_0, \vec{q}) - \Pi(-q_0, \vec{q})) = \Pi^o(-q_0, \vec{q}), \quad (2.2.32)$$

whereas nothing is said about the actual dependence on  $q_0$ . Summation and subtraction of the dispersion relation (2.2.29) for  $\Pi(q_0, \vec{q})$  and  $\Pi(-q_0, \vec{q})$  now result in the following separate dispersion relations for the even part  $\Pi^e(q_0, \vec{q})$  of the current-current correlation function

$$\begin{aligned} \Pi^e(q_0, \vec{q}) &= \frac{1}{2} \sum_{n=0}^{N-1} \frac{\Pi^{(n)}(0, \vec{q})}{n!} (q_0)^n (1 + (-1)^n) \\ &= \frac{1}{2\pi} \int_{-\infty}^{+\infty} ds \Delta\Pi(s, \vec{q}) \frac{q_0^N}{s^{N-1}} \frac{(1 + (-1)^N) + \frac{q_0}{s} (1 - (-1)^N)}{s^2 - q_0^2} \end{aligned} \quad (2.2.33)$$

and for the odd part of the correlation function

$$\begin{aligned} \Pi^o(q_0, \vec{q}) &= \frac{1}{2} \sum_{n=0}^{N-1} \frac{\Pi^{(n)}(0, \vec{q})}{n!} (q_0)^{n-1} (1 - (-1)^n) \\ &= \frac{1}{2\pi} \int_{-\infty}^{+\infty} ds \Delta\Pi(s, \vec{q}) \frac{q_0^{N-1}}{s^{N-1}} \frac{(1 - (-1)^N) + \frac{q_0}{s} (1 + (-1)^N)}{s^2 - q_0^2}. \end{aligned} \quad (2.2.34)$$

From these two equations we recognize that both functions,  $\Pi^e(q_0, \vec{q})$  and  $\Pi^o(q_0, \vec{q})$ , can only depend on  $q_0^2$ . Hence, one can write

$$\Pi(q_0, \vec{q}) = \Pi^e(q_0^2, \vec{q}) + q_0 \Pi^o(q_0^2, \vec{q}). \quad (2.2.35)$$

The not subtracted dispersion relations can be obtained from these expressions by setting  $N = 1$ . At this point we remark the similarity of the vacuum dispersion relation and the even in-medium dispersion relation, which can be seen by substituting  $s^2 = t$  in (2.2.33). This is not the case for the odd in-medium dispersion relation (2.2.34).

Due to the reality of  $\Delta\Pi(s)$  for the vacuum and in-medium case, we can read off from the corresponding dispersion relations

$$\Pi(q^{2*}) = \Pi^*(q^2) \quad (2.2.36)$$

for the vacuum case and

$$\Pi(q_0^*, \vec{q}) = \Pi^*(q_0, \vec{q}) \quad (2.2.37)$$

for the in-medium case. By the definition of  $\Delta\Pi(s)$  we can then write

$$\Delta\Pi(s) = \text{Im}\Pi(s) \quad (2.2.38)$$

for both, vacuum and medium.

By the dispersion relations an exact relation between the current-current correlation function at arbitrary (complex) values of  $q_0$  or  $q^2$  respectively off the real axis (positive real axis) and its values at the real axis (positive real axis) is given. This enables us to relate properties of the current-current correlation function at real (physical) values of the energy  $q_0$  for the in-medium case and positive real values of the momentum squared  $q^2$  for the vacuum case to the hadronic properties of the correlation function encoded in the discontinuities along the real axis.

## 2.3 Operator Product Expansion

We now relate the correlation function to the quark degrees of freedom encoded in the respective currents. This can be done by applying the operator product expansion [Wi69]. Intuitively, it is clear that such a relation can only be valid at large external momenta  $q^2$ . At low momentum the fundamental degrees of freedom are hadrons, while we can only observe the quark structure of the hadron at high external momenta. In fact, the operator product expansion has only been proven in perturbation theory [Zi72]. Therefore, we restrict ourselves to the high momentum regime when applying the operator product expansion.

Considering the product of two local field operators,  $j(x)j^\dagger(y)$ , for  $x \rightarrow y$  one can show that this product is not well defined. Instead, it is singular [Mu87]. This also holds true for the time-ordered product of two local field operators,  $T[\Psi(x)\Psi^\dagger(y)]$ , as can be seen by applying Wick's theorem to the time-ordered product<sup>6</sup>

$$T[j(x)j^\dagger(y)] = :j(x)j^\dagger(y): + \underbrace{j(x)j^\dagger(y)}, \quad (2.3.1)$$

introducing the free-field propagators and setting  $x = y$ . The singularities are then contained in the free-field propagators. For matrix elements of two interacting local field operators this can also be seen by investigating the Lehman representation in coordinate space for  $x \rightarrow y$ . The same holds true for operator products which are not time ordered.

Wilson proposed [Wi69] that an operator product can be written as a sum of c-number functions  $C_O(x - y)$ , which are singular for  $x \rightarrow y$ , and non-singular operators  $O$ . Being non-singular means that the singularities of the operator product for  $x \rightarrow y$  are completely contained in the coefficient functions  $C_O(x - y)$ . For the time-ordered product, this expansion therefore reads

$$T[j(x)j^\dagger(y)] = \sum_O C_O(x - y)O, \quad (2.3.2)$$

where  $C_O(x - y)$  are so-called Wilson coefficients or coefficient functions, being singular and  $O$  being finite in the limit  $x \rightarrow y$ . The operators in the sum can be ordered according to their mass dimension and, in principle, the sum runs over all possible products of field

---

<sup>6</sup>:  $\dots :$  means normal ordering and  $\underbrace{\quad}$  indicates a contraction.

operators of the theory under consideration. We list all operators and their mass-dimension that are considered throughout this work

$$D_\mu : \dim_m = 1 , \quad (2.3.3a)$$

$$q : \dim_m = \frac{3}{2} , \quad (2.3.3b)$$

$$\mathcal{G}_{\mu\nu} : \dim_m = 2 , \quad (2.3.3c)$$

and the operator products

$$\bar{q}q : \dim_m = 3 , \quad (2.3.4a)$$

$$\bar{q}D_\mu q : \dim_m = 4 , \quad (2.3.4b)$$

$$G^2 : \dim_m = 4 , \quad (2.3.4c)$$

$$\bar{q}D_\mu D_\nu q : \dim_m = 5 , \quad (2.3.4d)$$

$$\bar{q}\sigma^{\mu\nu}\mathcal{G}_{\mu\nu}q : \dim_m = 5 . \quad (2.3.4e)$$

In [Zi72] a generalized form of normal ordered products and Wick's theorem were used to proof this expansion in perturbation theory. Moreover, one can show that, in the framework of a theory which contains non-perturbative effects, a consistent separation of large distance and short distance physics is necessary. All the non-perturbative effects must be contained in the operators  $O$ , while the coefficients are completely determined by perturbative physics.

It is important to note that (2.3.2) can only be understood as an asymptotic expansion. This is clear, because convergence of the series is by no means obvious and the series of partial sums could have more than one accumulation point, i.e. being divergent. But the series is supposed to be a good approximation to the operator product, when truncated and only a finite number of terms is taken [Sh78] into account. Then it has to fulfill [It80]

$$\lim_{x \rightarrow y} \frac{\text{T} [j(x)j^\dagger(y)] - \sum_{O_{max}} C_O(x-y)O}{C_{O_{max}}(x-y)} = 0 \quad \forall O_{max} , \quad (2.3.5)$$

being merely the definition for a divergent series which is asymptotic to the operator product for  $x \rightarrow y$ , i.e. an asymptotic expansion of the divergent operator product. In contrast to a Taylor expansion of a function  $f(x)$  at  $x = 0$ , where the quality of the approximation increases with increasing number of terms that have been taken into account, the asymptotic series of a, possibly divergent, function  $g(x)$  at  $x = 0$  has to be truncated at some order  $N$  to give the best approximation that can be achieved.<sup>7</sup> Taking more or less terms into account, the approximation gets worse. Thereby,  $N$  depends on the value of  $x$  at which point the function  $g(x)$  is to be approximated by the asymptotic series, i.e.  $x$

<sup>7</sup>A Laurent expansion would only be a possible expansion if the function  $g(x)$  has isolated singularities. Moreover, such an expansion would mean, that the series is convergent inside some ring around the singularity. Instead, an asymptotic expansion can also be used to approximate functions  $g(x)$  that are well defined in some region, e.g.  $x > 0$ , have a divergence at  $x = 0$  and are ill defined for  $x < 0$ . In such a case it is impossible to find a Laurent series for the function  $g(x)$  at  $x = 0$  with maximum radius of convergence being  $R > 0$ .

determines the point where the asymptotic series has to be truncated. We will use this property of asymptotic expansions for the analysis of our sum rule.

As the operator product expansion is an expansion at operator level, the coefficient functions are state independent. They are completely determined by the structure of the operator product. This means that the choice of a certain current to express the quark structure of the considered particle completely determines the coefficient functions. Therefore, the coefficient functions must be the same for all particles that have the same quantum numbers.

Calculating matrix elements of (2.3.2) using the non-perturbative vacuum ground state or the in-medium ground state  $|\Omega\rangle$ , one obtains

$$\langle\Omega|T[j(x)j^\dagger(y)]|\Omega\rangle = \sum_O C_O(x-y)\langle\Omega|O|\Omega\rangle. \quad (2.3.6)$$

The matrix elements of the operators  $\langle\Omega|O|\Omega\rangle$  on the r.h.s. of (2.3.6) are called condensates. If one would work in perturbation theory using the perturbative ground state, only the unity operator would give a contribution to the sum, because all the other matrix elements would vanish. But as we have to include non-perturbative effects and by (2.1.2), this is not true anymore. In this sense, by introducing non-vanishing matrix elements we were able to deal with non-perturbative physics. From (2.3.6) we also see that the whole medium dependence must be contained in the condensates, because the Wilson coefficients are state independent.

There is a subtlety about the last point. In fact, the operator product expansion differs in vacuum and in medium. But this is not a result of vanishing Wilson coefficients. Rather, it is a result of matrix elements of certain operators that vanish in vacuum, but do not vanish in medium. Therefore, the complete medium dependence is contained in the condensates, although the operator product expansions themselves already differ.

On the other side, the condensates can be considered at this stage as phenomenological parameters used to reproduce the properties of the correlation function in the non-perturbative, i.e. hadronic, region. Knowledge of the current-current correlation function in the low momentum regime, i.e. the hadronic properties of the particle under investigation, together with the dispersion relations reviewed in subsection 2.2 will result in restrictions for the correlator in the large-momentum regime. By virtue of the operator product expansion, this gives us valuable information about the condensates.<sup>8</sup>

Moreover, instead of reproducing hadronic properties which are related to the non-perturbative character of the theory, e.g. hadron masses, from first principles of quantum chromodynamic, the condensates are used to reproduce hadron properties which depend on the large-distance behavior of the theory. As the condensates are expectation values of the ground state, they can give us valuable information about the dynamical structure of the theory. Some of the most popular condensates are shown in fig. 2.3.1. They can be read as particles, propagating in the ground state of QCD, being annihilated by virtual particles from the ground state and creating another real particle (the remaining virtual particle becomes real) somewhere else. During this work we will meet these and other diagrams,

---

<sup>8</sup>Strictly speaking, QCD sum rules give us information about certain combinations of condensates.

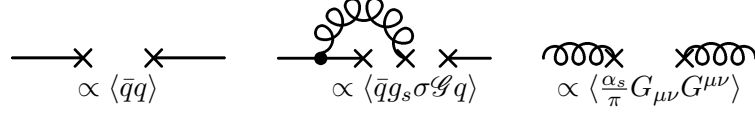


**Figure 2.3.1:** Graphical visualization of the chiral condensate (left panel), the mixed quark-gluon condensate (middle panel) and the pure gluon condensate (right panel). Plain lines depict quarks, curly lines gluons and crosses symbolize annihilation of the corresponding particles with virtual particles from the ground state.

where the coupling of particles to condensates is depicted in a similar way, embedded in larger diagrams. Although Feynman diagram techniques are applicable, we prefer to use them only as visualizations of the formulas which are evaluated and as an intuitive notation in order to indicate the terms that have to be inserted for further calculations.

However, because the operators  $O$  appearing in the sum (2.3.2) are completely determined by the theory, they do not depend on the specific currents used to calculate the operator product. Of course, a certain operator could be absent from the sum, if the corresponding Wilson coefficient vanishes due to the structure of the currents, but the operator itself is independent of this. Hence, the condensates can be considered as universal parameters in the sense that their knowledge is not restricted to a specific sum rule. Knowledge of the condensates from the investigation of one sum rule gives the possibility to make restrictions for other sum rules.

Instead of going to higher and higher orders in the perturbative expansion (2.1.4) we apply the operator product expansion to (2.1.1):

$$\Pi^{OPE}(q) = \sum_O C_O(q) \langle \Omega | O | \Omega \rangle. \quad (2.3.7)$$

In doing so we introduce the notion of condensates in order to reproduce or to predict hadronic properties, which can not be understood from a perturbative point of view. A graphical representation can be found in fig. 2.3.2.

Recapitulatory we recall that the singular behavior of operator products like  $j(x)j^\dagger(y)$  for  $x \rightarrow y$  gives rise to the operator product expansion (2.3.2), while the non-perturbative large distance behavior gives rise to the introduction of condensates  $\langle \Omega | O | \Omega \rangle$ .

## 2.4 Fock Schwinger Gauge and Background Field Method

In this section we will discuss the so-called Fock-Schwinger gauge, which enables us to give simple expressions for gluon fields and quark propagators. These are then used to develop simple techniques for the calculation of the operator product expansion. This section follows closely [No83].

The Fock-Schwinger gauge reads

$$(x^\mu - x_0^\mu) \mathcal{A}_\mu(x) = 0. \quad (2.4.1)$$



$$\begin{array}{c}
\text{QCD Quark-} \\
\text{Propagator}
\end{array}
= \frac{\text{perturbative}}{\text{contribution}}$$

$$\begin{array}{c}
+ \underbrace{\begin{array}{c} \propto \langle \bar{q}q \rangle \\ \text{---} \times \text{---} \end{array}}_{\text{non-perturbative contribution}} + \begin{array}{c} \propto \langle \frac{\alpha_s}{\pi} G_{\mu\nu} G^{\mu\nu} \rangle \\ \text{---} \text{---} \times \text{---} \text{---} \end{array} + \begin{array}{c} \propto \langle \bar{q} g_s \sigma \mathcal{G} q \rangle \\ \text{---} \bullet \text{---} \times \text{---} \times \text{---} \end{array} + \dots
\end{array}$$

**Figure 2.3.2:** Graphical representation of an operator product expansion. To expand the exact propagator, one can go to higher orders in the perturbative expansion, only including scattering events of the quark. On the other side, creation and annihilation processes emerging from the complicated structure of the QCD ground state can also be taken into account.

Usually one chooses  $x_0^\mu = 0$ . Obviously, this gauge is not translation invariant. The invariance is broken due to the special role of  $x_0$ . Therefore, a shift in space-time would destroy the gauge condition. But, as we will see, this condition is crucial to the techniques used in the calculations performed afterwards. Hence, we must restrict ourselves to one selected frame. By (2.4.1) we can write

$$0 = \partial_\mu (y^\nu A_\nu^A(y)) = A_\mu^A(y) + y^\nu \partial_\mu A_\nu^A(y). \quad (2.4.2)$$

Furthermore, using (A.9) one obtains

$$y^\nu \partial_\mu A_\nu^A = y^\nu G_{\mu\nu}^A + y^\nu \partial_\nu A_\mu^A, \quad (2.4.3)$$

where the non-Abelian term in (A.9) vanishes due to the gauge condition (2.4.1). Together with (2.4.2) one ends up with

$$A_\mu^A(y) + y^\nu \partial_\nu A_\mu^A = y^\nu G_{\nu\mu}^A. \quad (2.4.4)$$

Substituting  $y^\nu = \alpha x^\nu$  and inserting (2.4.4) again leads to

$$\frac{d}{d\alpha} (\alpha A_\mu(\alpha x)) = \alpha x^\nu G_{\nu\mu}^A(\alpha x). \quad (2.4.5)$$

Integration over  $\alpha$  from 0 to 1 finally yields

$$A_\mu^A(x) = \int_0^1 d\alpha \alpha x^\nu G_{\nu\mu}^A(\alpha x). \quad (2.4.6)$$

We observe that the Fock-Schwinger gauge (2.4.1) enables us to express the gluon fields in terms of the gluon field strength tensor. Expanding the gluon field  $\mathcal{A}_\mu$  in (2.4.1) in  $x$

$$x^\mu \left( \sum_{n=0}^{\infty} \frac{1}{n!} x^{\alpha_1} \dots x^{\alpha_n} \partial_{\alpha_1} \dots \partial_{\alpha_n} \mathcal{A}_\mu(0) \right) = 0 \quad (2.4.7)$$

for all  $x$ , we conclude

$$x^\mu x^{\alpha_1} \dots x^{\alpha_n} \partial_{\alpha_1} \dots \partial_{\alpha_n} \mathcal{A}_\mu(0) = 0. \quad (2.4.8)$$

As a direct consequence of the last equation one can show that

$$x^{\alpha_1} \dots x^{\alpha_n} (\partial_{\alpha_1} \dots \partial_{\alpha_n} \mathcal{G}_{\mu\nu})_{x=0} = x^{\alpha_1} \dots x^{\alpha_n} (D_{\alpha_1} \dots D_{\alpha_n} \mathcal{G}_{\mu\nu})_{x=0}. \quad (2.4.9)$$

Therefore, one can expand the gluon field strength tensor in (2.4.6) for small  $x$

$$\begin{aligned} \mathcal{A}_\mu(x) &= \int_0^1 d\alpha \alpha x^\nu \mathcal{G}_{\nu\mu}(\alpha x) \\ &= \int_0^1 d\alpha \alpha x^\nu \sum_{n=0}^{\infty} \frac{\alpha^n}{n!} x^{\alpha_1} \dots x^{\alpha_n} (\partial_{\alpha_1} \dots \partial_{\alpha_n} \mathcal{G}_{\nu\mu})_{x=0} \\ &= \int_0^1 d\alpha \alpha x^\nu \sum_{n=0}^{\infty} \frac{\alpha^n}{n!} x^{\alpha_1} \dots x^{\alpha_n} (D_{\alpha_1} \dots D_{\alpha_n} \mathcal{G}_{\nu\mu})_{x=0}. \end{aligned} \quad (2.4.10)$$

Integration over  $\alpha$  then yields the covariant expansion for the gluon fields in terms of the gluon field strength tensor only:

$$\mathcal{A}_\mu(x) = \sum_{n=0}^{\infty} \frac{x^\nu}{n!(n+2)} x^{\alpha_1} \dots x^{\alpha_n} (D_{\alpha_1} \dots D_{\alpha_n} \mathcal{G}_{\nu\mu})_{x=0}. \quad (2.4.11)$$

The Fock-Schwinger gauge also provides a covariant expansion for the quark fields:

$$\Psi(x) = \sum_{n=0}^{\infty} \frac{1}{n!} x^{\alpha_1} \dots x^{\alpha_n} \left( \vec{D}_{\alpha_1} \dots \vec{D}_{\alpha_n} \Psi \right)_{x=0}, \quad (2.4.12a)$$

$$\bar{\Psi}(x) = \sum_{k=0}^{\infty} \frac{1}{k!} x^{\alpha_1} \dots x^{\alpha_k} \left( \bar{\Psi} \overleftarrow{D}_{\alpha_k} \dots \overleftarrow{D}_{\alpha_1} \right)_{x=0}. \quad (2.4.12b)$$

The method used to simulate the non-perturbative vacuum and medium effects of the physical ground state is the background field method. When a quark is propagating it interacts with the virtual particles emerging from the ground state. These particles can effectively be modeled by a classic weak gluonic background field, and the interaction is then described by a propagation within this field. As it is a weak field, it is possible to give a perturbative expansion of the quark propagator in terms of the coupling constant:

$$\begin{aligned} iS(x, y) &= iS^{(0)}(x - y) \\ &+ \sum_{n=1}^{\infty} \int iS^{(0)}(x - z_1) g \hat{A}(z_1) iS^{(0)}(z_1 - z_2) \dots g \hat{A}(z_n) iS^{(0)}(z_n - y) dz_1 \dots dz_n, \end{aligned} \quad (2.4.13)$$

where  $S^{(0)}(x - y)$  denotes the free propagator satisfying

$$(i\hat{\partial}_x - m)S^{(0)}(x - y) = \delta^{(4)}(x - y). \quad (2.4.14)$$

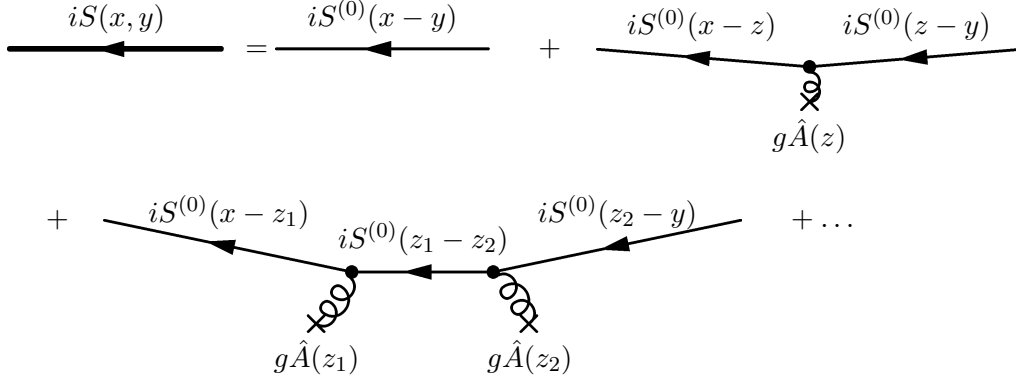


**Figure 2.4.1:** Perturbative quark propagator in a weak gluonic background field. The gluons are supposed to emerge from the ground state.

The expansion is depicted in fig. 2.4.1. If we think about the gluons emerging from the ground state, the fields can be understood as operators acting on the Fock space and creating an additional gluon. Thus we use a classical expansion for the quark propagator, but also bring into account creation or annihilation of gluons from the ground state.

The Fourier transformed free propagator reads

$$S^{(0)}(p) = \int d^4x e^{ipx} S^{(0)}(x) = \frac{\hat{p} + m}{p^2 - m^2}. \quad (2.4.15)$$

Using (2.4.14) one can show that (2.4.13) satisfies

$$(i\hat{\partial}_x + g\hat{A}(x) - m)S(x, y) = \delta^{(4)}(x - y), \quad (2.4.16)$$

telling that  $S(x)$  is indeed the propagator of a quark in a weak gluonic background field. In order to ensure the gauge condition (2.4.1), one has to permit shifts in space-time. Hence, one is not allowed to perform the transformation  $x \rightarrow x' = x - y$ . This means that, as a result of the gauge, the propagator does not only depend on the differences of the coordinates, i.e.  $x - y$ . Thus,  $S(x, y)$  and  $S(x - y, 0)$  are different quantities. Let us introduce the Fourier transformed expressions

$$S(p) = \int d^4x e^{ipx} S(x, 0), \quad (2.4.17)$$

$$\tilde{S}(p) = \int d^4x e^{-ipx} S(0, x), \quad (2.4.18)$$

$$A_\mu(p) = \int d^4x e^{ipx} A_\mu(x), \quad (2.4.19)$$

where we also introduce the quantity  $\tilde{S}(p)$  in order to ensure the gauge condition. We first calculate the Fourier transform of  $A_\mu(x)$  giving

$$A_\mu(p) = \sum_{n=0}^{\infty} (-i)^{n+1} \frac{(2\pi)^4}{n!(n+2)} \left( \vec{D}_{\alpha_1} \dots \vec{D}_{\alpha_n} \mathcal{G}_{\rho\mu}(0) \right) \left( \partial^\rho \partial^{\alpha_1} \dots \partial^{\alpha_n} \delta^{(4)}(p) \right), \quad (2.4.20)$$

where  $\partial$  denotes a derivative with respect to the momentum. The transformed expression of (2.4.13) then reads

$$S(p) = S^{(0)}(p) + \sum_{n=1}^{\infty} (-g)^n S^{(0)}(p) \times \int \frac{d^4 k_1}{(2\pi)^4} \dots \frac{d^4 k_n}{(2\pi)^4} \hat{A}(p - k_1) S^{(0)}(k_1) \hat{A}(k_1 - k_2) \dots S^{(0)}(k_n). \quad (2.4.21)$$

By partial integration we now observe for an arbitrary function  $f(k)$

$$\int \frac{d^4 k}{(2\pi)^4} g \hat{A}(p - k) f(k) = (\gamma \tilde{A}) f(p), \quad (2.4.22)$$

where we have defined

$$\tilde{A}_\mu = \sum_{n=0}^{\infty} \tilde{A}_\mu^{(n)} \quad (2.4.23)$$

with

$$\begin{aligned} \tilde{A}_\mu^{(0)} &= i \frac{g}{2} \mathcal{G}_{\mu\nu} \partial^\nu, \\ \tilde{A}_\mu^{(n)} &= - \frac{(-i)^{n+1} g}{n!(n+2)} (D_{\alpha_1} \dots D_{\alpha_n} \mathcal{G}_{\mu\nu}(0)) \partial^\nu \partial^{\alpha_1} \dots \partial^{\alpha_n} \end{aligned} \quad (2.4.24)$$

which is now a derivative operator. This enables us to give a more comfortable expression for the perturbative quark propagator. Successive partial integration of the momentum integrals in (2.4.21) and using (2.4.22) yield

$$S(p) = \sum_{n=0}^{\infty} S^{(n)}(p) \quad (2.4.25)$$

with

$$\begin{aligned} S^{(n)}(p) &= (-1)^n S^{(n-1)}(p) (\gamma \tilde{A}) S^{(0)}(p) \\ &= (-1)^n S^{(0)}(p) (\gamma \tilde{A}) S^{(n-1)}(p) \\ &= (-1)^n S^{(0)}(p) \underbrace{(\gamma \tilde{A}) S^{(0)}(p) \times \dots \times S^{(0)}(p)}_n (\gamma \tilde{A}) S^{(0)}(p). \end{aligned} \quad (2.4.26)$$

Here the derivatives contained in  $(\gamma \tilde{A})$  act on all functions to the right of them. Moreover, performing the same steps for  $\tilde{S}(p)$ , one can show that  $S(p) = \tilde{S}(p)$ . Although (2.4.13) is not translational invariant, the Fourier transform of  $S(x, 0)$  and  $S(0, x)$  are identical. The corresponding expression for  $\tilde{S}(p)$  in terms of  $\tilde{A}_\mu$  reads

$$\tilde{S}(p) = S^{(0)}(p) + \sum_{n=1}^{\infty} (-1)^n S^{(0)}(p) \underbrace{\left( \gamma \overleftarrow{\tilde{A}} \right) S^{(0)}(p) \times \dots \times S^{(0)}(p) \left( \gamma \overleftarrow{\tilde{A}} \right)}_n S^{(0)}(p) \quad (2.4.27)$$

which is equal to (2.4.25). Using a very useful formula for further calculations

$$\frac{\partial}{\partial p_\rho} S^{(0)}(p) = -S^{(0)}(p) \gamma^\rho S^{(0)}(p), \quad (2.4.28)$$

which can be confirmed by a direct calculation, we write out the first terms of (2.4.26) in lowest order of the gluon field  $\tilde{A}_\mu$

$$S^{(0)}(p) = \frac{\hat{p} + m}{p^2 - m^2}, \quad (2.4.29)$$

$$S^{(1)}(p) = i \frac{g}{2} \mathcal{G}_{\mu\nu}(0) S^{(0)}(p) \gamma^\mu S^{(0)}(p) \gamma^\nu S^{(0)}(p), \quad (2.4.30)$$

$$S^{(2)}(p) = \left(i \frac{g}{2}\right)^2 \mathcal{G}_{\mu\nu}(0) \mathcal{G}_{\kappa\lambda}(0) T^{\mu\nu\kappa\lambda}(p), \quad (2.4.31)$$

where we have defined

$$\begin{aligned} T^{\mu\nu\kappa\lambda}(p) := & S^{(0)}(p) \gamma^\mu S^{(0)}(p) \gamma^\nu S^{(0)}(p) \gamma^\kappa S^{(0)}(p) \gamma^\lambda S^{(0)}(p) \\ & + S^{(0)}(p) \gamma^\mu S^{(0)}(p) \gamma^\kappa S^{(0)}(p) \gamma^\nu S^{(0)}(p) \gamma^\lambda S^{(0)}(p) \\ & + S^{(0)}(p) \gamma^\mu S^{(0)}(p) \gamma^\kappa S^{(0)}(p) \gamma^\lambda S^{(0)}(p) \gamma^\nu S^{(0)}(p). \end{aligned} \quad (2.4.32)$$

The operator product expansion of the current-current correlator is then obtained by applying Wick's theorem to the operator product  $j(x)j^\dagger(0)$  in terms of quark fields. While pure quark condensates directly enter in virtue of Wick's theorem, gluonic operators and gluonic condensates enter via quark-gluon interactions of the current-quarks with the background field. On the one hand side the perturbative expansion of the quark propagator contributes, on the other side, the covariant expansion of the quark fields (2.4.12) together with the field equations (A.28) of chromodynamics contribute.

If we restrict ourselves to small distances in (2.1.1), a restriction to large momenta is required. Nevertheless, unlike the expectation that perturbative methods are adequate in this energy regime, especially for the example of D mesons, non-perturbative effects will prohibit us from a pure perturbative treatment even in the high energy regime. Details about this effect and about calculating the operator product expansion by applying the background field method can be found in chapter 3 for the example of the D meson.

## 2.5 Sum Rules

Now we have collected all the necessary tools and are able to set up the sum rules. Therefore, we return to the dispersion relations in vacuum (2.2.25) and in medium (2.2.33), (2.2.34). We now suggest that the current-current correlator  $\Pi(q)$  for large space-like momenta  $q^2 = -Q^2 \ll 0$  is determined by its quark structure, represented via the operator product expansion, i.e.  $\Pi(q) = \Pi_{OPE}(q)$  for  $q^2 \rightarrow -\infty$ . While it is determined by hadronic properties, i.e. the excitation spectrum  $\Delta\Pi_{ph}(q)$  (here the subscript 'ph' exposes the phenomenological character), encoded by the Lehmann representation of the ground state matrix element of the two composite field operators  $j(x)$  and  $j^\dagger(0)$ . Hence, we have

to split up the integrals into a low-momentum and a large-momentum contribution. For the vacuum case the sum rules read

$$\begin{aligned} \Pi_{OPE}(q^2) - \sum_{n=0}^{N-1} \frac{\Pi_{ph}^{(n)}(0)}{n!} (q^2)^n \\ = \frac{1}{\pi} \int_0^{s_0} \left( \frac{q^2}{s} \right)^N \frac{\Delta \Pi_{ph}(s)}{s - q^2} ds + \frac{1}{\pi} \int_{s_0}^{+\infty} \left( \frac{q^2}{s} \right)^N \frac{\Delta \Pi_{OPE}(s)}{s - q^2} ds, \end{aligned} \quad (2.5.1)$$

where we introduced the threshold parameter  $s_0$ .<sup>9</sup> Similar, for the in-medium case the sum rules for the even part read

$$\begin{aligned} \Pi_{OPE}^e(q_0^2, \vec{q}) - \frac{1}{2} \sum_{n=0}^{N-1} \frac{\Pi_{ph}^{(n)}(0, \vec{q})}{n!} (q_0)^n (1 + (-1)^n) \\ = \frac{1}{2\pi} \int_{s_0^-}^{s_0^+} ds \Delta \Pi_{ph}(s, \vec{q}) \frac{q_0^N}{s^{N-1}} \frac{(1 + (-1)^N) + \frac{q_0}{s} (1 - (-1)^N)}{s^2 - q_0^2} \\ + \frac{1}{2\pi} \left( \int_{-\infty}^{s_0^-} + \int_{s_0^+}^{+\infty} \right) ds \Delta \Pi_{OPE}(s, \vec{q}) \frac{q_0^N}{s^{N-1}} \frac{(1 + (-1)^N) + \frac{q_0}{s} (1 - (-1)^N)}{s^2 - q_0^2}, \end{aligned} \quad (2.5.2)$$

and for the odd part

$$\begin{aligned} \Pi_{OPE}^o(q_0^2, \vec{q}) - \frac{1}{2q_0} \sum_{n=0}^{N-1} \frac{\Pi_{ph}^{(n)}(0, \vec{q})}{n!} (q_0)^n (1 - (-1)^n) \\ = \frac{1}{2\pi q_0} \int_{s_0^-}^{s_0^+} ds \Delta \Pi_{ph}(s, \vec{q}) \frac{q_0^N}{s^{N-1}} \frac{(1 - (-1)^N) + \frac{q_0}{s} (1 + (-1)^N)}{s^2 - q_0^2} \\ + \frac{1}{2\pi q_0} \left( \int_{-\infty}^{s_0^-} + \int_{s_0^+}^{+\infty} \right) ds \Delta \Pi_{OPE}(s, \vec{q}) \frac{q_0^N}{s^{N-1}} \frac{(1 - (-1)^N) + \frac{q_0}{s} (1 + (-1)^N)}{s^2 - q_0^2}. \end{aligned} \quad (2.5.3)$$

If the full hadronic spectrum would be known, it would not be necessary to split up the integrals. Usually, the threshold parameters  $s_0^\pm$  are chosen to cover the lowest-lying hadronic excitation, while higher momentum contributions are collected at the OPE side. This recipe, also called semi-local quark hadron duality, is by no means obvious, but rather relies upon its success in many applications.

## 2.6 Borel Transformed Sum Rules

In section 2.3 we mentioned that convergence of the operator product expansion is not ensured. Instead it diverges and can only be considered as an asymptotic expansion. The infinite sum approximates the current-current correlation function for  $x \approx 0$  if it

---

<sup>9</sup>The quantity  $s_0$  differs from the threshold parameter introduced in section 2.2 to characterize the regions of analyticity.

is truncated at a certain mass dimension, only taking into account a finite number of operators.

One way to deal with asymptotic series is to consider the Borel transformed sum. The Borel transform of a function  $f(Q^2)$  is defined as [Fu92]

$$\mathcal{B}[f](M^2) := \lim_{\substack{n \rightarrow \infty \\ Q^2 = nM^2}} \frac{(Q^2)^{n+1}}{n!} \left( -\frac{d}{dQ^2} \right)^n f(Q^2), \quad (2.6.1)$$

with  $Q^2 \geq 0$ . Sometimes [Na04] a slightly different definition is used

$$\mathcal{B}[f](M^2)' := \lim_{\substack{n \rightarrow \infty \\ Q^2 = nM^2}} \frac{(Q^2)^{n+1}}{n!} \left( -\frac{d}{dQ^2} \right)^{n+1} f(Q^2), \quad (2.6.2)$$

and the connection between both is given by

$$\mathcal{B}[f](M^2) = M^2 \mathcal{B}[f](M^2)'. \quad (2.6.3)$$

In order to spell out the Borel transformed sum rules, we have to give the transformed expressions for typical functions which appear in the OPE. For simple functions  $f$ , e.g.  $f(Q^2) = (Q^2)^n \ln Q^2$  or  $f(Q^2) = 1/(Q^2 + m^2)^n$ , the transformed expressions can be calculated directly from (2.6.1) by using general rules for the  $n$ th derivative, e.g. the Leibniz rule

$$\left( \frac{d}{dx} \right)^n (uv) = \sum_{m=0}^n \binom{n}{m} \left( \frac{d^m}{dx^m} u \right) \left( \frac{d^{n-m}}{dx^{n-m}} v \right). \quad (2.6.4)$$

As can be seen from (2.6.1) all functions which are merely finite polynomials in  $Q^2$  vanish under Borel transformation. For more complex functions, direct calculations are rather difficult. Instead, one can use the connection between the Borel transformation and the Laplace transformation [Wi46], which is an integral transformation. The Laplace transform of a function  $g(t)$  is defined as [Br01]

$$\mathcal{L}[g](s) := \int_0^\infty e^{-st} g(t) dt. \quad (2.6.5)$$

Here  $g(t)$  is assumed to be piecewise smooth for  $t \geq 0$  and to be bounded by  $e^{\alpha t}$  for  $t \rightarrow \infty$ ;  $g(t) \leq e^{\alpha t}$  for some  $\alpha > 0$ . The integral converges for  $\text{Re } s > \alpha$  and is an analytic function in  $s$  in that area.

Now, the beneficial point is that an inverse operation to the Laplace transformation is given by (see chapter VII.6 in [Wi46])<sup>10</sup>

$$g(t) = \lim_{n \rightarrow \infty} \frac{1}{n!} \binom{n}{t}^{n+1} \left[ -\mathcal{L}[g] \left( \frac{n}{t} \right) \right]^{(n)}, \quad (2.6.6)$$

<sup>10</sup>Another representation of the inversion of the Laplace transform is given by the Bromwich integral  $g(t) = \frac{1}{2\pi i} \int_{c-i\infty}^{c+i\infty} e^{pt} \mathcal{L}[g](p) dp$  for  $t > 0$ .

where  $[\dots]^{(n)}$  denotes the  $n$ th derivative. Setting  $t = 1/M^2$  and  $n/t = nM^2 = Q^2$  one obtains

$$g\left(\frac{1}{M^2}\right) = \lim_{\substack{n \rightarrow \infty \\ Q^2 = nM^2}} \frac{(Q^2)^{n+1}}{n!} \left(-\frac{d}{dQ^2}\right)^n \mathcal{L}[g](Q^2). \quad (2.6.7)$$

Comparison with (2.6.1) shows that the Borel transform obeys

$$\mathcal{B}[f](M^2) = g(1/M^2), \quad (2.6.8)$$

if the function  $f$  is the Laplace transform of  $g$  [Ra81]. This enables us to give the Borel transformed expressions for a broad range of functions if we are able to identify them as the Laplace transform of other known functions. Moreover, we can now safely use well known properties of the Laplace transformation to simplify many calculations, e.g. the momentum shift

$$f(s-a) \xrightarrow{\mathcal{L}^{-1}} e^{at}g(t), \quad (2.6.9)$$

giving for the Borel transformation

$$\mathcal{B}[f(Q^2 + m^2)](M^2) = e^{-m^2/M^2} \mathcal{B}[f(Q^2)](M^2). \quad (2.6.10)$$

Although, by the above criteria, the Borel transformation can be performed for a broad range of functions, we will merely need the transform of one type of functions during this work, namely

$$f(s) = \frac{1}{s^{\alpha+1}} \frac{1}{(\ln s)^{\beta+1}}. \quad (2.6.11)$$

If  $\text{Re } \alpha > -1$  and  $\text{Re } s > 1$ , then  $f(s)$  is the Laplace transform of the transcendental function  $\mu(t, \beta, \alpha)$  [Er55b]

$$\int_0^\infty e^{-st} \mu(t, \beta, \alpha) dt = \frac{1}{s^{\alpha+1}} \frac{1}{(\ln s)^{\beta+1}}, \quad (2.6.12)$$

where  $\mu(t, \beta, \alpha)$  is defined by the following integral representation

$$\mu(x, \beta, \alpha) = \int_0^\infty \frac{x^{\alpha+1} t^\beta dt}{\Gamma(\beta+1) \Gamma(\alpha+t+1)}. \quad (2.6.13)$$

By repeated partial integration one can bring this into a form that is more convenient for further calculations:

$$\mu(x, -n, \alpha) = (-1)^{n-1} \left(\frac{d}{du}\right)^{n-1} \frac{x^{\alpha+u}}{\Gamma(\alpha+u+1)} \Big|_{u=0} \quad (2.6.14)$$

with  $n = 1, 2, \dots$ . In particular we get

$$\mu(x, -1, \alpha) = \frac{x^\alpha}{\Gamma(\alpha+1)}, \quad (2.6.15)$$

$$\mu(x, -2, \alpha) = \frac{x^\alpha}{\Gamma(\alpha+1)} \left[ -\ln x + \frac{\Gamma'(\alpha+1)}{\Gamma(\alpha+1)} \right] \quad (2.6.16)$$



with

$$\Gamma'(n) = -(n-1)! \left[ \frac{1}{n} + \gamma_E - \sum_{k=1}^n \frac{1}{k} \right] \quad (2.6.17)$$

and  $\gamma_E$  being the Euler constant

$$\gamma_E = \lim_{n \rightarrow \infty} \left( \sum_{k=1}^n \frac{1}{k} - \ln n \right). \quad (2.6.18)$$

From (2.6.12) we are now able to represent the Borel transform of (2.6.11) without performing too many elaborate calculations by means of the initial definition of the Borel transformation (2.6.1)

$$\mathcal{B} \left[ \frac{1}{(Q^2)^{\alpha+1}} \frac{1}{(\ln Q^2)^{\beta+1}} \right] (M^2) = \mu \left( \frac{1}{M^2}, \beta, \alpha \right). \quad (2.6.19)$$

In particular, for  $\beta = -1$  and  $\alpha = n-1$  the result reads

$$\mathcal{B} \left[ \frac{1}{(Q^2)^n} \right] (M^2) = \mu \left( \frac{1}{M^2}, -1, n-1 \right) = \frac{1}{(n-1)!} \frac{1}{(M^2)^{n-1}}, \quad (2.6.20)$$

and for  $\beta = -2$  and  $\alpha = n-1$  we get

$$\begin{aligned} \mathcal{B} \left[ \frac{1}{(Q^2)^n} \ln Q^2 \right] (M^2) &= \mu \left( \frac{1}{M^2}, -2, n-1 \right) \\ &= \frac{1}{(n-1)!} \frac{1}{(M^2)^{n-1}} \left[ \ln M^2 - \frac{1}{n} - \gamma_E + \sum_{k=1}^n \frac{1}{k} \right]. \end{aligned} \quad (2.6.21)$$

Let us now apply the Borel transformation to the subtracted dispersion relations (2.2.25), as well as (2.2.33) and (2.2.34). As the operator product expansion is only valid for large space like momenta, i.e.  $q^2 \ll 0$ , we can substitute  $q^2 = -Q^2$ . Furthermore the limiting procedure in the definition of the Borel transformation is not in conflict with the operator product expansion. For the dispersion relation in vacuum we get

$$\begin{aligned} \Pi_{OPE}(Q^2) - \sum_{n=0}^{N-1} \frac{\Pi_{ph}^{(n)}(0)}{n!} (-Q^2)^n \\ = \frac{1}{\pi} \int_0^{s_0} \left( -\frac{Q^2}{s} \right)^N \frac{\Delta \Pi_{ph}(s)}{s+Q^2} ds + \frac{1}{\pi} \int_{s_0}^{+\infty} \left( -\frac{Q^2}{s} \right)^N \frac{\Delta \Pi_{OPE}(s)}{s+Q^2} ds. \end{aligned} \quad (2.6.22)$$

For the in-medium dispersion relations we introduce  $q_0^2 = -\omega^2$ . This is equivalent to the

consideration of imaginary values for the energy  $q_0$ . For the even part one obtains

$$\begin{aligned} \Pi_{OPE}^e(\omega^2, \vec{q}) &= \frac{1}{2} \sum_{n=0}^{N-1} \frac{\Pi_{ph}^{(n)}(0, \vec{q})}{n!} (\omega^2)^{n/2} (1 + (-1)^n) \\ &= \left[ \frac{1}{\pi} \int_{s_0^-}^{s_0^+} ds \frac{\Delta \Pi_{ph}(s, \vec{q})}{s^2 + \omega^2} + \frac{1}{\pi} \left( \int_{-\infty}^{s_0^-} + \int_{s_0^+}^{+\infty} \right) ds \frac{\Delta \Pi_{OPE}(s, \vec{q})}{s^2 + \omega^2} \right] \\ &\times \frac{1}{2} \left( \frac{(-\omega^2)^{N/2}}{s^{N-1}} (1 + (-1)^N) + \frac{(-\omega^2)^{(N+1)/2}}{s^N} (1 - (-1)^N) \right), \end{aligned} \quad (2.6.23)$$

and for the odd part

$$\begin{aligned} \Pi_{OPE}^o(\omega^2, \vec{q}) &= \frac{1}{2} \sum_{n=0}^{N-1} \frac{\Pi_{ph}^{(n)}(0, \vec{q})}{n!} (\omega^2)^{(n-1)/2} (1 - (-1)^n) \\ &= \left[ \frac{1}{\pi} \int_{s_0^-}^{s_0^+} ds \frac{\Delta \Pi_{ph}(s, \vec{q})}{s^2 + \omega^2} + \frac{1}{\pi} \left( \int_{-\infty}^{s_0^-} + \int_{s_0^+}^{+\infty} \right) ds \frac{\Delta \Pi_{OPE}(s, \vec{q})}{s^2 + \omega^2} \right] \\ &\times \frac{1}{2} \left( \frac{(-\omega^2)^{(N-1)/2}}{s^{N-1}} (1 - (-1)^N) + \frac{(-\omega^2)^{N/2}}{s^N} (1 + (-1)^N) \right). \end{aligned} \quad (2.6.24)$$

Application of the Borel transformation (2.6.1) to the vacuum dispersion relation (2.6.22) yields

$$\begin{aligned} \mathcal{B} \left[ \left( -\frac{Q^2}{s} \right)^N \frac{1}{s + Q^2} \right] (M^2) &= \frac{e^{-s/M^2}}{(-s)^N} \mathcal{B} \left[ \frac{(Q^2 - s)^N}{Q^2} \right] (M^2) \\ &= \frac{e^{-s/M^2}}{(-s)^N} \mathcal{B} \left[ \frac{(-s)^N}{Q^2} \right] (M^2) = e^{-s/M^2}, \end{aligned} \quad (2.6.25)$$

where we have used that only the term  $\propto 1/Q^2$  survives the Borel transformation. Hence, one finally ends up with

$$\begin{aligned} \mathcal{B} [\Pi_{OPE}(Q^2)] (M^2) &= \frac{1}{\pi} \int_0^{s_0} e^{-s/M^2} \Delta \Pi_{ph}(s) ds + \frac{1}{\pi} \int_{s_0}^{+\infty} e^{-s/M^2} \Delta \Pi_{OPE}(s) ds. \end{aligned} \quad (2.6.26)$$

In the same way, we obtain for the in medium dispersion relation (2.6.23) by applying the Borel transformation (2.6.1) with respect to  $\omega^2$

$$\begin{aligned} \mathcal{B} \left[ \frac{(-\omega^2)^{N/2}}{s^{N-1}} \frac{1}{s^2 + \omega^2} \right] (M^2) &= (-1)^{N/2} \frac{e^{-s^2/M^2}}{s^{N-1}} \mathcal{B} \left[ \frac{(\omega^2 - s^2)^{N/2}}{\omega^2} \right] (M^2) \\ &= (-1)^{N/2} \frac{e^{-s^2/M^2}}{s^{N-1}} \mathcal{B} \left[ \frac{(-s^2)^{N/2}}{\omega^2} \right] (M^2) = (-1)^N s e^{-s^2/M^2}, \end{aligned} \quad (2.6.27)$$

where we have used that, due to the factor  $(1 + (-1)^N)$  in the first term of the last line in (2.6.23),  $N/2$  can only have integer values. The same holds true for  $(N + 1)/2$  in the second term. Thus, we arrive at

$$\begin{aligned} & \mathcal{B} [\Pi_{OPE}^e(\omega^2, \vec{q})] (M^2) \\ &= \left[ \frac{1}{\pi} \int_{s_0^-}^{s_0^+} ds \Delta\Pi_{ph}(s, \vec{q}) + \frac{1}{\pi} \left( \int_{-\infty}^{s_0^-} + \int_{s_0^+}^{+\infty} \right) ds \Delta\Pi_{OPE}(s, \vec{q}) \right] s e^{-s^2/M^2}. \end{aligned} \quad (2.6.28)$$

For the odd part we use (2.6.25) and obtain

$$\begin{aligned} & \mathcal{B} [\Pi_{OPE}^o(\omega^2, \vec{q})] (M^2) \\ &= \left[ \frac{1}{\pi} \int_{s_0^-}^{s_0^+} ds \Delta\Pi_{ph}(s, \vec{q}) + \frac{1}{\pi} \left( \int_{-\infty}^{s_0^-} + \int_{s_0^+}^{+\infty} \right) ds \Delta\Pi_{OPE}(s, \vec{q}) \right] e^{-s^2/M^2}. \end{aligned} \quad (2.6.29)$$

As a byproduct we see that the subtraction terms vanish under Borel transformation, as they are polynomials in  $Q^2$ .

In section 2.2 we reviewed the method of subtracted dispersion relations. They enable us to suppress polynomial contributions to the dispersion relations from the integral over the infinite circle and ensure the convergence of the dispersion integral. From the definition of the Borel transformation we see that all functions that are merely polynomials in  $Q^2$  vanish. Hence, by applying (2.6.1) to the dispersion relations (2.2.27) or (2.2.17) one gets rid of the polynomial contribution from the outer circle integral. Thus, we do not need to consider subtracted dispersion relations and could have started from the non-subtracted dispersion relation. The result, however, is the same. The divergence of the operator product expansion makes it necessary to introduce the Borel transformation.

We note the occurrence of the exponential weighting function in the Borel transformed sum rules (2.6.26), (2.6.28) and (2.6.29). This weighting function gives a possible physical interpretation of the transformation. It emphasizes the contribution of the lowest lying hadronic excitations in contrast to the exponential suppression of higher energy contributions.



## 3 Sum Rules for D Mesons

We are now well equipped to approach the sum rules for D mesons. Therefore we will briefly summarize the main properties of D mesons that are necessary to formulate the sum rules. Then we will calculate the operator product expansion up to next-to-leading order in  $\alpha_s$  and mass dimension 5. Afterward we will set up the sum rule.

### 3.1 D Mesons

Mesons are bosonic hadrons consisting of an even number of valence quarks. Systems with one constituent being a charm quark and the other being one of the light quark flavors "up" or "down" are called D mesons. The lowest lying excitations are  $D^\pm$ ,  $D^0$  and  $\bar{D}^0$ . They are pseudoscalar particles having negative parity, and they belong to the isotopic doublet having isospin 1/2. Their spin is  $J = 0$ . Thus, their quark constituents point to the following interpolating currents

$$j_{D^+}(x) = i\bar{d}\gamma_5 c, \quad (3.1.1)$$

$$j_{D^-}(x) = i\bar{c}\gamma_5 d, \quad (3.1.2)$$

$$j_{D^0}(x) = i\bar{u}\gamma_5 c, \quad (3.1.3)$$

$$j_{\bar{D}^0}(x) = i\bar{c}\gamma_5 u, \quad (3.1.4)$$

where the quark field operators in Heisenberg picture are denoted by  $u, d, c$ . From the definitions the currents fulfill

$$(j_{D^+}(x))^\dagger = j_{D^-}(x), \quad (3.1.5a)$$

$$(j_{D^0}(x))^\dagger = j_{\bar{D}^0}(x). \quad (3.1.5b)$$

The current-current correlation functions are defined as (2.1.1). Using the translation properties of Heisenberg operators (2.2.4), we obtain the following connection between the current-current correlators

$$\Pi_{D^+}(-q) = \Pi_{D^-}(q), \quad (3.1.6)$$

$$\Pi_{D^0}(-q) = \Pi_{\bar{D}^0}(q). \quad (3.1.7)$$

Of course, the current-current correlation function for  $D^0$  can be obtained from  $D^+$  by the replacement  $d \rightarrow u$ .

## 3.2 Operator Product Expansion for the D Meson

The OPE of the product of two nonlocal composite field operators is an expansion at operator level which can be proven for small distances, i.e. in the perturbative region (see discussion in subsection 2.3). This means that the Wilson coefficients are independent of the states we use to calculate scalar products. Moreover, if we restrict the momentum  $q$  to large space like values  $q^2 < 0$  we can use perturbative techniques to calculate Wilson coefficients. Wick's theorem is such a technique and enables us to evaluate time ordered products in terms of normal ordered products and Wick contracted operators:

$$T[A \dots Z] = :A \dots Z: + : \underbrace{AB} \dots Z : + \dots + : \underbrace{AB} \dots \underbrace{YZ} :, \quad (3.2.1)$$

whereas a contraction ' $\underbrace{\phantom{AB}}$ ' is defined as

$$\underbrace{AB} := \langle 0 | T[AB] | 0 \rangle \quad (3.2.2)$$

and normal ordering ' $: \dots :$ ' means that all annihilation operators are brought to the right of the operator product. At this point it is important to note that normal ordering only refers to the perturbative field operators. In order to expand a field operator in creation and annihilation operators it is necessary to give a unique and covariant Fourier decomposition of the field operators into positive and negative frequency parts. This is always possible for free field operators. It is also possible for field operators calculated in perturbation theory, because these operators are merely expanded in terms of free field operators. But, generally speaking, it is not possible to decompose an interacting field operator into positive and negative frequencies in a covariant way.<sup>1</sup> In other words, normal ordering refers accordingly to perturbation theory [Ro69]. In this sense Wick's theorem is a perturbative tool. The perturbative ground state  $|0\rangle$  is defined to satisfy

$$a|0\rangle = 0 \quad (3.2.3)$$

being an important assumption in the derivation of Wick's theorem. One cannot use the physical ground state  $|\Omega\rangle$  instead (cf. (2.1.2)).

We now apply Wick's theorem to the correlation function  $\Pi_{D^+}(q)$  of the two currents  $j(x), j^\dagger(0)$  and thereby introduce normal ordered products and Wick contracted terms, whereas the normal ordered terms do not vanish due to (2.1.2):

$$\begin{aligned} \Pi_{D^+}(q) &= i \int d^4x e^{iqx} \langle \Omega | T [i\bar{d}(x)\gamma_5 c(x) i\bar{c}(0)\gamma_5 d(0)] | \Omega \rangle \\ &= -i \int d^4x e^{iqx} \gamma_{5,ij} \gamma_{5,kl} \langle \Omega | : \bar{d}_i(x) d_l(0) c_j(x) \bar{c}_k(0) : + : \bar{d}_i(x) \underbrace{c_j(x) \bar{c}_k(0)} : d_l(0) : \\ &\quad + : \underbrace{\bar{d}_i(x) c_j(x) \bar{c}_k(0)} d_l(0) : + : \underbrace{\bar{d}_i(x) d_l(0) c_j(x) \bar{c}_k(0)} : | \Omega \rangle \\ &= -i \int d^4x e^{iqx} \langle \Omega | : \text{Tr}_{C,D} [\gamma_5 S_d(0, x) \gamma_5 S_c(x, 0)] : + i : \bar{d}(x) \gamma_5 S_c(x, 0) \gamma_5 d(0) : \\ &\quad + i : \bar{c}(0) \gamma_5 S_d(0, x) \gamma_5 c(x) : + : \bar{d}(x) \gamma_5 c(x) \bar{c}(0) \gamma_5 c(0) : | \Omega \rangle, \end{aligned} \quad (3.2.4)$$

<sup>1</sup>For interaction picture field operators it is always possible to define a covariant Fourier decomposition, because they fulfill the free equations of motion.

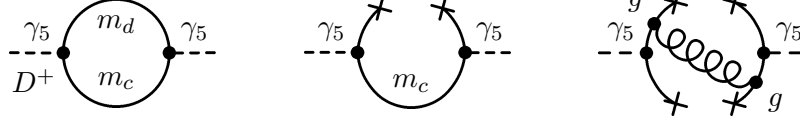


**Figure 3.2.1:** Contributions  $\Pi^{(0)}$ ,  $\Pi^{(2)}$  and  $\Pi^{(4)}$  (from left to the right) to the OPE for the D meson. Dashed lines depict the D meson, continuous lines represent heavy or light quarks, curly lines represent gluons, and the crosses symbolize the creation or annihilation of a quark by virtual particles.  $\gamma_5$  exposes the pseudoscalar character of the particle. All lines represent perturbative propagators.

where the trace  $\text{Tr}_{\text{C,D}}$  refers to color and Dirac indices. In the last step we have used

$$iS_{ij}(x, y) = \langle 0 | T [q_i(x) \bar{q}_j(y)] | 0 \rangle = \underbrace{q_i(x) \bar{q}_j(y)} . \quad (3.2.5)$$

Again, we have to emphasize the usage of the vacuum state  $|0\rangle$  which leads to the perturbative propagator, describing the propagation of a quark in a weak gluonic background field.

Let us introduce the following notation

$$\Pi_{D^+}(q) = \Pi^{(0)}(q) + \Pi^{(2)}(q) + \Pi^{(4)}(q) , \quad (3.2.6)$$

$$\Pi^{(0)}(q) = -i \int d^4x e^{iqx} \langle \Omega | : \text{Tr}_{\text{C,D}} [\gamma_5 S_d(0, x) \gamma_5 S_c(x, 0)] : | \Omega \rangle , \quad (3.2.7)$$

$$\Pi^{(2)}(q) = \int d^4x e^{iqx} \langle \Omega | : \bar{d}(x) \gamma_5 S_c(x, 0) \gamma_5 d(0) : + : \bar{c}(0) \gamma_5 S_d(0, x) \gamma_5 c(x) : | \Omega \rangle , \quad (3.2.8)$$

$$\Pi^{(4)}(q) = -i \int d^4x e^{iqx} \langle \Omega | : \bar{d}(x) \gamma_5 c(x) \bar{c}(0) \gamma_5 c(0) : | \Omega \rangle , \quad (3.2.9)$$

where the labels (0), (2) and (4) denote the numbers of non-contracted quark fields or, more illustratively, the number of quarks which participate in the formation of a condensate. These contributions are depicted graphically in fig. 3.2.1.

Each diagram can give a contribution to the Wilson coefficients belonging to operator products, where the number of quark field operators is equal to or larger than the number of quarks which couple to condensates. In the language of mass dimensions, this means that each diagram of fig. 3.2.1 can contribute to condensates with mass dimension  $\geq n$ , where  $n$  is the number of non-contracted quark fields.

The left diagram for  $\Pi^{(0)}$ , in principle, could give contributions to all Wilson coefficients. It is the diagrammatic description of two quarks propagating in a weak gluonic background field. The respective quark propagators can be calculated in perturbation theory using the Fock-Schwinger gauge. Beside the purely perturbative result it also gives contributions to other Wilson coefficients, e.g. gluonic operators like  $G^2$ ,  $G^3$  or higher powers in the gluon field strength.

The middle diagram for  $\Pi^{(2)}$  belongs to condensates containing at least two quark field operators. It can be read as one quark propagating in a background field and the other one propagating, being annihilated by a virtual quark and, therefore, creating another real quark propagating somewhere else (the other virtual quark becomes real). This diagram not only gives contributions to two-quark condensates but also to condensates containing gluon operators or with more quark field operators, e.g. the four-quark condensates.

The right diagram for  $\Pi^{(4)}$  is dedicated to condensates containing at least four quark field operators. It contributes only in first-order perturbation theory, as indicated by the exchange of one gluon. Otherwise this diagram would not be connected and no momentum could flow. This is why this gluon is a so-called hard one, meaning that it carries high momentum. Hence, this diagram can not be evaluated by the weak background field method. Instead, it requires the introduction of condensates at the next-to-leading order perturbative expansion (2.1.4) in  $\alpha_s$ . As mentioned above, it is not the only source of four-quark condensates. However, as four-quark condensates are of mass dimension 6, and their numerical importance is supposed to be small, they will not be considered throughout this work.

We now proceed with the calculation of the contribution of the fully contracted term  $\Pi^{(0)}(q)$ . Inserting the Fourier transformed propagators (2.4.19)

$$\begin{aligned}\Pi^{(0)}(q) &= -i \int d^4x e^{iqx} \langle \Omega | : \text{Tr}_{\text{C,D}} [\gamma_5 S_d(0, x) \gamma_5 S_c(x, 0)] : | \Omega \rangle \\ &= -i \int \frac{d^4p}{(2\pi)^4} \langle : \text{Tr}_{\text{C,D}} [\gamma_5 S_c(p+q) \gamma_5 S_d(p)] : \rangle \\ &= \Pi^{\text{per}}(q) + \Pi^{G^2}(q) + \dots ,\end{aligned}\tag{3.2.10}$$

where we have introduced the notation

$$\Pi^{\text{per}}(q) = -i \int \frac{d^4p}{(2\pi)^4} \langle : \text{Tr}_{\text{C,D}} [\gamma_5 S_c^{(0)}(p) \gamma_5 S_d^{(0)}(p-q)] : \rangle\tag{3.2.11}$$

with  $S^{(0)}$  as the free propagator.  $\Pi^{G^2}(q)$ , to be discussed in section 3.2.2, corresponds to the insertion of higher-order propagators, e.g.  $S^{(1)}$ ,  $S^{(2)}$ , and lowest-order gluon fields. Therefore, it will lead to the gluon condensate. The dots in (3.2.10) stand for higher-order insertions of propagators and/or higher-order insertions of gluon fields, while  $\Pi^{\text{per}}(q)$  follows from the insertion of lowest-order perturbation propagators. It is the Wilson coefficient of the unity operator. This term appears in the OPE as well as in the lowest-order perturbative calculation of the correlation function (2.1.4). We also added the perturbative correction  $\propto \alpha_s$ , being the next-to-leading order term in (2.1.4), which is not included in (3.2.11).<sup>2</sup> The corresponding diagrams are shown in fig. 3.2.2.

Both terms,  $\Pi^{\text{per}}$  and  $\Pi^{G^2}$ , are not well defined in the limit  $m_d \rightarrow 0$  as they are infrared divergent. The occurrence of these divergences at the perturbative level signals some influence of the long-distance behavior at small distances [Sp88]. As (3.2.11) is just

<sup>2</sup>Only weak fields, i.e. soft gluons can be modeled by the background field, while a perturbative expansion also includes hard gluons. They can not be modeled by a weak field.



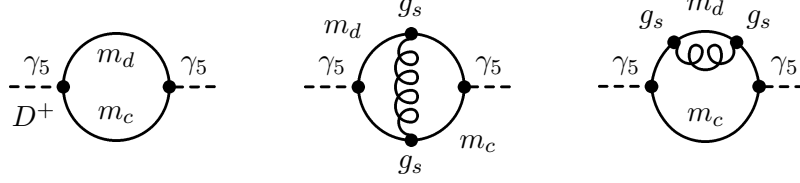


**Figure 3.2.2:** Diagrams regarding to the perturbative calculation of the correlation function  $\Pi_{D^+}$ . In contrast to fig. 3.2.1, solid lines depict the free quark propagator. Curly lines stand for the free gluon propagator. The left diagram is the lowest-order contribution  $\Pi^{(0)}$ . The middle and right ones are higher-order perturbative corrections to  $\Pi^{per}$ .

the Wilson coefficient of the unity operator, it must not be governed by non-perturbative physics. In order to perform a consistent separation of scales, these divergences must be absorbed into the condensates [Tk83]. In section 3.2.4 we will come back to this item again and we will show how this procedure works in vacuum and in medium.

The infrared stable Wilson coefficient for the unity operator can only be obtained within the  $\overline{\text{MS}}$  scheme [Tk83]. It can be obtained from the imaginary part of the correlation function in form of a twice subtracted dispersion relation [Al83]

$$\Pi_{D^+}^{per}(\omega^2) = c_0(\omega^2) = c_0(0) + \omega^2 c'_0 + \frac{\omega^4}{\pi} \int_{m_c^2}^{\infty} ds \frac{\text{Im}\Pi_{D^+}^{per}(s)}{s^2(s - \omega^2)}, \quad (3.2.12)$$

where  $\text{Im}\Pi_{D^+}^{per}(s)$  in first order of  $\alpha_s$  and for  $m_d = 0$  reads

$$\begin{aligned} \text{Im}\Pi_{D^+}^{per}(q^2) &= \frac{3}{8\pi} \frac{(q^2 - m_c^2)^2}{q^2} \left\{ 1 + \frac{4\alpha_s(q^2)}{3\pi} \left[ \frac{9}{4} + 2\text{Li}_2\left(\frac{m_c^2}{q^2}\right) + \ln\left(\frac{q^2}{m_c^2}\right) \ln\left(\frac{q^2}{q^2 - m_c^2}\right) \right. \right. \\ &\quad \left. \left. + \frac{3}{2} \ln\left(\frac{m_c^2}{q^2 - m_c^2}\right) + \ln\left(\frac{q^2}{q^2 - m_c^2}\right) + \frac{m_c^2}{q^2} \ln\left(\frac{q^2 - m_c^2}{m_c^2}\right) + \frac{m_c^2}{q^2 - m_c^2} \ln\left(\frac{q^2}{m_c^2}\right) \right] \right\}. \end{aligned} \quad (3.2.13)$$

Here, the Spence function is defined as  $\text{Li}_2(x) = -\int_0^x t^{-1} \ln(1-t) dt$ . Borel transformation with respect to  $\omega^2$  of (3.2.12) gives the common result

$$\mathcal{B}[c_0(\omega^2)](M^2) = \frac{1}{\pi} \int_{m_c^2}^{\infty} ds e^{-s/M^2} \text{Im}\Pi_{D^+}^{per}(s). \quad (3.2.14)$$

Before we turn to the calculation of the other Wilson coefficients we will give a list of all projections that are essential in the calculation of the OPE.

### 3.2.1 Projections

Condensates are vacuum expectation values of quantum field operators. They reflect basic properties of the QCD ground state. Condensates are assumed to be color singlets, Lorentz

invariants and invariants under parity transformations and time reversal. Therefore, one has to project out color, spinor and Lorentz indices from several structures that appear during our calculations. Vacuum expectation values which are not invariant under parity transformations and time reversal are supposed to vanish. In the following description we adopt the method described in [Ji93].

Up to mass dimension 5 we meet the following structures

$$\begin{aligned} \langle : \bar{q}_i^a q_j^b : \rangle, \quad \langle : (\bar{q}_i D_\mu)^a q_j^b : \rangle, \quad \langle : (\bar{q}_i D_\mu D_\nu)^a q_j^b : \rangle, \\ \langle : G_{\mu\nu}^A G_{\kappa\lambda}^B : \rangle, \quad \langle : \bar{q}_i^a \mathcal{G}_{\mu\nu}^{ab} q_j^b : \rangle. \end{aligned} \quad (3.2.15)$$

The meaning of various indices is explained in appendix A. The last structure is already invariant under color rotations, thus one does not need to take care of color projections for this one. One can expand the remaining other condensates using an orthogonal basis. For  $N_c \times N_c$  dimensional matrices such a set is given by the generators  $t$  of  $SU(N_c)$  (A.6) supplemented by the unity matrix  $\mathbb{1}$  in  $N_c$  dimensions; an appropriate scalar product is given by the trace operation  $(A, B) = \text{Tr}(AB)$ . Using (A.8) the prescription for the expansion in terms of the generators of  $SU(N_c)$  reads as follows

$$\begin{aligned} M_{ab} &= \sum_A c_A t_{ab}^A + c_{\mathbb{1}} \mathbb{1}_{ab}, \\ c_A &= \frac{2}{\text{Tr}_C(t^A t^A)} \text{Tr}_C(t^A M) \quad \text{and} \quad c_{\mathbb{1}} = \frac{1}{N_c} \text{Tr}_C(M). \end{aligned} \quad (3.2.16)$$

In order to retain just color singlets the only non-vanishing expansion coefficient is  $c_{\mathbb{1}}$ . All the other coefficients belong to vacuum expectation values which do not transform as scalars under color transformations.

The projection of spinor indices proceeds in an analog way. A complete set is given by the elements  $O_k$  of the Clifford algebra, i.e.  $O_k \in \{\mathbb{1}, \gamma_\mu, \sigma_{\mu<\nu}, i\gamma_5 \gamma_\mu, \gamma_5\}$ , satisfying  $\text{Tr}_D(O_i O^j) = 4\delta_i^j$ . The expansion reads

$$\langle : \bar{q}_i A_{\mu\nu\dots} q_j : \rangle = \sum_k d_k O_{ji}^k, \quad d_k = \frac{1}{4} \langle : \bar{q} O_k A_{\mu\nu\dots} q : \rangle \quad (3.2.17)$$

resulting in

$$\begin{aligned} \langle : \bar{q}_i A_{\mu\nu\dots} q_j : \rangle &= \frac{1}{4} \left( \langle : \bar{q} A_{\mu\nu\dots} q : \rangle \mathbb{1}_{ji} + \langle : \bar{q} \gamma_\mu A_{\mu\nu\dots} q : \rangle \gamma_{ji}^\mu + \frac{1}{2} \langle : \bar{q} \sigma_{\mu\nu} A_{\mu\nu\dots} q : \rangle \sigma_{ji}^{\mu\nu} \right. \\ &\quad \left. - \langle : \bar{q} \gamma_5 \gamma_\mu A_{\mu\nu\dots} q : \rangle \gamma_5 \gamma_{ji}^\mu + \langle : \bar{q} \gamma_5 A_{\mu\nu\dots} q : \rangle \gamma_{5,ji} \right). \end{aligned} \quad (3.2.18)$$

Together with color projection one gets

$$\begin{aligned} \langle : \bar{q}_i^a A_{\mu\nu\dots} q_j^b : \rangle &= \frac{\delta^{ab}}{12} \left( \langle : \bar{q} A_{\mu\nu\dots} q : \rangle \mathbb{1}_{ji} + \langle : \bar{q} \gamma_\mu A_{\mu\nu\dots} q : \rangle \gamma_{ji}^\mu + \frac{1}{2} \langle : \bar{q} \sigma_{\mu\nu} A_{\mu\nu\dots} q : \rangle \sigma_{ji}^{\mu\nu} \right. \\ &\quad \left. - \langle : \bar{q} \gamma_5 \gamma_\mu A_{\mu\nu\dots} q : \rangle \gamma_5 \gamma_{ji}^\mu + \langle : \bar{q} \gamma_5 A_{\mu\nu\dots} q : \rangle \gamma_{5,ji} \right). \end{aligned} \quad (3.2.19)$$

Here  $A_{\mu\nu\dots}$  stands for an arbitrary operator with Lorentz indices  $\mu\nu\dots$ . [Ji93] states that terms corresponding to the projection onto  $\sigma_{\mu\nu}, \gamma_5\gamma_\mu, \gamma_5$  do not appear due to parity and/or time reversal. This statement can be misunderstood. It is true for  $\gamma_5\gamma_\mu, \gamma_5$ , however not for  $\sigma_{\mu\nu}$ , which does not contribute because there is no independent Lorentz structure that reflects the symmetry properties of  $\sigma_{\mu\nu}$ . In fact, it contributes if the gluon field strength tensor enters the operator product (i.e.  $A_{\mu\nu} = \mathcal{G}_{\mu\nu}$ ).

A striking difference of vacuum and in-medium projections appears when projecting Lorentz indices. It is important to note that this projection is not an expansion in terms of a complete orthogonal set. It strongly depends on the structures available to perform the projection. In vacuum, there are only two independent objects, the metric tensor  $g_{\mu\nu}$  and the total antisymmetric symbol  $\epsilon_{\mu\nu\alpha\beta}$ , being a pseudo-tensor under parity transformations. In medium the condensates also depend on the medium's four-velocity  $v_\mu$  which, therefore, is an additional structure for projections. As a result, also pseudo-vectorial structures can be invariant under parity transformations.

Now we give a list of the in-medium projections up to mass dimension 5. Terms that violate time reversal or parity invariance are omitted. Equations of motion (A.32) enable us to rewrite the condensates in terms of canonical condensates [Gr94].

(i) Condensates of mass dimension 3:

$$\langle : \bar{q}q : \rangle = \langle : \bar{q}q : \rangle, \quad (3.2.20)$$

$$\langle : \bar{q}\gamma_\mu q : \rangle = \langle : \bar{q}\hat{v}q : \rangle \frac{v_\mu}{v^2}. \quad (3.2.21)$$

A condensate of the type  $\langle : \bar{q}\sigma_{\mu\nu}q : \rangle$  occurs neither in vacuum nor in a medium since there is no possibility to create an antisymmetric structure in the Lorentz indices  $\mu, \nu$ . Condensates of the type  $\langle : \bar{q}\gamma_5\gamma_\mu q : \rangle, \langle : \bar{q}\gamma_5 q : \rangle$  can not be projected onto structures that are invariant under parity transformations.

(ii) Condensates of mass dimension 4:

$$\langle : \bar{q}D_\mu q : \rangle = -\langle : \bar{q}\hat{v}q : \rangle i \frac{m_q v_\mu}{v^2}, \quad (3.2.22)$$

$$\begin{aligned} \langle : \bar{q}\gamma_\mu D_\nu q : \rangle &= -\langle : \bar{q}q : \rangle i \frac{m_q}{4} g_{\mu\nu} \\ &\quad - \left[ i \frac{m_q}{4} \langle : \bar{q}q : \rangle + \langle : \bar{q}\hat{v} \frac{(vD)}{v^2} q : \rangle \right] \frac{1}{3} \left( g_{\mu\nu} - 4 \frac{v_\mu v_\nu}{v^2} \right), \end{aligned} \quad (3.2.23)$$

$$\begin{aligned} \langle : G_{\mu\nu}^A G_{\kappa\lambda}^B : \rangle &= \frac{\delta^{AB}}{96} (g_{\mu\alpha} g_{\nu\beta} - g_{\mu\beta} g_{\nu\alpha}) \langle : G^2 : \rangle \\ &\quad - \frac{\delta^{AB}}{24} \langle : \frac{\alpha_s}{\pi} \left( \frac{(vG)^2}{v^2} - \frac{G^2}{4} \right) : \rangle S_{\mu\nu\kappa\lambda}. \end{aligned} \quad (3.2.24)$$

Again, terms of the form  $\langle : \bar{q}\gamma_5\gamma_\mu D_\mu q : \rangle, \langle : \bar{q}\gamma_5 D_\mu q : \rangle$  do not have a projection due to the requirement of parity invariance. The same holds true for  $\langle : \bar{q}\sigma_{\mu\nu} D_\kappa q : \rangle$ , which can be contracted with  $\epsilon_{\mu\nu\kappa\lambda} v^\lambda$  giving an odd term with respect to parity.

(iii) Condensates of mass dimension 5:

$$\begin{aligned} \langle : \bar{q} D_\mu D_\nu q : \rangle &= -\langle : \bar{q} q : \rangle \frac{m_q^2}{4} g_{\mu\nu} + \langle : \bar{q} g \sigma \mathcal{G} q : \rangle \frac{1}{8} g_{\mu\nu} \\ &\quad - \left[ \frac{m_q^2}{4} \langle : \bar{q} q : \rangle - \frac{1}{8} \langle : \bar{q} g \sigma \mathcal{G} q : \rangle + \langle : \bar{q} \frac{(vD)^2}{v^2} q : \rangle \right] \frac{1}{3} \left( g_{\mu\nu} - 4 \frac{v_\mu v_\nu}{v^2} \right), \end{aligned} \quad (3.2.25)$$

$$\begin{aligned} \langle : \bar{q} \gamma_\mu D_\nu D_\alpha q : \rangle &= \frac{1}{v^4} \langle : \bar{q} \hat{v} (vD)^2 q : \rangle \left( \frac{2v_\mu v_\nu v_\alpha}{v^2} - \frac{1}{3} (v_\mu g_{\nu\alpha} + v_\nu g_{\mu\alpha} + v_\alpha g_{\mu\nu}) \right) \\ &\quad - \frac{1}{6v^2} \langle : \bar{q} \hat{v} g \sigma G q : \rangle \left( \frac{v_\mu v_\nu v_\alpha}{v^2} - v_\mu g_{\nu\alpha} \right) + \frac{m_q^2}{3v^2} \langle : \bar{q} \hat{v} q : \rangle \left( \frac{v_\mu v_\nu v_\alpha}{v^2} - v_\mu g_{\nu\alpha} \right) \\ &\quad + \frac{im_q}{3v^2} \langle : \bar{q} (vD) q : \rangle \left( \frac{2v_\mu v_\nu v_\alpha}{v^2} - v_\nu g_{\mu\alpha} - v_\alpha g_{\mu\nu} \right), \end{aligned} \quad (3.2.26)$$

$$\begin{aligned} \langle : \bar{q} \gamma_5 \gamma_\mu D_\nu D_\alpha q : \rangle &= -\frac{1}{6v^2} \epsilon_{\mu\nu\alpha\beta} v^\beta \left[ \frac{i}{2} \langle : \bar{q} \hat{v} g \sigma G q : \rangle + im_q^2 \langle : \bar{q} \hat{v} q : \rangle + im_q^2 \langle : \bar{q} (vD) q : \rangle \right], \end{aligned} \quad (3.2.27)$$

$$\begin{aligned} \langle : \bar{q} \sigma_{\mu\nu} D_\alpha D_\beta q : \rangle &= -\frac{i}{24} (g_{\mu\alpha} g_{\nu\beta} - g_{\mu\beta} g_{\nu\alpha}) \langle : \bar{q} g \sigma \mathcal{G} q : \rangle \\ &\quad - \left[ \frac{i}{8} \langle : \bar{q} g \sigma \mathcal{G} q : \rangle - m_q \langle : \bar{q} \hat{v} \frac{(vD)}{v^2} q : \rangle - i \langle : \bar{q} \frac{(vD)^2}{v^2} q : \rangle \right] S_{\mu\nu\alpha\beta}, \end{aligned} \quad (3.2.28)$$

$$\langle : \bar{q} \gamma_5 \gamma_\alpha \mathcal{G}_{\mu\nu} q : \rangle = \frac{1}{6v^2} \langle : \bar{q} \hat{v} g \sigma G q : \rangle \epsilon_{\alpha\mu\nu\sigma} v^\sigma, \quad (3.2.29)$$

$$\begin{aligned} \langle : \bar{q} g \sigma_{\alpha\beta} \mathcal{G}_{\mu\nu} q : \rangle &= \langle : \bar{q} g \sigma \mathcal{G} q : \rangle \frac{1}{12} (g_{\alpha\mu} g_{\beta\nu} - g_{\alpha\nu} g_{\beta\mu}) \\ &\quad + \left[ \frac{1}{12} \langle : \bar{q} g \sigma \mathcal{G} q : \rangle - i \frac{2m_q}{3} \langle : \bar{q} \hat{v} \frac{(vD)}{v^2} q : \rangle - \frac{2}{3} \langle : \bar{q} \frac{(vD)^2}{v^2} q : \rangle \right] S_{\alpha\beta\mu\nu}, \end{aligned} \quad (3.2.30)$$

where we have defined

$$S_{\alpha\beta\mu\nu} = \left( g_{\alpha\mu} g_{\beta\nu} - g_{\alpha\nu} g_{\beta\mu} - 2 \left( g_{\alpha\mu} \frac{v_\beta v_\nu}{v^2} - g_{\alpha\nu} \frac{v_\beta v_\mu}{v^2} + g_{\beta\nu} \frac{v_\alpha v_\mu}{v^2} - g_{\beta\mu} \frac{v_\alpha v_\nu}{v^2} \right) \right). \quad (3.2.31)$$

We have explicitly separated the medium specific contributions from the vacuum projections. Medium specific contributions are either condensates that contain the medium four-velocity  $v$  or combinations of condensates that appear in vacuum and medium. The latter ones are always written with angled brackets. Applying vacuum projections to the medium specific terms makes them zero in the vacuum limit.

In order to give an example for this procedure we briefly proof (3.2.29). Due to Lorentz covariance we write

$$\langle : \bar{q} \gamma_5 \gamma_\alpha \mathcal{G}_{\mu\nu} q : \rangle = A \epsilon_{\alpha\mu\nu\sigma} v^\sigma. \quad (3.2.32)$$

Our aim is to determine the Lorentz scalar  $A$ . Using (A.31), we can write for any four-vector  $v_\mu$

$$\hat{v}\sigma^{\mu\nu}\mathcal{G}_{\mu\nu} = iv_\alpha\gamma^\alpha\gamma^\mu\gamma^\nu\mathcal{G}_{\mu\nu}. \quad (3.2.33)$$

Expanding the product of Dirac matrices in terms of the Clifford algebra, one obtains

$$\gamma^\alpha\gamma^\mu\gamma^\nu = g^{\mu\nu}\gamma^\alpha + g^{\nu\alpha}\gamma^\mu + g^{\alpha\mu}\gamma^\nu + i\epsilon^{\sigma\alpha\mu\nu}\gamma_5\gamma_\sigma. \quad (3.2.34)$$

Due to the equations of motion (A.28) and by the definition of the gluon field strength tensor, one can show that

$$\langle : \bar{d}v^\mu\gamma^\nu\mathcal{G}_{\mu\nu}d : \rangle = 0. \quad (3.2.35)$$

Altogether, this gives the relation

$$\langle : \bar{d}\hat{v}\sigma^{\mu\nu}\mathcal{G}_{\mu\nu}d : \rangle = -\langle : \bar{d}\gamma_5\gamma_\sigma\mathcal{G}_{\mu\nu}d : \rangle\epsilon^{\sigma\alpha\mu\nu}v_\alpha. \quad (3.2.36)$$

Contracting (3.2.32) with  $\epsilon^{\alpha\mu\nu\sigma}$  and using  $\epsilon^{\alpha\mu\nu\sigma}\epsilon_{\alpha\mu\nu}{}^\tau = -6g^{\sigma\tau}$ , one can show the desired relation (3.2.29).

Let us define the operator  $\hat{T}$  in such a way that it creates a traceless expression with respect to Lorentz indices. For two Lorentz indices  $\hat{T}$  reads

$$\hat{T}(O_{\mu\nu}) = O_{\mu\nu} - \frac{g_{\mu\nu}}{4}O_\alpha^\alpha \quad (3.2.37)$$

and we immediately observe that the medium specific terms in (3.2.23) and in (3.2.25) originate from the contraction of  $v^\mu v^\nu/v^2$  with a certain traceless expression:

$$\frac{v^\mu v^\nu}{v^2} \langle : \bar{q} \hat{T}(\gamma_\mu D_\nu) q : \rangle = \left[ i \frac{m_q}{4} \langle : \bar{q} q : \rangle + \langle : \bar{q} \hat{v} \frac{(vD)}{v^2} q : \rangle \right], \quad (3.2.38)$$

$$\frac{v^\mu v^\nu}{v^2} \langle : \bar{q} \hat{T}(D_\mu D_\nu) q : \rangle = \left[ \frac{m_q^2}{4} \langle : \bar{q} q : \rangle - \frac{1}{8} \langle : \bar{q} g \sigma \mathcal{G} q : \rangle + \langle : \bar{q} \frac{(vD)^2}{v^2} q : \rangle \right]. \quad (3.2.39)$$

This is clear since the additional medium contributions can be obtained by performing the complete projection of the structure to be projected minus the vacuum projection, which is proportional to products of the metric tensor,  $O_{\mu\nu} - \frac{g_{\mu\nu}}{4}g^{\alpha\beta}O_{\alpha\beta}$ . Therefore, the additional medium contributions must be traceless. The generalization to arbitrary Lorentz indices is obvious.

Now we can proceed with the calculation of the Wilson coefficients. We always consider the in-medium OPE; the vacuum OPE can be easily derived from these expressions by setting all medium specific contributions zero.

### 3.2.2 Gluon Condensates from $\Pi_{D+}^{(0)}$

We are going to calculate the contribution of the left diagram in fig. 3.2.1 to the gluon condensate  $\langle : G^2 : \rangle$ . This means, we consider an insertion of higher-order perturbative

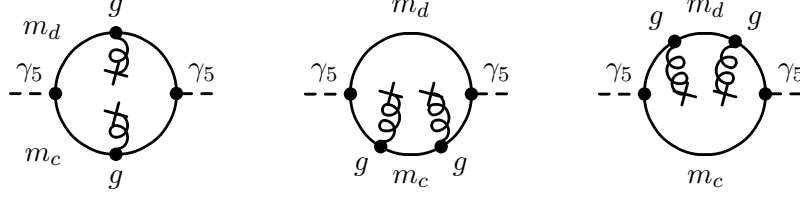


**Figure 3.2.3:** Contributing diagrams to the Wilson coefficient of  $\langle : \frac{\alpha_s}{\pi} G^2 : \rangle$ .

quark propagators, namely  $S_c^{(1)}, S_d^{(1)}$  or  $S_c^{(2)}, S_d^{(0)}$  or  $S_c^{(0)}, S_d^{(2)}$ , and lowest-order gluon fields, thus, taking into account first order quark-gluon interactions in a weak background field. The gluon condensate, therefore, is of next-to-leading order in  $\alpha_s$ . Let us introduce the following notation for the three different contributions

$$\Pi_{D^+}^{G^2}(q) = \Pi_{D^+}^{G^2,1}(q) + \Pi_{D^+}^{G^2,2}(q) + \Pi_{D^+}^{G^2,3}(q), \quad (3.2.40)$$

with

$$\Pi_{D^+}^{G^2,1}(q) = -i \int \frac{d^4 p}{(2\pi)^4} \langle : \text{Tr}_{\text{C,D}} \left[ \gamma_5 S_c^{(1)}(p) \gamma_5 S_d^{(1)}(p-q) \right] : \rangle, \quad (3.2.41)$$

$$\Pi_{D^+}^{G^2,2}(q) = -i \int \frac{d^4 p}{(2\pi)^4} \langle : \text{Tr}_{\text{C,D}} \left[ \gamma_5 S_c^{(2)}(p) \gamma_5 S_d^{(0)}(p-q) \right] : \rangle, \quad (3.2.42)$$

$$\Pi_{D^+}^{G^2,3}(q) = -i \int \frac{d^4 p}{(2\pi)^4} \langle : \text{Tr}_{\text{C,D}} \left[ \gamma_5 S_c^{(0)}(p+q) \gamma_5 S_d^{(2)}(p) \right] : \rangle. \quad (3.2.43)$$

The change of variables in the last expression is just for calculational convenience. These terms can be visualized by the diagrams in fig. 3.2.3. All line codes in this and the following subsection are according to the line codes used in fig. 3.2.2.

The occurring integrals can be calculated for Euclidean momenta after performing a Wick rotation. The results can be found in many textbooks about quantum field theory, e.g. [It80]. We list the necessary expressions in  $D$  dimensions. The limit  $D \rightarrow 4$  can safely be taken as there will not be any divergences for the required integrals in (3.2.41), (3.2.42) and (3.2.43) which are connected to dimensional regularization and the limit  $D \rightarrow 4$ .<sup>3</sup> In the following equations all momenta are in Euclidean space-time.

For simplicity we introduce the following notation:

$$\mathbf{I}_{ijk}(q^2, m_1^2, m_2^2) := \int_0^1 d\alpha \frac{\alpha^i (1-\alpha)^j}{[\alpha(1-\alpha)q^2 + \alpha m_1^2 + (1-\alpha)m_2^2]^k}. \quad (3.2.44)$$

Obviously, the mass dimension of these integrals is always  $2k$ . There are useful relations among these integrals which sometimes simplify their calculation or, at least, give a good

<sup>3</sup>Terms which are divergent in the limit  $m_d \rightarrow 0$  will occur. They require a different treatment. See section 3.2.4.

possibility to check the results:

$$\frac{\partial}{\partial m_1^2} \mathcal{I}_{ijk}(q^2, m_1^2, m_2^2) = -k \mathcal{I}_{i+1,j,k+1}(q^2, m_1^2, m_2^2), \quad (3.2.45)$$

$$\frac{\partial}{\partial m_2^2} \mathcal{I}_{ijk}(q^2, m_1^2, m_2^2) = -k \mathcal{I}_{i,j+1,k+1}(q^2, m_1^2, m_2^2), \quad (3.2.46)$$

$$\frac{\partial}{\partial q^2} \mathcal{I}_{ijk}(q^2, m_1^2, m_2^2) = -k \mathcal{I}_{i+1,j+1,k+1}(q^2, m_1^2, m_2^2). \quad (3.2.47)$$

With this notation the required integrals read

$$\begin{aligned} & \int \frac{d^D p}{(2\pi)^D} \frac{1}{[(p-q) + m_1^2]^n (p^2 + m_2^2)^p} \\ &= \frac{1}{(4\pi)^{D/2}} \frac{\Gamma(n+p-\frac{D}{2})}{\Gamma(n)\Gamma(p)} \mathcal{I}_{n-1,p-1,n+p-D/2}(q^2, m_1^2, m_2^2), \end{aligned} \quad (3.2.48)$$

$$\begin{aligned} & \int \frac{d^D p}{(2\pi)^D} \frac{p_\mu}{[(p-q) + m_1^2]^n (p^2 + m_2^2)^p} \\ &= \frac{q_\mu}{(4\pi)^{D/2}} \frac{\Gamma(n+p-\frac{D}{2})}{\Gamma(n)\Gamma(p)} \mathcal{I}_{n,p-1,n+p-D/2}(q^2, m_1^2, m_2^2), \end{aligned} \quad (3.2.49)$$

$$\begin{aligned} & \int \frac{d^D p}{(2\pi)^D} \frac{p_\mu p_\nu}{[(p-q) + m_1^2]^n (p^2 + m_2^2)^p} = \frac{1}{(4\pi)^{D/2}} \frac{1}{\Gamma(n)\Gamma(p)} \\ & \times \left\{ \frac{g_{\mu\nu}}{2} \Gamma\left(n+p-\frac{D}{2}-1\right) \mathcal{I}_{n-1,p-1,n+p-D/2-1}(q^2, m_1^2, m_2^2) \right. \\ & \left. + q_\mu q_\nu \Gamma\left(n+p-\frac{D}{2}\right) \mathcal{I}_{n+1,p-1,n+p-D/2}(q^2, m_1^2, m_2^2) \right\}. \end{aligned} \quad (3.2.50)$$

In order to get the expression belonging to three Lorentz indices we have to take the first derivative of (3.2.50) with respect to  $q^\kappa$  and obtain

$$\begin{aligned} & \int \frac{d^D p}{(2\pi)^D} \frac{p_\mu p_\nu p_\kappa}{[(p-q) + m_1^2]^n (p^2 + m_2^2)^p} = q_\kappa \int \frac{d^D p}{(2\pi)^D} \frac{p_\mu p_\nu}{[(p-q) + m_1^2]^n (p^2 + m_2^2)^p} \\ & + \frac{1}{2(n-1)} \frac{\partial}{\partial q^\kappa} \int \frac{d^D p}{(2\pi)^D} \frac{p_\mu p_\nu}{[(p-q) + m_1^2]^{n-1} (p^2 + m_2^2)^p}. \end{aligned} \quad (3.2.51)$$

Inserting (3.2.49) and making use of  $x\Gamma(x) = \Gamma(x+1)$  leads to the final result for the desired integral:

$$\begin{aligned} & \int \frac{d^D p}{(2\pi)^D} \frac{p_\mu p_\nu p_\kappa}{[(p-q) + m_1^2]^n (p^2 + m_2^2)^p} = \frac{1}{(4\pi)^{D/2}} \frac{1}{\Gamma(n)\Gamma(p)} \\ & \times \left\{ \frac{g_{\mu\nu} q_\kappa + g_{\mu\kappa} q_\nu + g_{\nu\kappa} q_\mu}{2} \Gamma\left(n+p-\frac{D}{2}-1\right) \mathcal{I}_{n,p-1,n+p-D/2+1}(q^2, m_1^2, m_2^2) \right. \\ & \left. + q_\mu q_\nu q_\kappa \Gamma\left(n+p-\frac{D}{2}\right) \mathcal{I}_{n+2,p-1,n+p-D/2}(q^2, m_1^2, m_2^2) \right\}. \end{aligned} \quad (3.2.52)$$

For concrete evaluations one can use algebraic software. Solving the required integrals for both masses  $m_1$  and  $m_2$  being non-zero leads to cumbersome expressions. On the other side, it is not possible to set one mass equal to zero from the beginning, because the integrals contain structures like  $m_d^{-1}$  and  $\ln m_d$ , while  $m_d \ln m_d$  terms vanish in the limit  $m_d \rightarrow 0$ . In order to extract the corresponding terms  $\propto m_d^{-1}$  one has to multiply the integral with the lowest power  $n$  of  $m_d$  that gives a finite result for the mass going to zero. What remains is the corresponding coefficient for the  $m_d^{-n}$  term. All the other coefficients can be obtained by taking suitable derivatives of  $m_d^n I_{ijk}$  with respect to  $m_d$  and setting afterward  $m_d$  equal to zero. The terms  $\propto \ln m_d$  can be obtained by taking the first derivative of  $I_{ijk}$  and extracting the term  $\propto m_d^{-1}$  from that expression in the same way.

Sometimes, some additional manipulations have to be made in order to obtain meaningful expressions. Using

$$\arctan z = \frac{1}{2i} \ln \frac{1+iz}{1-iz} \quad (3.2.53)$$

one gets

$$\arctan \left( i \frac{q^2 - m^2}{q^2 + m^2} \right) = \frac{1}{2i} \ln \frac{m^2}{q^2}, \quad (3.2.54)$$

which is a source of mass logarithms. Another source of terms  $\propto \ln m_d$  arises from a slightly different expression, namely

$$\arctan \left( i \frac{q^2 + m_1^2 + m_2^2}{\sqrt{-2q^2 m_2^2 - q^4 - 2q^2 m_1^2 - m_1^4 + 2m_1^2 m_2^2 - m_2^4}} \right) \xrightarrow{m_2=0} \arctan(-i), \quad (3.2.55)$$

which is not well defined. Expanding the fraction in  $m_2$  and keeping only the lowest power, which is the dominant contribution for  $m_2 \rightarrow 0$ , leads to

$$\arctan \left( i \frac{q^2 + m_1^2 + m_2^2}{\sqrt{-2q^2 m_2^2 - q^4 - 2q^2 m_1^2 - m_1^4 + 2m_1^2 m_2^2 - m_2^4}} \right) \xrightarrow{m_2 \approx 0} \frac{1}{2i} \ln \frac{q^2 m_2^2}{(q^2 + m_1^2)^2}. \quad (3.2.56)$$

This term arises in the medium contribution of  $\Pi^{G^2,3}$  and causes an infrared divergent Wilson coefficient. It prohibits us from taking the limit  $m_d \rightarrow 0$  at this stage.

These formulas now enable us to calculate the gluon contribution of the completely contracted term. Inserting the appropriate propagator terms and evaluating the trace over color indices we get

$$\begin{aligned} \Pi^{G^2,1}(q) = & - \left( i \frac{g}{2} \right)^2 \frac{\delta^{AB}}{2} \langle : G_{\mu\nu}^A G_{\kappa\lambda}^B : \rangle \int \frac{d^4 p}{(2\pi)^4} \text{Tr}_D \left[ \gamma_5 S_c^{(0)}(p) \gamma^\mu S^{(0)}(p) \gamma^\nu S^{(0)}(p) \right. \\ & \times \left. \gamma_5 S^{(0)}(p-q) \gamma^\kappa S^{(0)}(p-q) \gamma^\lambda S^{(0)}(p-q) \right], \end{aligned} \quad (3.2.57)$$



$$\Pi^{G^2,2}(q) = -i \left(i\frac{g}{2}\right)^2 \frac{\delta^{AB}}{2} \langle : G_{\mu\nu}^A G_{\kappa\lambda}^B : \rangle \int \frac{d^4 p}{(2\pi)^4} \text{Tr}_D \left[ \gamma_5 T_c^{\mu\nu\kappa\lambda}(p) \gamma_5 S_d^{(0)}(p-q) \right] , \quad (3.2.58)$$

$$\Pi^{G^2,3}(q) = -i \left(i\frac{g}{2}\right)^2 \frac{\delta^{AB}}{2} \langle : G_{\mu\nu}^A G_{\kappa\lambda}^B : \rangle \int \frac{d^4 p}{(2\pi)^4} \text{Tr}_D \left[ \gamma_5 S_c^{(0)}(p+q) \gamma_5 T_d^{\mu\nu\kappa\lambda}(p) \right] \quad (3.2.59)$$

with  $T^{\mu\nu\kappa\lambda}$  defined in (2.4.32). We now see the advantage of separating vacuum projections from medium projections as we are now able to calculate the results for the vacuum case and the additional medium contributions separately. For the vacuum case we obtain for  $m_d \approx 0$  and for Euclidean momenta

$$\Pi^{G^2,1}(q) = \frac{1}{8} \langle : \frac{\alpha_s}{\pi} G^2 : \rangle \frac{1}{q_E^2 + m_c^2} , \quad (3.2.60)$$

$$\Pi^{G^2,2}(q) = -\frac{1}{24} \langle : \frac{\alpha_s}{\pi} G^2 : \rangle \frac{1}{q_E^2 + m_c^2} , \quad (3.2.61)$$

$$\Pi^{G^2,3}(q) = \langle : \frac{\alpha_s}{\pi} G^2 : \rangle \left( \frac{1}{12} \frac{m_c}{m_d} \frac{1}{q_E^2 + m_c^2} - \frac{1}{24} \frac{1}{q_E^2 + m_c^2} - \frac{1}{24} \frac{m_c^2}{(q_E^2 + m_c^2)^2} \right) . \quad (3.2.62)$$

We recognize that the term  $\propto m_d^{-1}$  prohibits us from regarding one quark to be massless in the vacuum case. For the additional medium contributions we obtain for  $m_d \approx 0$  and for Euclidean momenta

$$\begin{aligned} \Pi^{G^2,1}(q) &= \langle : \frac{\alpha_s}{\pi} \left( \frac{(vG)^2}{v^2} - \frac{G^2}{4} \right) : \rangle \left( q_E^2 - 4 \frac{(vq)_E^2}{v_E^2} \right) \\ &\quad \times \left( -\frac{1}{3} \frac{m_c^2}{q_E^6} \ln \left( \frac{m_c^2}{q_E^2 + m_c^2} \right) + \frac{1}{6q_E^2} \frac{1}{q_E^2 + m_c^2} - \frac{1}{3q_E^4} \right) , \end{aligned} \quad (3.2.63)$$

$$\begin{aligned} \Pi^{G^2,2}(q) &= \langle : \frac{\alpha_s}{\pi} \left( \frac{(vG)^2}{v^2} - \frac{G^2}{4} \right) : \rangle \left( q_E^2 - 4 \frac{(vq)_E^2}{v_E^2} \right) \left( \frac{1}{9q_E^4} + \frac{1}{18q_E^2} \frac{1}{q_E^2 + m_c^2} \right. \\ &\quad \left. + \frac{1}{9q_E^4} \ln \left( \frac{m_c^2}{q_E^2 + m_c^2} \right) + \frac{m_c^2}{9q_E^6} \ln \left( \frac{m_c^2}{q_E^2 + m_c^2} \right) \right) , \end{aligned} \quad (3.2.64)$$

$$\begin{aligned} \Pi^{G^2,3}(q) &= \langle : \frac{\alpha_s}{\pi} \left( \frac{(vG)^2}{v^2} - \frac{G^2}{4} \right) : \rangle \left( q_E^2 - 4 \frac{(vq)_E^2}{v_E^2} \right) \left( \frac{2}{9q_E^4} - \frac{1}{18q_E^2} \frac{1}{q_E^2 + m_c^2} \right. \\ &\quad - \frac{1}{6q_E^2} \frac{m_c^2}{(q_E^2 + m_c^2)^2} - \left( \frac{1}{9q_E^4} - \frac{2m_c^2}{9q_E^6} \right) \ln \left( \frac{m_c^2}{q_E^2 + m_c^2} \right) \\ &\quad - \frac{1}{9q_E^2} \left( \frac{m_c^2}{(q_E^2 + m_c^2)^2} - \frac{1}{q_E^2 + m_c^2} \right) \ln \left( \frac{m_d^2}{m_c^2} \right) \\ &\quad \left. - \frac{2}{9q_E^2} \left( \frac{m_c^2}{(q_E^2 + m_c^2)^2} - \frac{1}{q_E^2 + m_c^2} \right) \ln \left( \frac{m_c^2}{q_E^2 + m_c^2} \right) \right) . \end{aligned} \quad (3.2.65)$$

Here, we observe the occurrence of a term  $\propto \ln m_d$ , which again prohibits us from taking the limit  $m_d \rightarrow 0$ . The divergent terms cancel, however, after the introduction of physical condensates. This will be described in detail in section 3.2.4.

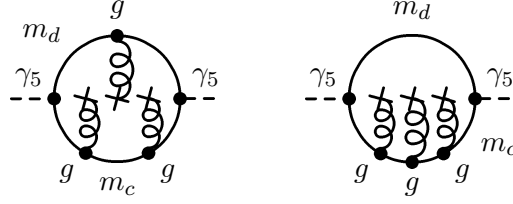


**Figure 3.2.4:** Contributing diagrams to the Wilson coefficient of  $\langle G^3 \rangle$ .

Summation of all contributions and transformation to Minkowski momenta gives the contribution of the completely contracted term to the gluonic operator:

$$\begin{aligned} \Pi^{G^2}(q) = & \langle \frac{\alpha_s}{\pi} G^2 \rangle \left( -\frac{1}{24} \frac{1}{q^2 - m_c^2} - \frac{1}{12} \frac{m_c}{m_d} \frac{1}{q^2 - m_c^2} - \frac{1}{24} \frac{m_c^2}{(q^2 - m_c^2)^2} \right) \\ & + \langle \frac{\alpha_s}{\pi} \left( \frac{(vG)^2}{v^2} - \frac{G^2}{4} \right) \rangle \left( q^2 - 4 \frac{(vq)^2}{v^2} \right) \left( -\frac{1}{6q^2} \frac{1}{q^2 - m_c^2} - \frac{1}{6q^2} \frac{m_c^2}{(q^2 - m_c^2)^2} \right. \\ & - \frac{1}{9q^2} \left( \frac{m_c^2}{(q^2 - m_c^2)^2} + \frac{1}{q^2 - m_c^2} \right) \ln \left( \frac{m_d^2}{m_c^2} \right) \\ & \left. - \frac{2}{9q^2} \left( \frac{m_c^2}{(q^2 - m_c^2)^2} + \frac{1}{q^2 - m_c^2} \right) \ln \left( -\frac{m_c^2}{q^2 - m_c^2} \right) \right). \end{aligned} \quad (3.2.66)$$

If it would not be necessary to introduce physical condensates instead of normal ordered ones,  $\Pi^{G^2}(q)$  would already contain the complete Wilson coefficient for the gluon condensate. But as already mentioned above we have to absorb the divergences into the condensates leading to a mixing of the condensates. Therefore, additional terms enter the OPE and give further contributions to the Wilson coefficients of the gluonic condensates.

It is worth emphasizing that the completely contracted term also gives contributions to other Wilson coefficients. Of course, inserting higher-order propagators, like  $S_c^{(3)}$  together with  $S_d^{(0)}$  or  $S_c^{(2)}$  together with  $S_d^{(1)}$  (or the same with  $d \leftrightarrow c$ ), and the gluon field in the lowest order leads to the  $\langle G^3 \rangle$  condensate (see fig. 3.2.4). It is of mass dimension 6 and  $\propto g^3$  and will therefore not be considered here.

The completely contracted term also contributes to quark condensates. Insertion of  $S_c^{(1)}$  together with  $S_d^{(0)}$  or vice versa and the next-to-leading order gluon field will give rise to a di-quark condensate. These terms are depicted in fig. 3.2.5. This can be seen by applying the equation of motion of the gluon field strength tensor. An insertion of  $S_c^{(1)}$  together with  $S_d^{(1)}$  and the next-to-leading order gluon field will result in a four-quark condensate, which is exhibited in fig. 3.2.6. Finally, the insertion of  $S_c^{(1)}$  and the next-to-leading order gluon field together with  $S_d^{(1)}$  and the lowest order gluon field (or vice versa) will cause a mixed quark-gluon condensate, see fig. 3.2.7.

These are just some examples of diagrams emerging from  $\Pi^{(0)}(q)$  which give contributions to the Wilson coefficients of other condensates apart from the gluon condensate

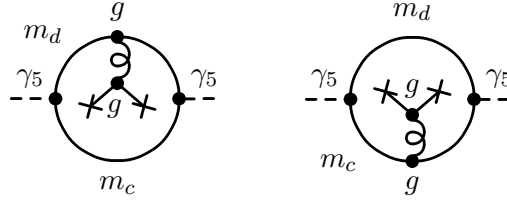


**Figure 3.2.5:** Contributing diagrams to the Wilson coefficient of di-quark condensates from the completely contracted term.

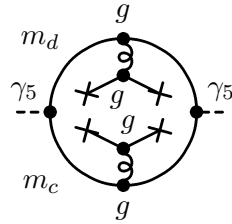


**Figure 3.2.6:** Contributing diagram to the Wilson coefficient of four-quark condensates from the completely contracted term.

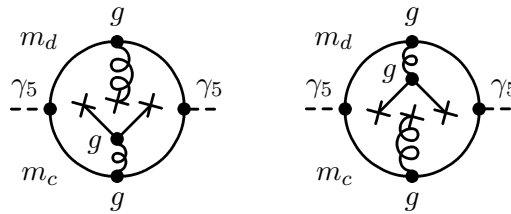


**Figure 3.2.7:** Contributing diagrams to the Wilson coefficient of the mixed quark-gluon condensate.

$\langle : G^2 : \rangle$  and must not be taken as a complete list. They are of higher order in  $\alpha_s$  or mass dimension and are not considered throughout this work. Also, some of the above mentioned contributions might vanish due to projection properties or vanishing traces. At least they will give different results for vacuum and medium analysis.

### 3.2.3 Quark Condensates from $\Pi_{D+}^{(2)}$

Let us now turn to the computation of the Wilson coefficients belonging to operators which emerge from the calculation of  $\Pi_{D+}^{(2)}$ . As the mass of the charm quark is supposed to be large, at least much larger than the light quark masses, it does not couple to condensates. This means that it is too heavy to be created from the vacuum. Therefore  $\langle : \bar{c} \dots c : \rangle \rightarrow 0$ . Later we will see that the physical heavy charm quark condensate can be expressed by other condensates due to the heavy-quark mass expansion in section 3.2.4. One can show that this happens in the already mentioned framework of a consistent separation of scales and the absorption of divergences into the physical condensates [Tk83].  $\Pi_{D+}^{(2)}$  reduces to

$$\Pi^{(2)}(q) = \int d^4x e^{iqx} \langle : \bar{d}(x) \gamma_5 S^c(x, 0) \gamma_5 d(0) : \rangle \quad (3.2.67)$$

which is exhibited by the middle diagram in fig. 3.2.1. So we have not missed anything by leaving out the adequate diagram with a cut charm quark line as this diagram does not contribute.

Applying the covariant expansion of the quark fields and carrying out the Fourier transformation (2.4.19), one obtains (summation over color indices  $a, b$  is to be understood)

$$\Pi^{(2)}(q) = \sum_{k=0}^{\infty} \frac{(-i)^k}{k!} \langle : \left( \bar{d}_i \overleftarrow{D}_{\alpha_1} \dots \overleftarrow{D}_{\alpha_k} \right)^a (\gamma_5 \partial^{\alpha_1} \dots \partial^{\alpha_k} S_c(q) \gamma_5)^{ij}_{ab} d_j^b : \rangle. \quad (3.2.68)$$

The quark fields and their covariant derivatives are to be calculated at the origin, i.e.  $x = 0$ . From here we can go to higher quark field derivatives or to higher orders in the perturbative propagator or to higher orders in the gluon field, which enters through the perturbative quark propagator. The quark fields are of mass dimension  $3/2$ . Each covariant derivative and the gluon fields  $\tilde{A}_\mu$  enlarge the mass dimension by one unit. Thus working in lowest order of the gluon fields the following terms have to be considered up to mass dimension 5:

$$\begin{aligned} \Pi^{(2)}(q) = & \langle : \bar{d}_i^a \left( \gamma_5 S_c^{(0)}(q) \gamma_5 \right)^{ij}_{ab} d_j^b : \rangle - i \langle : \left( \bar{d} \overleftarrow{D}_\mu \right)_i^a \left( \gamma_5 \partial^\mu S_c^{(0)}(q) \gamma_5 \right)^{ij}_{ab} d_j^b : \rangle \\ & - \frac{1}{2} \langle : \left( \bar{d} \overleftarrow{D}_\mu \overleftarrow{D}_\nu \right)_i^a \left( \gamma_5 \partial^\mu \partial^\nu S_c^{(0)}(q) \gamma_5 \right)^{ij}_{ab} d_j^b : \rangle \\ & + \langle : \bar{d}_i^a \left( \gamma_5 S_c^{(1)}(q) \gamma_5 \right)^{ij}_{ab} d_j^b : \rangle. \end{aligned} \quad (3.2.69)$$

If one investigates the vacuum OPE, the second term is not present. In this case the individual terms can be given a diagrammatic interpretation as in fig. 3.2.8. The right diagram corresponds to the insertion of the next-to-leading order perturbative heavy quark

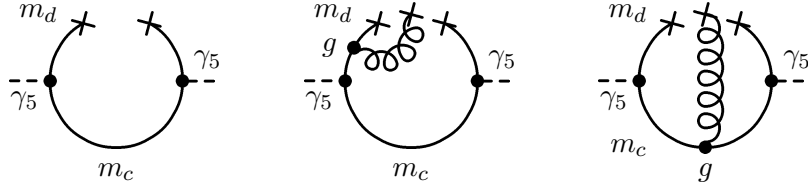


**Figure 3.2.8:** Diagrams for  $\Pi^{(2)}$  calculated in vacuum.

propagator which is the last term in (3.2.69). The left and middle diagrams reflect the covariant expansion of the quark fields.

Unfortunately, there is no such simple diagrammatic interpretation for all the occurring terms when the in-medium case is considered, since new types of condensates appear. For completeness and later purposes we give the result of projecting color and Dirac indices

$$\begin{aligned}
\Pi^{(2)}(q) = & \langle : \bar{d} d : \rangle \frac{m_c}{q^2 - m_c^2} - \langle : \bar{d} \vec{D}_\mu d : \rangle i \frac{2m_c q^\mu}{(q^2 - m_c^2)^2} \\
& - \langle : \bar{d} \gamma_\lambda d : \rangle \frac{q^\lambda}{q^2 - m_c^2} + i \langle : \bar{d} \gamma_\lambda \vec{D}_\mu d : \rangle \left( 2 \frac{q^\mu q^\lambda}{(q^2 - m_c^2)^2} - \frac{g^{\mu\lambda}}{q^2 - m_c^2} \right) \\
& + \langle : \bar{d} \vec{D}_\mu \vec{D}_\nu d : \rangle \left( \frac{m_c g^{\mu\nu}}{(q^2 - m_c^2)^2} - 4 \frac{m_c q^\mu q^\nu}{(q^2 - m_c^2)^3} \right) \\
& + \langle : \bar{d} \gamma_\lambda \vec{D}_\mu \vec{D}_\nu d : \rangle \left( 4 \frac{q^\mu q^\nu q^\lambda}{(q^2 - m_c^2)^3} - \frac{q^\mu g^{\nu\lambda} + q^\nu g^{\mu\lambda} + q^\lambda g^{\mu\nu}}{(q^2 - m_c^2)^2} \right) \\
& - \langle : \bar{d} g \sigma_{\alpha\beta} \mathcal{G}_{\mu\nu} d : \rangle \frac{m_c}{4} \frac{g^{\alpha\mu} g^{\beta\nu} - g^{\alpha\nu} g^{\beta\mu}}{(q^2 - m_c^2)^2} + \langle : \bar{d} g \gamma_5 \gamma_\alpha \mathcal{G}_{\mu\nu} d : \rangle \frac{g}{2} \frac{\epsilon^{\alpha\mu\nu\kappa} q_\kappa}{(q^2 - m_c^2)^2} .
\end{aligned} \tag{3.2.70}$$

The results for the complete projections of the condensates onto invariant structures read:<sup>4</sup>

$$\langle : \bar{d}_i^a \left( \gamma_5 S_c^{(0)}(q) \gamma_5 \right)_{ab}^{ij} d_j^b : \rangle = \langle : \bar{d} d : \rangle \frac{m_c}{q^2 - m_c^2} - \langle : \bar{d} \hat{v} d : \rangle \frac{(vq)}{v^2} \frac{1}{q^2 - m_c^2} , \tag{3.2.71}$$

$$\begin{aligned}
& - i \langle : \left( \bar{d} \overleftarrow{D}_\mu \right)_i^a \left( \gamma_5 \partial^\mu S_c^{(0)}(q) \gamma_5 \right)_{ab}^{ij} d_j^b : \rangle \\
& = \langle : \bar{d} d : \rangle \frac{1}{2} \left( \frac{m_d m_c^2}{(q^2 - m_c^2)^2} - \frac{m_d}{q^2 - m_c^2} \right) - \langle : \bar{d} \hat{v} d : \rangle 2 \frac{(vq)}{v^2} \frac{m_d m_c}{(q^2 - m_c^2)^2} \\
& + \left[ \frac{m_d}{12} \langle : \bar{d} d : \rangle - \frac{1}{3} \langle : \bar{d} \hat{v} \frac{(ivD)}{v^2} d : \rangle \right] 2 \left( q^2 - 4 \frac{(vq)^2}{v^2} \right) \frac{1}{(q^2 - m_c^2)^2} ,
\end{aligned} \tag{3.2.72}$$

<sup>4</sup>To apply the projection formulas given in section 3.2.1 we have to make use of the translation invariance of the condensates [Ji93], e.g.  $\langle \bar{q} \Gamma D_\mu q \rangle = -\langle \bar{q} \Gamma \overleftarrow{D}_\mu q \rangle$  and  $\langle \bar{q} \Gamma D_\mu D_\nu q \rangle = -\langle \bar{q} \Gamma \overleftarrow{D}_\mu D_\nu q \rangle = \langle \bar{q} \Gamma \overleftarrow{D}_\mu \overleftarrow{D}_\nu q \rangle$ .

$$\begin{aligned}
& -\frac{1}{2}\langle : \left( \bar{d} \overleftarrow{D}_\mu \overleftarrow{D}_\nu \right)_i^a \left( \gamma_5 \partial^\mu \partial^\nu S_c^{(0)}(q) \gamma_5 \right)_{ab}^{ij} d_j^b : \rangle \\
& = \langle : \bar{d} d : \rangle \frac{m_d^2 m_c^3}{(q^2 - m_c^2)^3} - \langle : \bar{d} g \sigma \mathcal{G} d : \rangle \frac{1}{2} \frac{m_c^3}{(q^2 - m_c^2)^3} \\
& + \left[ \frac{m_d^2}{12} \langle : \bar{d} d : \rangle + \frac{1}{3} \langle : \bar{d} \frac{(vD)^2}{v^2} d : \rangle - \frac{1}{24} \langle : \bar{d} g \sigma \mathcal{G} d : \rangle \right] \\
& \times 4 \left( q^2 - 4 \frac{(vq)^2}{v^2} \right) \frac{m_c}{(q^2 - m_c^2)^3} \\
& - \langle : \bar{d} \hat{v} (vD)^2 d : \rangle 4 \left( q^2 - 2 \frac{(vq)^2}{v^2} \right) \frac{(vq)}{v^4} \frac{1}{(q^2 - m_c^2)^3} \\
& + \langle : \bar{d} \hat{v} g \sigma \mathcal{G} d : \rangle \left( \frac{2}{3} \frac{(vq)}{v^2} \left( q^2 - \frac{(vq)^2}{v^2} \right) \frac{1}{(q^2 - m_c^2)^3} - \frac{1}{2} \frac{(vq)}{v^2} \frac{1}{(q^2 - m_c^2)^2} \right) \\
& + \langle : \bar{d} \hat{v} d : \rangle \left( \frac{(vq)}{v^2} \frac{m_d^2}{(q^2 - m_c^2)^2} - \frac{4}{3} \frac{(vq)}{v^2} \left( q^2 - \frac{(vq)^2}{v^2} \right) \frac{m_d^2}{(q^2 - m_c^2)^2} \right) \\
& + \langle : \bar{d} (ivD) d : \rangle \left( 2 \frac{(vq)}{v^2} \frac{m_d}{(q^2 - m_c^2)^2} - \frac{8}{3} \frac{(vq)}{v^2} \left( q^2 - \frac{(vq)^2}{v^2} \right) \frac{m_d}{(q^2 - m_c^2)^3} \right), \tag{3.2.73}
\end{aligned}$$

$$\begin{aligned}
& \langle : \bar{d}_i^a \left( \gamma_5 S_c^{(1)}(q) \gamma_5 \right)_{ab}^{ij} d_j^b : \rangle \\
& = -\langle : \bar{d} g \sigma \mathcal{G} d : \rangle \frac{1}{2} \frac{m_c}{(q^2 - m_c^2)^2} - \langle : \bar{d} \hat{v} g \sigma \mathcal{G} d : \rangle \frac{1}{2} \frac{m_c}{(q^2 - m_c^2)^2}. \tag{3.2.74}
\end{aligned}$$

Summing up all contributions one eventually obtains

$$\begin{aligned}
\Pi_{D^+}^{(2)}(q) & = \langle : \bar{d} d : \rangle \left( \frac{m_c}{q^2 - m_c^2} - \frac{1}{2} \frac{m_d}{q^2 - m_c^2} + \frac{1}{2} \frac{m_d m_c^2}{(q^2 - m_c^2)^2} + \frac{m_d^2 m_c^3}{(q^2 - m_c^2)^3} \right) \\
& - \langle : \bar{d} g \sigma \mathcal{G} d : \rangle \frac{1}{2} \left( \frac{m_c^3}{(q^2 - m_c^2)^3} + \frac{m_c}{(q^2 - m_c^2)^2} \right) \\
& + \left[ \frac{m_d}{12} \langle : \bar{d} d : \rangle - \frac{1}{3} \langle : \bar{d} \hat{v} \frac{(ivD)}{v^2} d : \rangle \right] 2 \left( q^2 - 4 \frac{(vq)^2}{v^2} \right) \frac{1}{(q^2 - m_c^2)^2} \\
& + \left[ \frac{m_d^2}{12} \langle : \bar{d} d : \rangle + \frac{1}{3} \langle : \bar{d} \frac{(vD)^2}{v^2} d : \rangle - \frac{1}{24} \langle : \bar{d} g \sigma \mathcal{G} d : \rangle \right] \\
& \times 4 \left( q^2 - 4 \frac{(vq)^2}{v^2} \right) \frac{m_c}{(q^2 - m_c^2)^3} \\
& - \langle : \bar{d} \hat{v} d : \rangle \frac{(vq)}{v^2} \left( \frac{1}{q^2 - m_c^2} + 2 \frac{m_d m_c}{(q^2 - m_c^2)^2} - \frac{m_d^2}{(q^2 - m_c^2)^2} \right) \\
& + \frac{4}{3} \left( q^2 - \frac{(vq)^2}{v^2} \right) \frac{m_d^2}{(q^2 - m_c^2)^2} \\
& - \langle : \bar{d} \hat{v} (vD)^2 d : \rangle 4 \left( q^2 - 2 \frac{(vq)^2}{v^2} \right) \frac{(vq)}{v^4} \frac{1}{(q^2 - m_c^2)^3}
\end{aligned}$$

$$\begin{aligned}
& + \langle : \bar{d} \hat{v} g \sigma \mathcal{G} d : \rangle \frac{(vq)}{v^2} \left( \frac{2}{3} \left( q^2 - \frac{(vq)^2}{v^2} \right) \frac{1}{(q^2 - m_c^2)^3} - \frac{1}{(q^2 - m_c^2)^2} \right) \\
& + \langle : \bar{d} (i v D) d : \rangle \frac{(vq)}{v^2} \left( 2 \frac{m_d}{(q^2 - m_c^2)^2} - \frac{8}{3} \left( q^2 - \frac{(vq)^2}{v^2} \right) \frac{m_d}{(q^2 - m_c^2)^3} \right).
\end{aligned} \tag{3.2.75}$$

These results account for masses  $m_{d,c}$  being non-zero and for any arbitrary frame. Additional structures emerging from  $\Pi^{(2)}(q)$  are exhibited in fig. 3.2.9 (four-quark condensates) and fig. 3.2.10 ( $\langle \bar{q} G^2 q \rangle$  condensate). The left diagram of fig. 3.2.9 results from an insertion of the next-to-leading order heavy quark propagator and the next-to-leading order gluon field. Application of the equation of motion for the gluon fields then yields the four-quark condensate. The right diagram corresponds to the consideration of higher covariant quark field derivatives. The diagrams of fig. 3.2.10 originate from the insertion of the next-to-next-to-leading order heavy quark propagator (middle panel) or higher covariant field derivatives together with the next-to-leading order heavy quark propagator (left panel) or higher covariant field derivatives together with the lowest order heavy quark propagator (right panel). They will lead to the  $\langle \bar{q} G^2 q \rangle$  condensate which is of mass dimension 7.

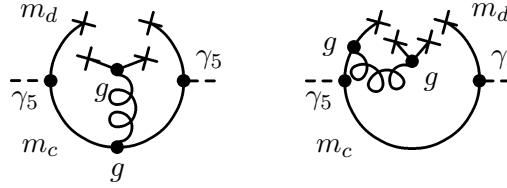


**Figure 3.2.9:** Diagrams for  $\Pi^{(2)}$  which contribute to  $\langle \bar{q} q \sum_n \bar{n} n \rangle$ .

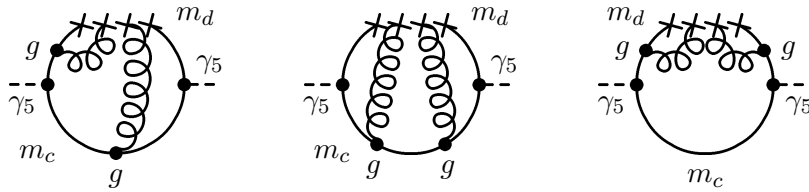


**Figure 3.2.10:** Diagrams for  $\Pi^{(2)}$  which contribute to  $\langle \bar{q} G^2 q \rangle$ .

### 3.2.4 Physical Condensates and Heavy-Quark Mass Expansion

In order to perform a consistent separation of scales, which means that the coefficient functions are only determined by the short distance behavior, while the non-perturbative effects are encoded in the condensates, all the infrared divergences have to be absorbed into the condensates. In [Ch82, Tk83] it has been shown that the dependence of the

coefficient functions on the masses is polynomial only when they are calculated in the  $\overline{\text{MS}}$  scheme.<sup>5</sup> In contrast, using normal ordered operators is not a minimal subtraction scheme. By introducing normal ordered condensates the mass-logarithms do not simply disappear, but have been absorbed into the coefficient functions [Tk83]. Thereby, the needed separation of scales has been avoided. Moreover, these arguments can be taken as a formalization of the heuristic arguments of [Sh78] to introduce non-vanishing vacuum averages and the need for a proper separation of short-distance and long-distance behavior.

The method we used to calculate Wilson coefficients naturally leads to the introduction of normal ordered condensates. In order to express the normal ordered condensates by physical condensates which emerge from operator products renormalized in the  $\overline{\text{MS}}$  scheme and shall contain all the non-perturbative physics,<sup>6</sup> we note Wick's theorem for an arbitrary equal-time operator product of two quark fields. In doing so we partly follow [Gr94] to get

$$\begin{aligned} T[\bar{q}(x) (O[D_\mu] q)(y)] &=: \bar{q}(x) O[D_\mu] q(y) : + \langle 0 | T[\bar{q}(x) (O[D_\mu] q)(y)] | 0 \rangle \\ &=: \bar{q}(x) O[D_\mu] q(y) : - O[D_\mu](y)_{ij}^{ab} \langle 0 | T[q_j^b(y) \bar{q}_i^a(x)] | 0 \rangle \\ &=: \bar{q}(x) O[D_\mu] q(y) : - i \text{Tr}_{C,D} [O[D_\mu](y) S(y, x)] . \end{aligned} \quad (3.2.76)$$

Here,  $O[D_\mu](y)$  denotes an arbitrary function of gluon fields, covariant derivatives and Dirac structures. If  $O[D_\mu](y)$  contains any Fock operators one gets additional terms of the type  $\bar{q} \langle 0 | T[O[A_\mu] q] | 0 \rangle$  which vanish when the expectation value is evaluated using the physical ground state  $|\Omega\rangle$  and the result stays the same. We emphasize the occurrence of the perturbative propagator and not the exact propagator in the last line. Setting  $x = 0$  and introducing the Fourier transformed expressions for the operator function and the quark propagator one obtains

$$\begin{aligned} T[\bar{q}(0) (O[D_\mu] q)(y)] &=: \bar{q}(0) O[D_\mu] q(y) : \\ &\quad - i \int \frac{d^4 p}{(2\pi)^4} e^{-ipy} \text{Tr}_{C,D} \left[ O[-ip_\mu - i\tilde{A}_\mu] S(p) \right] . \end{aligned} \quad (3.2.77)$$

$O[-ip_\mu - i\tilde{A}_\mu]$  denotes the Fourier transformed operator function with  $\tilde{A}_\mu$  defined in (2.4.23). The derivatives are now contained in the gluon fields. Therefore, the ordering among the Lorenz indices is important as the field operators act on everything to the right. A generalization of (3.2.77) to  $x \neq 0$  would require translation invariance of the perturbative propagator  $S(x, y)$ , which is broken due to the Fock-Schwinger gauge (see section 2.4). Setting  $y = 0$  and calculating the expectation value using  $|\Omega\rangle$ , results in

$$\begin{aligned} \langle \Omega | \bar{q} O[D_\mu] q | \Omega \rangle &= \langle \Omega | : \bar{q} O[D_\mu] q : | \Omega \rangle \\ &\quad - i \int \frac{d^4 p}{(2\pi)^4} \langle \Omega | \text{Tr}_{C,D} \left[ O[-ip_\mu - i\tilde{A}_\mu] S(p) \right] | \Omega \rangle . \end{aligned} \quad (3.2.78)$$

<sup>5</sup>One can also work in  $\overline{\text{MS}}$  scheme. However, because dimensional regularization in  $D = 4 - \epsilon$  dimensions and absorption of the divergence for  $\epsilon \rightarrow 0$  is crucial for a proper separation of the long and short distance behavior, some minimal subtraction scheme has to be used. Thus, we prefer to employ the  $\overline{\text{MS}}$  scheme.

<sup>6</sup>Many authors prefer to talk about non-normal ordered condensates, but due to the arguments given above we think the term physical condensate is better justified



We define (3.2.78) as the connection between physical condensates and normal ordered condensates. Renormalizing the physical condensates by absorbing the divergent terms of  $\Pi^{(0)}$  on the r.h.s. of (3.2.78) cancels out the infrared divergences and yields infrared stable Wilson coefficients.

The integrals do not depend on  $p$ , therefore, the Lorentz structure can be projected out before the integration is performed. Evaluation of the integrals can then be done in Euclidean space in the framework of dimensional regularization and renormalization in  $\overline{\text{MS}}$  scheme. It is important to note that the result for the physical condensates is still obtained in Minkowskian space. Up to order  $\alpha_s$ , one gets the following equations

$$\langle \bar{q}q \rangle = \langle : \bar{q}q : \rangle - i \int \frac{d^4 p}{(2\pi)^4} \langle \text{Tr} [S_0(p) + S_2(p)] \rangle, \quad (3.2.79)$$

$$\langle \bar{q}\gamma_\mu q \rangle = \langle : \bar{q}\gamma_\mu q : \rangle, \quad (3.2.80)$$

$$\langle \bar{q}iD_\mu q \rangle = \langle : \bar{q}iD_\mu q : \rangle, \quad (3.2.81)$$

$$\langle \bar{q}\gamma_\mu iD_\nu q \rangle = \langle : \bar{q}\gamma_\mu iD_\nu q : \rangle - i \int \frac{d^4 p}{(2\pi)^4} \langle \text{Tr} [\gamma_\mu p_\nu \{S_0(p) + S_2(p)\}] \rangle, \quad (3.2.82)$$

$$\begin{aligned} \langle \bar{q}iD_\mu iD_\nu q \rangle &= \langle : \bar{q}iD_\mu iD_\nu q : \rangle \\ &\quad - i \int \frac{d^4 p}{(2\pi)^4} \langle \text{Tr} [p_\mu p_\nu \{S_0(p) + S_2(p)\} + \tilde{A}_\mu \tilde{A}_\nu S_0(p)] \rangle, \end{aligned} \quad (3.2.83)$$

$$\langle \bar{q}\gamma_\lambda iD_\mu iD_\nu q \rangle = \langle : \bar{q}\gamma_\lambda iD_\mu iD_\nu q : \rangle, \quad (3.2.84)$$

$$\langle \bar{q}g\sigma\mathcal{G}q \rangle = \langle : \bar{q}g\sigma\mathcal{G}q : \rangle - i \int \frac{d^4 p}{(2\pi)^4} \langle \text{Tr} [\sigma^{\mu\nu} \mathcal{G}_{\mu\nu} S_1(p)] \rangle, \quad (3.2.85)$$

$$\langle \bar{q}g\gamma_\lambda \sigma\mathcal{G}q \rangle = \langle : \bar{q}g\gamma_\lambda \sigma\mathcal{G}q : \rangle, \quad (3.2.86)$$

where the expectation value is calculated with the physical ground state  $|\Omega\rangle$ . As  $\langle : \frac{\alpha_s}{\pi} G^2 : \rangle$  is already of order  $\alpha_s$  we set  $\langle : \frac{\alpha_s}{\pi} G^2 : \rangle \rightarrow \langle \frac{\alpha_s}{\pi} G^2 \rangle$ . In all cases above, where normal-ordered and the physical condensates are matching, i.e. in (3.2.80), (3.2.81), (3.2.84) and (3.2.86), the integral vanishes in all orders of  $\alpha_s$  and the identity is exact, if one works in lowest order of the field  $\tilde{A}_\mu = \tilde{A}_\mu^{(0)}$ .<sup>7</sup> To clarify this, one has to note that  $S(p)$  is merely the product of  $S^{(0)}(p)$  and  $(\gamma\tilde{A})$ , where each  $(\gamma\tilde{A})$  brings in two additional Dirac matrices (2.4.28). In order to get a non-vanishing integral, the integrand must be even in  $p$ , requiring an even number of Dirac matrices. By this it is clear that  $\int d^4 p p_\mu \text{Tr}_{\text{C,D}} [S(p)] = 0$  and similar terms are zero. Each  $\tilde{A}_\mu$  brings in one additional Dirac matrix, and by this  $\int d^4 p \text{Tr}_{\text{C,D}} [\tilde{A}_\mu S(p)]$  vanishes. Hence, only if the number of Lorentz indices (i.e. the sum of Dirac matrices and covariant derivatives in the condensates) is even, physical and normal ordered condensates differ. Dimensional regularization and minimal subtraction

<sup>7</sup>This corresponds to taking the lowest-order term of the covariant Taylor expansion of the gluon field  $A_\mu(x)$  for small  $x$ , which is sufficient as we set  $y = 0$  in (3.2.78). Therefore, only the lowest-order term in the expansion (2.4.11) and its Fourier transformed expression (2.4.20) is of importance. Thus the lowest-order term of (2.4.23) is sufficient in all orders of  $\alpha_s$ .

yield

$$\langle \bar{q}q \rangle = \langle : \bar{q}q : \rangle + \frac{3}{4\pi^2} m_q^3 \left( \ln \frac{\mu^2}{m_q^2} + 1 \right) - \frac{1}{12m_q} \langle \frac{\alpha_s}{\pi} G^2 \rangle, \quad (3.2.87a)$$

$$\langle \bar{q}g\sigma\mathcal{G}q \rangle = \langle : \bar{q}g\sigma\mathcal{G}q : \rangle - \frac{1}{2} m_q \ln \frac{\mu^2}{m_q^2} \langle \frac{\alpha_s}{\pi} G^2 \rangle, \quad (3.2.87b)$$

$$\begin{aligned} \langle \bar{q}\gamma_\mu iD_\nu q \rangle &= \langle : \bar{q}\gamma_\mu iD_\nu q : \rangle + \frac{3}{16\pi^2} m_q^4 g_{\mu\nu} \left( \ln \frac{\mu^2}{m_q^2} + 1 \right) - \frac{g_{\mu\nu}}{48} \langle \frac{\alpha_s}{\pi} G^2 \rangle \\ &\quad + \frac{1}{18} \left( g_{\mu\nu} - 4 \frac{v_\mu v_\nu}{v^2} \right) \left( \ln \frac{\mu^2}{m_q^2} - \frac{1}{3} \right) \langle \frac{\alpha_s}{\pi} \left( \frac{(vG)^2}{v^2} - \frac{G^2}{4} \right) \rangle, \end{aligned} \quad (3.2.87c)$$

$$\begin{aligned} \langle \bar{q}iD_\mu iD_\nu q \rangle &= \langle : \bar{q}iD_\mu iD_\nu q : \rangle + \frac{3m_q^5}{16\pi^2} g_{\mu\nu} \left( \ln \frac{\mu^2}{m_q^2} + 1 \right) \\ &\quad + \frac{m_q}{16} g_{\mu\nu} \left( \ln \frac{\mu^2}{m_q^2} - \frac{1}{3} \right) \langle \frac{\alpha_s}{\pi} G^2 \rangle \\ &\quad - \frac{m_q}{36} \left( g_{\mu\nu} - 4 \frac{v_\mu v_\nu}{v^2} \right) \left( \ln \frac{\mu^2}{m_q^2} + \frac{2}{3} \right) \langle \frac{\alpha_s}{\pi} \left( \frac{(vG)^2}{v^2} - \frac{G^2}{4} \right) \rangle. \end{aligned} \quad (3.2.87d)$$

These are the required relations for the purpose of obtaining infrared stable Wilson coefficients. They reproduce the definitions made to render the vacuum OPE free from mass singularities [Ja92] and also give the correct expressions for the in-medium OPE. It is worth to check these equations for self-consistency. If we contract (3.2.87c) with the metric tensor, (3.2.87a) is reproduced. Contracting (3.2.87d) with the metric tensor, the result can be verified from (3.2.87a) and (3.2.87b) by using the equations of motion (A.28) and the identity (A.32). Of course, this only gives us confidence for the vacuum parts of these equations, as the in-medium parts are traceless and vanish if contracted with the metric tensor.

We want to remark, that the condensates are mixing under this procedure. Not only the condensates of equal mass dimension are mixing, but also condensates of different mass dimensions.

If we now consider the heavy-mass limit in the renormalized version of (3.2.87a), where the perturbative contribution is canceled by the corresponding infrared divergence, we meet again the heavy-quark mass expansion [Sh78, Ge83]

$$\langle \bar{q}q \rangle \approx -\frac{1}{12m_q} \langle \frac{\alpha_s}{\pi} G^2 \rangle + \dots, \quad (3.2.88)$$

$$\langle \bar{q}g\sigma\mathcal{G}q \rangle \approx -\frac{1}{2} m_q \ln \frac{\mu^2}{m_q^2} \langle \frac{\alpha_s}{\pi} G^2 \rangle + \dots. \quad (3.2.89)$$

The idea behind this expansion is, that the interaction of the heavy quark with the physical ground state mainly happens via gluon interactions, because the quark itself is too heavy to couple directly to a condensate.

Before calculating the infrared stable Wilson coefficients, we would like to remark that the medium specific combinations of condensates appearing in (3.2.75) do not have any

contribution to the vacuum condensates when the physical condensates are inserted since  $\langle \frac{\alpha_s}{\pi} G^2 \rangle$  cancels in all in-medium combinations. Using (3.2.37) or directly inserting (3.2.87) into (3.2.75) yields

$$\left[ \frac{m_d}{12} \langle : \bar{d}d : \rangle - \frac{1}{3} \langle : \bar{d} \hat{v} \frac{(ivD)}{v^2} d : \rangle \right] = \left[ \frac{m_d}{12} \langle \bar{d}d \rangle - \frac{1}{3} \langle \bar{d} \hat{v} \frac{(ivD)}{v^2} d \rangle \right. \\ \left. - \frac{1}{18} \left( \ln \frac{\mu^2}{m_d^2} - \frac{1}{3} \right) \langle \frac{\alpha_s}{\pi} \left( \frac{(vG)^2}{v^2} - \frac{G^2}{4} \right) \rangle \right]. \quad (3.2.90)$$

We emphasize the occurrence of the  $\ln m_d^2$  term which does not vanish in the limit  $m_d \rightarrow 0$ . This term cancels out by the gluonic in-medium contribution of the completely contracted term mentioned before. The same happens for the second medium specific contribution. Here, no logarithmic terms, which correspond to infrared divergent contributions, appear, i.e.

$$\left[ \frac{m_d^2}{12} \langle : \bar{d}d : \rangle + \frac{1}{3} \langle : \bar{d} \frac{(vD)^2}{v^2} d : \rangle - \frac{1}{24} \langle : \bar{d} g \sigma \mathcal{G} d : \rangle \right] \\ = \left[ \frac{m_d^2}{12} \langle \bar{d}d \rangle + \frac{1}{3} \langle \bar{d} \frac{(vD)^2}{v^2} d \rangle - \frac{1}{24} \langle \bar{d} g \sigma \mathcal{G} d \rangle \right. \\ \left. + \frac{m_d}{36} \left( \ln \frac{\mu^2}{m_d^2} + \frac{2}{3} \right) \langle \frac{\alpha_s}{\pi} \left( \frac{(vG)^2}{v^2} - \frac{G^2}{4} \right) \rangle \right]. \quad (3.2.91)$$

This is clear as the medium contributions emerge from traceless expressions, while the vacuum contributions of the physical condensates and of the perturbative contribution, which is also a pure vacuum contribution, are again proportional to products of the metric tensor. Therefore, it is clear that they cancel from the medium specific terms.

At this point we explicitly note the difference of a neat separation of scales in vacuum and in medium. This has already been indicated in (3.2.66) by the occurrence of the additional light-quark mass logarithm in the Wilson coefficient of the medium specific gluon condensate. Hence, for in-medium sum rules the procedure of passing over from normal-ordered condensates to condensates renormalized in  $\overline{\text{MS}}$  scheme differs from the vacuum case.

### 3.2.5 Operator Mixing

Expressing the normal ordered condensates in (3.2.75) in terms of physical condensates (3.2.87), the complete contribution of  $\Pi^{(2)}(q)$  reads

$$\Pi_{D^+}^{(2d)}(q) = \langle \bar{d}d \rangle \left( \frac{m_c}{q^2 - m_c^2} - \frac{1}{2} \frac{m_d}{q^2 - m_c^2} + \frac{1}{2} \frac{m_d m_c^2}{(q^2 - m_c^2)^2} + \frac{m_d^2 m_c^3}{(q^2 - m_c^2)^3} \right) \\ - \langle \bar{d} g \sigma \mathcal{G} d \rangle \frac{1}{2} \left( \frac{m_c^3}{(q^2 - m_c^2)^3} + \frac{m_c}{(q^2 - m_c^2)^2} \right) \\ + \langle \frac{\alpha_s}{\pi} G^2 \rangle \left( \frac{1}{12} \frac{m_c}{m_d} \frac{1}{q^2 - m_c^2} - \frac{1}{24} \frac{1}{q^2 - m_c^2} + \frac{1}{24} \frac{m_c^2}{(q^2 - m_c^2)^2} \right)$$

$$\begin{aligned}
& + \frac{1}{12} \frac{m_d m_c^3}{(q^2 - m_c^2)^3} - \frac{m_d}{4} \ln \frac{\mu^2}{m_d^2} \left( \frac{m_c^3}{(q^2 - m_c^2)^3} + \frac{m_c}{(q^2 - m_c^2)^2} \right) \\
& + \left[ \frac{m_d}{12} \langle \bar{d}d \rangle - \frac{1}{3} \langle \bar{d} \hat{v} \frac{(viD)}{v^2} d \rangle \right] 2 \left( q^2 - 4 \frac{(vq)^2}{v^2} \right) \frac{1}{(q^2 - m_c^2)^2} \\
& + \left\langle \frac{\alpha_s}{\pi} \left( \frac{(vG)^2}{v^2} - \frac{G^2}{4} \right) \right\rangle \frac{1}{9} \left( q^2 - 4 \frac{(vq)^2}{v^2} \right) \\
& \times \left( \frac{m_c m_d}{(q^2 - m_c^2)^3} \left( \ln \frac{\mu^2}{m_d^2} + \frac{2}{3} \right) - \frac{1}{(q^2 - m_c^2)^2} \left( \ln \frac{\mu^2}{m_d^2} - \frac{1}{3} \right) \right) \\
& + \left[ \frac{m_d^2}{12} \langle \bar{d}d \rangle + \frac{1}{3} \langle \bar{d} \frac{(vD)^2}{v^2} d \rangle - \frac{1}{24} \langle \bar{d} g \sigma \mathcal{G} d \rangle \right] \\
& \times 4 \left( q^2 - 4 \frac{(vq)^2}{v^2} \right) \frac{m_c}{(q^2 - m_c^2)^3} \\
& + \langle \bar{d} \hat{v} d \rangle \frac{vq}{v^2} \left( -\frac{1}{q^2 - m_c^2} - 2 \frac{m_d m_c}{(q^2 - m_c^2)^2} + \frac{m_d^2}{(q^2 - m_c^2)^2} \right. \\
& \left. - \frac{4}{3} \left( q^2 - \frac{(vq)^2}{v^2} \right) \frac{m_d^2}{(q^2 - m_c^2)^3} \right) \\
& - \langle \bar{d} \hat{v} (vD)^2 d \rangle 4 \frac{vq}{v^4} \frac{q^2 - 2 \frac{(vq)^2}{v^2}}{(q^2 - m_c^2)^3} \\
& + \langle \bar{d} \hat{v} g \sigma \mathcal{G} d \rangle \frac{vq}{v^2} \left( \frac{2}{3} \frac{q^2 - \frac{(vq)^2}{v^2}}{(q^2 - m_c^2)^3} - \frac{1}{(q^2 - m_c^2)^2} \right) \\
& + \langle \bar{d} (viD) d \rangle \frac{vq}{v^2} \left( 2 \frac{m_d}{(q^2 - m_c^2)^2} - \frac{8}{3} \left( q^2 - \frac{(vq)^2}{v^2} \right) \frac{m_d}{(q^2 - m_c^2)^3} \right). \quad (3.2.92)
\end{aligned}$$

The terms that enter the Wilson coefficient of the unity operator are not displayed, because the infrared stable perturbative contribution has been given in (3.2.13). We are now in the position to calculate the complete OPE for the D meson in vacuum and in medium with infrared stable Wilson coefficients. The result is

$$\begin{aligned}
\Pi_{D^+}(q) &= \Pi^{per}(q) + \Pi^{G^2}(q) + \Pi^{(2)}(q) \quad (3.2.93) \\
&= \Pi^{per}(q) + \langle \bar{d}d \rangle \left( \frac{m_c}{q^2 - m_c^2} - \frac{1}{2} \frac{m_d}{q^2 - m_c^2} + \frac{1}{2} \frac{m_d m_c^2}{(q^2 - m_c^2)^2} + \frac{m_d^2 m_c^3}{(q^2 - m_c^2)^3} \right) \\
&- \langle \bar{d} g \sigma \mathcal{G} d \rangle \frac{1}{2} \left( \frac{m_c^3}{(q^2 - m_c^2)^3} + \frac{m_c}{(q^2 - m_c^2)^2} \right) \\
&+ \left\langle \frac{\alpha_s}{\pi} G^2 \right\rangle \left( -\frac{1}{12} \frac{1}{q^2 - m_c^2} + \frac{1}{12} \frac{m_d m_c^3}{(q^2 - m_c^2)^3} \right. \\
&- \frac{m_d}{4} \ln \frac{\mu^2}{m_d^2} \left( \frac{m_c^3}{(q^2 - m_c^2)^3} + \frac{m_c}{(q^2 - m_c^2)^2} \right) \Bigg) \\
&+ \left\langle \frac{\alpha_s}{\pi} \left( \frac{(vG)^2}{v^2} - \frac{G^2}{4} \right) \right\rangle \left( q^2 - 4 \frac{(vq)^2}{v^2} \right) \left( -\frac{1}{6q^2} \frac{1}{q^2 - m_c^2} - \frac{1}{6q^2} \frac{m_c^2}{(q^2 - m_c^2)^2} \right)
\end{aligned}$$

$$\begin{aligned}
& -\frac{1}{9q^2} \left( \frac{m_c^2}{(q^2 - m_c^2)^2} + \frac{1}{q^2 - m_c^2} \right) \ln \frac{\mu^2}{m_c^2} + \frac{1}{27q^2} \left( \frac{m_c^2}{(q^2 - m_c^2)^2} + \frac{1}{q^2 - m_c^2} \right) \\
& -\frac{2}{9q^2} \left( \frac{m_c^2}{(q^2 - m_c^2)^2} + \frac{1}{q^2 - m_c^2} \right) \ln \left( -\frac{m_c^2}{q^2 - m_c^2} \right) \\
& + \frac{m_d}{9q^2} \left( \frac{m_c^3}{(q^2 - m_c^2)^3} + \frac{m_c}{(q^2 - m_c^2)^2} \right) \left( \ln \frac{\mu^2}{m_d^2} + \frac{2}{3} \right) \\
& + \left[ \frac{m_d}{12} \langle \bar{d}d \rangle - \frac{1}{3} \langle \bar{d}\hat{v} \frac{(viD)}{v^2} d \rangle \right] \left( q^2 - 4 \frac{(vq)^2}{v^2} \right) \frac{2}{q^2} \left( \frac{m_c^2}{(q^2 - m_c^2)^2} + \frac{1}{q^2 - m_c^2} \right) \\
& + \langle \bar{d}\hat{v}d \rangle \frac{vq}{v^2} \left( -\frac{1}{q^2 - m_c^2} - 2 \frac{m_d m_c}{(q^2 - m_c^2)^2} + \frac{m_d^2}{(q^2 - m_c^2)^2} \right. \\
& \left. - \frac{4}{3} \left( q^2 - \frac{(vq)^2}{v^2} \right) \frac{m_d^2}{(q^2 - m_c^2)^3} \right) \\
& + \left[ \frac{m_d^2}{12} \langle \bar{d}d \rangle + \frac{1}{3} \langle \bar{d} \frac{(vD)^2}{v^2} d \rangle - \frac{1}{24} \langle \bar{d}g\sigma\mathcal{G}d \rangle \right] \\
& \times \left( q^2 - 4 \frac{(vq)^2}{v^2} \right) \frac{4}{q^2} \left( \frac{m_c^3}{(q^2 - m_c^2)^3} + \frac{m_c}{(q^2 - m_c^2)^2} \right) \\
& - \langle \bar{d}\hat{v}(vD)^2 d \rangle \frac{vq}{v^4} \left( q^2 - 2 \frac{(vq)^2}{v^2} \right) \frac{4}{q^2} \left( \frac{m_c^2}{(q^2 - m_c^2)^3} + \frac{1}{(q^2 - m_c^2)^2} \right) \\
& + \langle \bar{d}\hat{v}g\sigma\mathcal{G}d \rangle \frac{vq}{v^2} \left( \frac{2}{3} \frac{q^2 - \frac{(vq)^2}{v^2}}{(q^2 - m_c^2)^3} - \frac{1}{(q^2 - m_c^2)^2} \right) \\
& + \langle \bar{d}(viD)d \rangle \frac{vq}{v^2} \left( 2 \frac{m_d}{(q^2 - m_c^2)^2} - \frac{8}{3} \left( q^2 - \frac{(vq)^2}{v^2} \right) \frac{m_d}{(q^2 - m_c^2)^3} \right). \tag{3.2.94}
\end{aligned}$$

We emphasize the cancellation of the infrared divergent  $\ln m_d^2$  term in the Wilson coefficient of the medium specific gluon condensate and  $m_d^{-1}$  term in the Wilson coefficient of the vacuum gluon condensate. In some sense this result is still incomplete. In  $\Pi^{G^2}(q)$  we omitted all terms proportional to  $m_d$ , while we kept these terms in  $\Pi^{(2)}(q)$ . Because the gluon condensate enters the latter through the introduction of physical condensates in terms of  $m_d^{-1}$ , one would get wrong results omitting terms proportional to  $m_d$ . But we see that all divergent terms cancel and that we can now safely take the limit  $m_d \rightarrow 0$ :

$$\begin{aligned}
& \Pi_{D^+}(q) \\
& = \Pi^{per}(q) + \langle \bar{d}d \rangle \frac{m_c}{q^2 - m_c^2} - \langle \bar{d}g\sigma\mathcal{G}d \rangle \frac{1}{2} \left( \frac{m_c^3}{(q^2 - m_c^2)^3} + \frac{m_c}{(q^2 - m_c^2)^2} \right) \\
& - \langle \frac{\alpha_s}{\pi} G^2 \rangle \frac{1}{12} \frac{1}{q^2 - m_c^2} \\
& + \langle \frac{\alpha_s}{\pi} \left( \frac{(vG)^2}{v^2} - \frac{G^2}{4} \right) \rangle \left( q^2 - 4 \frac{(vq)^2}{v^2} \right) \left( -\frac{7}{54q^2} \left( \frac{m_c^2}{(q^2 - m_c^2)^2} + \frac{1}{q^2 - m_c^2} \right) \right. \\
& \left. - \frac{1}{9q^2} \left( \frac{m_c^2}{(q^2 - m_c^2)^2} + \frac{1}{q^2 - m_c^2} \right) \ln \frac{\mu^2}{m_c^2} \right)
\end{aligned}$$

$$\begin{aligned}
& -\frac{2}{9q^2} \left( \frac{m_c^2}{(q^2 - m_c^2)^2} + \frac{1}{q^2 - m_c^2} \right) \ln \left( -\frac{m_c^2}{q^2 - m_c^2} \right) \\
& - \langle \bar{d} \hat{v} \frac{(vD)}{v^2} d \rangle \left( q^2 - 4 \frac{(vq)^2}{v^2} \right) \frac{2}{3q^2} \left( \frac{m_c^2}{(q^2 - m_c^2)^2} + \frac{1}{q^2 - m_c^2} \right) \\
& - \langle \bar{d} \hat{v} d \rangle \frac{vq}{v^2} \frac{1}{q^2 - m_c^2} + \left[ \frac{1}{3} \langle \bar{d} \frac{(vD)^2}{v^2} d \rangle - \frac{1}{24} \langle \bar{d} g \sigma \mathcal{G} d \rangle \right] \\
& \times \left( q^2 - 4 \frac{(vq)^2}{v^2} \right) \frac{4}{q^2} \left( \frac{m_c^3}{(q^2 - m_c^2)^3} + \frac{m_c}{(q^2 - m_c^2)^2} \right) \\
& - \langle \bar{d} \hat{v} (vD)^2 d \rangle \frac{vq}{v^4} \left( q^2 - 2 \frac{(vq)^2}{v^2} \right) \frac{4}{q^2} \left( \frac{m_c^2}{(q^2 - m_c^2)^3} + \frac{1}{(q^2 - m_c^2)^2} \right) \\
& + \langle \bar{d} \hat{v} g \sigma \mathcal{G} d \rangle \frac{vq}{v^2} \left( \frac{2}{3} \frac{q^2 - \frac{(vq)^2}{v^2}}{(q^2 - m_c^2)^3} - \frac{1}{(q^2 - m_c^2)^2} \right). \tag{3.2.95}
\end{aligned}$$

Transformation into the rest frame of the medium,  $v = (1, \vec{0})$ , and considering the D meson at vanishing spatial momentum,  $q = (q_0, \vec{0})$ , we get

$$\begin{aligned}
& \Pi_{D^+}(q_0) \\
& = \Pi_{per}(q_0) + \langle \bar{d} d \rangle \frac{m_c}{q_0^2 - m_c^2} - \langle \bar{d} g \sigma \mathcal{G} d \rangle \frac{1}{2} \left( \frac{m_c^3}{(q_0^2 - m_c^2)^3} + \frac{m_c}{(q_0^2 - m_c^2)^2} \right) \\
& - \langle \frac{\alpha_s}{\pi} G^2 \rangle \frac{1}{12} \frac{1}{q_0^2 - m_c^2} \\
& + \langle \frac{\alpha_s}{\pi} \left( \frac{(vG)^2}{v^2} - \frac{G^2}{4} \right) \rangle \left( \frac{7}{18} \left( \frac{m_c^2}{(q_0^2 - m_c^2)^2} + \frac{1}{q_0^2 - m_c^2} \right) \right. \\
& + \frac{1}{3} \left( \frac{m_c^2}{(q_0^2 - m_c^2)^2} + \frac{1}{q_0^2 - m_c^2} \right) \ln \frac{\mu^2}{m_c^2} \\
& + \frac{2}{3} \left( \frac{m_c^2}{(q_0^2 - m_c^2)^2} + \frac{1}{q_0^2 - m_c^2} \right) \ln \left( -\frac{m_c^2}{q_0^2 - m_c^2} \right) \\
& + \langle d^\dagger i D_0 d \rangle 2 \left( \frac{m_c^2}{(q_0^2 - m_c^2)^2} + \frac{1}{q_0^2 - m_c^2} \right) - \langle d^\dagger d \rangle q_0 \frac{1}{q_0^2 - m_c^2} \\
& - \left[ \frac{1}{3} \langle \bar{d} D_0^2 d \rangle - \frac{1}{24} \langle \bar{d} g \sigma \mathcal{G} d \rangle \right] 12 \left( \frac{m_c^3}{(q_0^2 - m_c^2)^3} + \frac{m_c}{(q_0^2 - m_c^2)^2} \right) \\
& + \langle d^\dagger D_0^2 d \rangle q_0 4 \left( \frac{m_c^2}{(q_0^2 - m_c^2)^3} + \frac{1}{(q_0^2 - m_c^2)^2} \right) - \langle d^\dagger g \sigma \mathcal{G} d \rangle q_0 \frac{1}{(q_0^2 - m_c^2)^2}. \tag{3.2.96}
\end{aligned}$$

As it is easier to apply the Borel transformation to terms which have a uniform  $q_0^2$  structure, we performed elementary manipulations in the equation above in order to avoid terms like  $q_0^2/(q_0^2 - m_c^2)$ , although the expressions at this point could be simplified and shortened.

The even and the odd part of the operator product expansion read

$$\begin{aligned}
\Pi_{D^+}^e(q_0) &= c_0(q_0^2) + \langle \bar{d}d \rangle \frac{m_c}{q_0^2 - m_c^2} - \langle \bar{d}g\sigma\mathcal{G}d \rangle \frac{1}{2} \left( \frac{m_c^3}{(q_0^2 - m_c^2)^3} + \frac{m_c}{(q_0^2 - m_c^2)^2} \right) \\
&- \langle \frac{\alpha_s}{\pi} G^2 \rangle \frac{1}{12} \frac{1}{q_0^2 - m_c^2} \\
&+ \langle \frac{\alpha_s}{\pi} \left( \frac{(vG)^2}{v^2} - \frac{G^2}{4} \right) \rangle \left( \frac{7}{18} + \frac{1}{3} \ln \frac{\mu^2}{m_c^2} + \frac{2}{3} \ln \left( -\frac{m_c^2}{q_0^2 - m_c^2} \right) \right) \\
&\times \left( \frac{m_c^2}{(q_0^2 - m_c^2)^2} + \frac{1}{q_0^2 - m_c^2} \right) \\
&+ \langle d^\dagger i D_0 d \rangle 2 \left( \frac{m_c^2}{(q_0^2 - m_c^2)^2} + \frac{1}{q_0^2 - m_c^2} \right) \\
&- \left[ \frac{1}{3} \langle \bar{d} D_0^2 d \rangle - \frac{1}{24} \langle \bar{d}g\sigma\mathcal{G}d \rangle \right] 12 \left( \frac{m_c^3}{(q_0^2 - m_c^2)^3} + \frac{m_c}{(q_0^2 - m_c^2)^2} \right)
\end{aligned} \tag{3.2.97}$$

and

$$\begin{aligned}
\Pi_{D^+}^o(q_0^2) &= -\langle d^\dagger d \rangle \frac{1}{q_0^2 - m_c^2} + \langle d^\dagger D_0^2 d \rangle 4 \left( \frac{m_c^2}{(q_0^2 - m_c^2)^3} + \frac{1}{(q_0^2 - m_c^2)^2} \right) \\
&- \langle d^\dagger g\sigma\mathcal{G}d \rangle \frac{1}{(q_0^2 - m_c^2)^2} .
\end{aligned} \tag{3.2.98}$$

From these expressions we can immediately read off the corresponding results for the vacuum operator product expansion. For the vacuum case, only the first two lines in (3.2.97) are existent. All the other terms are medium specific condensates or medium specific combinations of condensates. The odd part only contains medium specific condensates and, thus, vanishes at zero density. It does not exist for the vacuum operator product expansion and in (2.2.35), as the vacuum current-current correlator is symmetric under reflections, which is mirrored by the fact that it only depends on  $q^2$ . Hence, (2.2.32) vanishes in vacuum.

### 3.3 Borel transformed Sum Rules for the D Meson

#### 3.3.1 OPE Terms

Before calculating the Borel transformed sum rules, we analytically continue the energy to complex values  $q_0 = i\omega$  getting

$$\begin{aligned}
\Pi_{D^+}^e(\omega^2) &= c_0(\omega^2) - \langle \bar{d}d \rangle \frac{m_c}{\omega^2 + m_c^2} + \langle \bar{d}g\sigma\mathcal{G}d \rangle \frac{1}{2} \left( \frac{m_c^3}{(\omega^2 + m_c^2)^3} - \frac{m_c}{(\omega^2 + m_c^2)^2} \right)
\end{aligned}$$

$$\begin{aligned}
& + \langle \frac{\alpha_s}{\pi} G^2 \rangle \frac{1}{12} \frac{1}{\omega^2 + m_c^2} \\
& + \langle \frac{\alpha_s}{\pi} \left( \frac{(vG)^2}{v^2} - \frac{G^2}{4} \right) \rangle \left( \frac{7}{18} + \frac{1}{3} \ln \frac{\mu^2}{m_c^2} + \frac{2}{3} \ln \left( \frac{m_c^2}{\omega^2 + m_c^2} \right) \right) \\
& \times \left( \frac{m_c^2}{(\omega^2 + m_c^2)^2} - \frac{1}{\omega^2 + m_c^2} \right) \\
& + \langle d^\dagger i D_0 d \rangle 2 \left( \frac{m_c^2}{(\omega^2 + m_c^2)^2} - \frac{1}{\omega^2 + m_c^2} \right) \\
& + \left[ \langle \bar{d} D_0^2 d \rangle - \frac{1}{8} \langle \bar{d} g \sigma \mathcal{G} d \rangle \right] 4 \left( \frac{m_c^3}{(\omega^2 + m_c^2)^3} - \frac{m_c}{(\omega^2 + m_c^2)^2} \right)
\end{aligned} \tag{3.3.1}$$

and

$$\begin{aligned}
& \Pi_{D^+}^o(\omega^2) \\
& = \langle d^\dagger d \rangle \frac{1}{\omega^2 + m_c^2} - \langle d^\dagger D_0^2 d \rangle 4 \left( \frac{m_c^2}{(\omega^2 + m_c^2)^3} - \frac{1}{(\omega^2 + m_c^2)^2} \right) \\
& - \langle d^\dagger g \sigma \mathcal{G} d \rangle \frac{1}{(\omega^2 + m_c^2)^2}.
\end{aligned} \tag{3.3.2}$$

The Borel transformed dispersion relation can now simply be read of from (3.2.97) and (3.2.98) by applying the results obtained in section 2.6.

$$\begin{aligned}
& \mathcal{B} [\Pi^e(\omega^2)] (M^2) \\
& = \frac{1}{\pi} \int_{m_c^2}^{\infty} ds e^{-s/M^2} \text{Im} \Pi_{D^+}^{per}(s) \\
& + e^{-m_c^2/M^2} \left( -m_c \langle \bar{d} d \rangle + \frac{1}{2} \left( \frac{m_c^3}{2M^4} - \frac{m_c}{M^2} \right) \langle \bar{d} g \sigma \mathcal{G} d \rangle + \frac{1}{12} \langle \frac{\alpha_s}{\pi} G^2 \rangle \right. \\
& + \left[ \left( \frac{7}{18} + \frac{1}{3} \ln \frac{\mu^2 m_c^2}{M^4} - \frac{2\gamma_E}{3} \right) \left( \frac{m_c^2}{M^2} - 1 \right) - \frac{2}{3} \frac{m_c^2}{M^2} \right] \langle \frac{\alpha_s}{\pi} \left( \frac{(vG)^2}{v^2} - \frac{G^2}{4} \right) \rangle \\
& \left. + 2 \left( \frac{m_c^2}{M^2} - 1 \right) \langle d^\dagger i D_0 d \rangle + 4 \left( \frac{m_c^3}{2M^4} - \frac{m_c}{M^2} \right) \left[ \langle \bar{d} D_0^2 d \rangle - \frac{1}{8} \langle \bar{d} g \sigma \mathcal{G} d \rangle \right] \right)
\end{aligned} \tag{3.3.3}$$

for the even part and for the odd part

$$\begin{aligned}
& \mathcal{B} [\Pi^o(\omega^2)] (M^2) \\
& = e^{-m_c^2/M^2} \left( \langle d^\dagger d \rangle - 4 \left( \frac{m_c^2}{2M^4} - \frac{1}{M^2} \right) \langle d^\dagger D_0^2 d \rangle - \frac{1}{M^2} \langle d^\dagger g \sigma \mathcal{G} d \rangle \right).
\end{aligned} \tag{3.3.4}$$

### 3.3.2 Comparison with Literature

In tabs. 3.3.1, 3.3.2 and 3.3.3 we compare our results with the various sum rules in the literature. In all these tables we list the Borel transformed Wilson coefficient  $c_{\hat{O}}/e^{-m_c^2/M^2}$ .

For the vacuum OPE we see that, apart from the Wilson coefficient for  $\langle \frac{\alpha_s}{\pi} G^2 \rangle$  in [Ha04] and the sign of the same coefficient in [Al83], everything seems to be correct. The coefficient



|         | $\langle \bar{d}d \rangle$ | $\langle \frac{\alpha_s}{\pi} G^2 \rangle$                  | $\langle \bar{d}g\sigma\mathcal{G}d \rangle$                                    |
|---------|----------------------------|---|---|
| (3.3.3) | $-m_c$                     | $\frac{1}{12}$  | $-\frac{1}{2} \frac{1}{M^2} \left(1 - \frac{1}{2} \frac{m_c^2}{M^2}\right) m_c$ |
| [Ha04]  | $-m_c$                     | $\frac{1}{12} \left(\frac{3}{2} - \frac{m_c^2}{M^2}\right)$ | $-\frac{1}{2} \frac{1}{M^2} \left(1 - \frac{1}{2} \frac{m_c^2}{M^2}\right) m_c$ |
| [Mo01]  | $-m_c$                     | $\frac{1}{12}$  | $-\frac{1}{2} \frac{1}{M^2} \left(1 - \frac{1}{2} \frac{m_c^2}{M^2}\right) m_c$ |
| [Al83]  | $-m_c$                     | $-\frac{1}{12}$   | $-\frac{1}{2} \frac{1}{M^2} \left(1 - \frac{1}{2} \frac{m_c^2}{M^2}\right) m_c$ |

**Table 3.3.1:** Comparison of Borel transformed vacuum sum rules for  $D$  mesons. From (3.3.3) only the vacuum part has been listed.

for the chiral condensate  $\langle \bar{d}d \rangle$  given in [Al83] contains the factor  $(\alpha_s(\mu^2)/\alpha_s(m^2))^{4/9}$  which emerges from the renormalization group analysis of the operator product  $\bar{d}d$  under a change of the normalization point. As the quark mass also depends on the normalization point, this factor can be absorbed into the mass [Sh78]. Hence, we omitted this term.

For the in-medium OPE, which we compare in tabs. 3.3.2 and 3.3.3, we see that the agreement with [Ha00] is rather poor. In contrast, apart from the Wilson coefficient of  $\langle \frac{\alpha_s}{\pi} \left( \frac{(vG)^2}{v^2} - \frac{G^2}{4} \right) \rangle$  where we obtain some additional terms, the consistency with [Zs06] becomes apparent. Unfortunately, it is not possible to compare directly our in-medium OPE to that of [Mo01], as it is somehow hidden in their work. Nevertheless, for the unprojected OPE, which one obtains before introducing physical condensates, the lowest order term in an expansion in the quark mass  $m_d$  is given. Although, this is less meaningful, because many calculations still have to be done from this point on, we compare our results of the same status of evaluations with their results. Using (A.28) as well as (A.30) we obtain from (3.2.70) up to lowest order in  $m_d$

$$\begin{aligned}
\Pi^{(2)}(q) = & \langle : \bar{d}d : \rangle \frac{m_c}{q^2 - m_c^2} - \langle : \bar{d}\vec{D}_\mu d : \rangle i \frac{2m_c q^\mu}{(q^2 - m_c^2)^2} \\
& - \langle : \bar{d}\gamma_\lambda d : \rangle \frac{q^\lambda}{q^2 - m_c^2} + i \langle : \bar{d}\gamma_\lambda \vec{D}_\mu d : \rangle 2 \frac{q^\mu q^\lambda}{(q^2 - m_c^2)^2} \\
& - \langle : \bar{d}\vec{D}_\mu \vec{D}_\nu d : \rangle 4 \frac{m_c q^\mu q^\nu}{(q^2 - m_c^2)^3} + \langle : \bar{d}\gamma_\lambda \vec{D}_\mu \vec{D}_\nu d : \rangle 4 \frac{q^\mu q^\nu q^\lambda}{(q^2 - m_c^2)^3} \\
& - \langle : \bar{d}g\sigma_{\alpha\beta}\mathcal{G}_{\mu\nu}d : \rangle \frac{m_c}{4} \frac{g^{\alpha\mu}g^{\beta\nu} - g^{\alpha\nu}g^{\beta\mu}}{(q^2 - m_c^2)^2} - \langle : \bar{d}\gamma_\lambda \sigma\mathcal{G}d : \rangle \frac{q^\lambda}{(q^2 - m_c^2)^2}, \quad (3.3.5)
\end{aligned}$$

where the last term emerges from the Wilson coefficient of the condensates  $\langle : \bar{d}\gamma_\lambda \vec{D}_\mu \vec{D}_\nu d : \rangle$

|         | $\langle \bar{d}d \rangle$ | $\langle \frac{\alpha_s}{\pi} G^2 \rangle$ | $\langle d^+ i D_0 d \rangle$            | $\langle \frac{\alpha_s}{\pi} \left( \frac{(vG)^2}{v^2} - \frac{G^2}{4} \right) \rangle$  |
|---------|----------------------------|--|--|---|
| (3.3.3) | $-m_c$                     | $\frac{1}{12}$                             | $2 \left( \frac{m_c^2}{M^2} - 1 \right)$ | $\left( \frac{7}{18} + \frac{1}{3} \ln \frac{\mu^2 m_c^2}{M^4} - \frac{2\gamma_E}{3} \right) \left( \frac{m_c^2}{M^2} - 1 \right) - \frac{2}{3} \frac{m_c^2}{M^2}$  |
| [Ha00]  | $-\frac{m_c}{2}$           | $\frac{1}{24} - \frac{m_c^2}{48M^2}$       | $\left( \frac{m_c^2}{M^2} - 1 \right)$   | $\frac{1}{6} \left( \frac{4}{3} - \frac{m_c^2}{6M^2} + \frac{m_c^6}{2M^6} + \left( 1 - \frac{m_c^2}{M^2} \right) \ln \left( \frac{m_c^2}{4\pi\mu^2} \right) \right. \\ \left. + e^{m_c^2/M^2} \left( -2\gamma_E - \ln \frac{m_c^2}{M^2} + \int_0^{\frac{m_c^2}{M^2}} dt \frac{1-e^{-t}}{t} \right) \right)$ |
| [Zs06]  | $-m_c$                     | $\frac{1}{12}$                             | $2 \left( \frac{m_c^2}{M^2} - 1 \right)$ | $\left( \frac{7}{18} + \frac{1}{3} \ln \frac{\mu^2}{m_c^2} \right) \left( \frac{m_c^2}{M^2} - 1 \right)$  |

**Table 3.3.2:** Comparison of Borel transformed in-medium sum rules for D mesons (even part) up to mass dimension 4.

|                         | (3.3.4) | [Ha00] | [Zs06] |
|-------------------------|---------|--------|--------|
| $\langle d^+ d \rangle$ | 1       | (*)    | 1      |

**Table 3.3.3:** Comparison of Borel transformed in-medium sum rules for D mesons (odd part) up to mass dimension 4. We cited [Ha00] as (\*), because it is not clear whether the odd part is considered or not.

and  $\langle : \bar{d} g \gamma_5 \gamma_\alpha \mathcal{G}_{\mu\nu} d : \rangle^8$ . The result given in [Mo01] reads

$$\begin{aligned}
\Pi^{(2)}(q) = & -\langle : \bar{d} \vec{D}_\mu d : \rangle i \frac{2m_c q^\mu}{(q^2 - m_c^2)^2} \\
& - \langle : \bar{d} \gamma_\lambda d : \rangle \frac{q^\lambda}{q^2 - m_c^2} + i \langle : \bar{d} \gamma_\lambda \vec{D}_\mu d : \rangle 2 \frac{q^\mu q^\lambda}{(q^2 - m_c^2)^2} \\
& - \langle : \bar{d} \vec{D}_\mu \vec{D}_\nu d : \rangle 4 \frac{m_c q^\mu q^\nu}{(q^2 - m_c^2)^3} + \langle : \bar{d} \gamma_\lambda \vec{D}_\mu \vec{D}_\nu d : \rangle 4 \frac{q^\mu q^\nu q^\lambda}{(q^2 - m_c^2)^3} \\
& - \langle : \bar{d} \gamma_\lambda \sigma \mathcal{G} d : \rangle \frac{1}{3} \frac{q^\lambda q^2}{(q^2 - m_c^2)^3}, \tag{3.3.6}
\end{aligned}$$

where the authors omitted the vacuum terms  $\langle : \bar{d} d : \rangle$  and  $\langle : \bar{d} g \sigma_{\alpha\beta} \mathcal{G}_{\mu\nu} d : \rangle$ , and only listed the additional in-medium contributions. We see there is a mismatch in the Wilson coefficient of the last term. The origin of this mismatch is unclear.

<sup>8</sup>The derivation of (3.2.29) only uses the property of  $v_\mu$  being a four-vector. Hence, one could also use the external momentum  $q_\mu$  for projection.

### 3.3.3 Perturbative Term

In order to write down the sum rules we make the assumption, that the large momentum contribution of  $\Delta\Pi_{OPE}(q)$  is mostly determined by the perturbative part of  $\Pi(q)$ . Hence, we assume

$$\begin{aligned}
& \frac{1}{\pi} \left( \int_{-\infty}^{s_0^-} + \int_{s_0^+}^{+\infty} \right) ds \Delta\Pi_{OPE}(s, \vec{q}) s e^{-s^2/M^2} \\
& \approx \frac{1}{\pi} \left( \int_{-\infty}^{s_0^-} + \int_{s_0^+}^{+\infty} \right) ds \Delta\Pi_{per}(s, \vec{q}) s e^{-s^2/M^2} \\
& = \frac{1}{\pi} \left( \int_{-\infty}^{s_0^-} + \int_{s_0^+}^{+\infty} \right) ds \text{Im}\Pi_{per}(s, \vec{q}) s e^{-s^2/M^2} \\
& = \frac{1}{2\pi} \left( \int_{(s_0^+)^2}^{+\infty} + \int_{(s_0^-)^2}^{+\infty} \right) ds \text{Im}\Pi_{per}(s, \vec{q}) e^{-s/M^2}, \tag{3.3.7}
\end{aligned}$$

where we have used (2.2.38) in the second last line and substituted  $s^2 \rightarrow s$  in the last line. Similarly, we obtain for the odd part

$$\begin{aligned}
& \frac{1}{\pi} \left( \int_{-\infty}^{s_0^-} + \int_{s_0^+}^{+\infty} \right) ds \Delta\Pi_{OPE}(s, \vec{q}) e^{-s^2/M^2} \\
& \approx \frac{1}{\pi} \left( \int_{-\infty}^{s_0^-} + \int_{s_0^+}^{+\infty} \right) ds \Delta\Pi_{per}(s, \vec{q}) e^{-s^2/M^2} \\
& = \frac{1}{2\pi} \left( \int_{(s_0^+)^2}^{+\infty} - \int_{(s_0^-)^2}^{+\infty} \right) ds \frac{1}{\sqrt{s}} \text{Im}\Pi_{per}(s, \vec{q}) e^{-s/M^2}. \tag{3.3.8}
\end{aligned}$$

Note that the integral over the perturbative contribution of the current-current correlation function given in (3.3.8) cancels from the spectral integral for the odd dispersion relation (2.6.29) if equal threshold parameters are assumed.

### 3.3.4 Pole + Continuum Ansatz

Furthermore, we employ the so called "pole + continuum" ansatz, see fig. 3.3.1. It consists of the assumption that only the lowest lying excitations contribute to the low-momentum properties of  $\Delta\Pi(q)$ . Higher excitations are described by the perturbative continuum. The last argument already led us to the results obtained in section 2.5 and to the relations (3.3.7) and (3.3.8). In the following we are working in the rest frame of the medium with the D meson being at rest,  $\vec{p}_\Omega = \vec{q} = 0$ . This means  $\Delta\Pi_{ph}(q)$  can be approximated from (2.2.12) by

$$\Delta\Pi_{ph}(s) = \pi F_+ \delta(s - (M_+ - M_\Omega)) - \pi F_- \delta(s + (M_- - M_\Omega)), \tag{3.3.9}$$

where we have introduced  $F_\pm = (2\pi)^3 \left| \langle \Omega | j^{(\dagger)}(0) | \alpha \rangle \right|^2$  and the subscript "minus" refers to the matrix element of the adjoint current,  $p_\alpha = (M_\alpha, \vec{0})$  and  $p_\Omega = (M_\Omega, \vec{0})$ . Hence, only

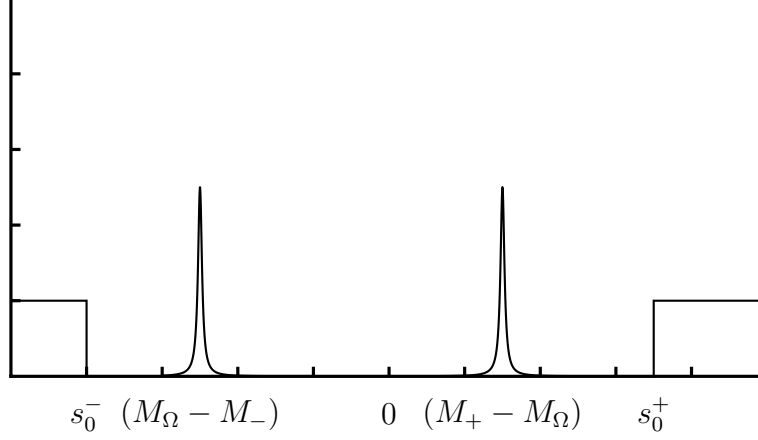


**Figure 3.3.1:** Schematic plot of  $\Delta\Pi^{ph}(s, \vec{0})$  as a function of  $s$  in the "pole + continuum" approximation.

the lowest lying excitation contributes as pole in our spectral function  $\Delta\Pi_{ph}(s)$ , while all higher excitations are modeled by the continuum. Assuming equal threshold parameters,  $s_0^+ = -s_0^- = \sqrt{s_0}$ , (3.3.7) together with (2.6.28) eventually leads us to the following relation for the even part

$$\begin{aligned} \mathcal{B} \left[ \Pi_{OPE}^e(\omega^2, \vec{0}) \right] (M^2) &= (M_+ - M_\Omega) F_+ e^{-(M_+ - M_\Omega)^2/M^2} + (M_- - M_\Omega) F_- e^{-(M_- - M_\Omega)^2/M^2} \\ &+ \frac{1}{\pi} \int_{s_0}^{+\infty} ds \operatorname{Im} \Pi_{per}(s) e^{-s/M^2} \end{aligned} \quad (3.3.10)$$

and for the odd part

$$\mathcal{B} \left[ \Pi_{OPE}^o(\omega^2, \vec{0}) \right] (M^2) = F_+ e^{-(M_+ - M_\Omega)^2/M^2} - F_- e^{-(M_- - M_\Omega)^2/M^2} . \quad (3.3.11)$$

Because we have chosen equal thresholds, there is no continuum contribution in (3.3.11) and, hence, no perturbative contribution to the odd sum rules. (The odd part of the operator product expansion can not have any perturbative contributions.)

For the vacuum sum rules we choose similar to (3.3.9) an ansatz for the phenomenological part of the current-current correlation function

$$\Delta\Pi_{ph}^{vac}(s) = \pi F_+ \delta(s^{1/2} - (M_+ - M_\Omega)) - \pi F_- \delta(s^{1/2} + (M_- - M_\Omega)) . \quad (3.3.12)$$

Because the integral of the vacuum dispersion relation (2.2.25) only runs over positive values of the squared energy, the term proportional to  $\delta(s^{1/2} + (M_- - M_\Omega))$  does not contribute.<sup>9</sup> Hence, there is no antiparticle contribution to the vacuum sum rules. Using

<sup>9</sup>Remember that  $M_- - M_\Omega > 0$  because  $M_\Omega$  is the lowest lying energy eigenstate.

the scaling property of Diracs  $\delta$  distribution

$$\delta(g(x)) = \sum_i \frac{\delta(x - x_i)}{|g'(x_i)|}, \quad (3.3.13)$$

where the  $x_i$  are the roots of  $g(x)$  and the sum is running over all roots, one can write

$$\Delta\Pi_{ph}^{vac}(s) = 2\pi F_+(M_+ - M_\Omega)\delta(s - (M_+ - M_\Omega)^2). \quad (3.3.14)$$

Thus, if we define  $\widetilde{M} = M_+$  to be the vacuum D meson mass and introduce

$$\widetilde{F} = 2F_+(\widetilde{M} - M_\Omega), \quad (3.3.15)$$

the following phenomenological ansatz for  $\Delta\Pi_{ph}^{vac}(s)$  is justified

$$\Delta\Pi_{ph}^{vac}(s) = \pi\widetilde{F}\delta(s - (\widetilde{M} - M_\Omega)^2). \quad (3.3.16)$$

It is not necessary to assume the equality of the threshold parameters  $s_0^+$  and  $s_0^-$ , because the correlator only depends on  $q^2$  and, hence,  $s_0^+ = s_0^-$  is naturally fulfilled. Therefore, we get the following relation for the vacuum case

$$\begin{aligned} \mathcal{B}[\Pi_{OPE}(Q^2)](M^2) \\ = \widetilde{F}e^{-(\widetilde{M}-M_\Omega)^2/M^2} + \frac{1}{\pi} \int_{s_0}^{\infty} e^{-s/M^2} \text{Im}\Pi_{per}(s)ds. \end{aligned} \quad (3.3.17)$$

### 3.3.5 Complete Sum Rules

We conclude this section by giving the complete sum rules for the vacuum and the in-medium case up to mass dimension 5 and next-to-leading order in  $\alpha_s$ . Therefore, we introduce  $m_\pm = M_\pm - M_\Omega$  and  $\widetilde{m} = \widetilde{M} - M_\Omega$  as the D meson mass.<sup>10</sup> For the vacuum case one obtains

$$\begin{aligned} \widetilde{F}e^{-\widetilde{m}^2/M^2} + \frac{1}{\pi} \int_{s_0}^{\infty} e^{-s/M^2} \text{Im}\Pi_{per}(s)ds &= \frac{1}{\pi} \int_{m_c^2}^{\infty} ds e^{-s/M^2} \text{Im}\Pi_{per}(s) \\ &+ e^{-m_c^2/M^2} \left( -m_c \langle \bar{d}d \rangle + \frac{1}{2} \left( \frac{m_c^3}{2M^4} - \frac{m_c}{M^2} \right) \langle \bar{d}g\sigma\mathcal{G}d \rangle + \frac{1}{12} \langle \frac{\alpha_s}{\pi} G^2 \rangle \right). \end{aligned} \quad (3.3.18)$$

Hence, the vacuum sum rules up to mass dimension 5 read

$$\begin{aligned} \widetilde{F}e^{-\widetilde{m}^2/M^2} &= \frac{1}{\pi} \int_{m_c^2}^{s_0} ds e^{-s/M^2} \text{Im}\Pi_{per}(s) \\ &+ e^{-m_c^2/M^2} \left( -m_c \langle \bar{d}d \rangle + \frac{1}{2} \left( \frac{m_c^3}{2M^4} - \frac{m_c}{M^2} \right) \langle \bar{d}g\sigma\mathcal{G}d \rangle + \frac{1}{12} \langle \frac{\alpha_s}{\pi} G^2 \rangle \right). \end{aligned} \quad (3.3.19)$$

<sup>10</sup>Actually, we have  $M_\Omega = 0$  for the vacuum sum rules, because the vacuum ground state has zero energy (see section 2.1).

Likewise, we get for the even part of the in-medium sum rules up to mass dimension 5

$$\begin{aligned}
m_+ F_+ e^{-m_+^2/M^2} + m_- F_- e^{-m_-^2/M^2} &= \frac{1}{\pi} \int_{m_c^2}^{s_0} ds e^{-s/M^2} \text{Im}\Pi_{per}(s) \\
&+ e^{-m_c^2/M^2} \left( -m_c \langle \bar{d}d \rangle + \frac{1}{2} \left( \frac{m_c^3}{2M^4} - \frac{m_c}{M^2} \right) \langle \bar{d}g\sigma\mathcal{G}d \rangle + \frac{1}{12} \langle \frac{\alpha_s}{\pi} G^2 \rangle \right. \\
&+ \left[ \left( \frac{7}{18} + \frac{1}{3} \ln \frac{\mu^2 m_c^2}{M^4} - \frac{2\gamma_E}{3} \right) \left( \frac{m_c^2}{M^2} - 1 \right) - \frac{2}{3} \frac{m_c^2}{M^2} \right] \langle \frac{\alpha_s}{\pi} \left( \frac{(vG)^2}{v^2} - \frac{G^2}{4} \right) \rangle \\
&\left. + 2 \left( \frac{m_c^2}{M^2} - 1 \right) \langle d^\dagger i D_0 d \rangle + 4 \left( \frac{m_c^3}{2M^4} - \frac{m_c}{M^2} \right) \left[ \langle \bar{d}D_0^2 d \rangle - \frac{1}{8} \langle \bar{d}g\sigma\mathcal{G}d \rangle \right] \right) , \quad (3.3.20)
\end{aligned}$$

and for the odd part

$$\begin{aligned}
F_+ e^{-m_+^2/M^2} - F_- e^{-m_-^2/M^2} \\
= +e^{-m_c^2/M^2} \left( \langle d^\dagger d \rangle - 4 \left( \frac{m_c^2}{2M^4} - \frac{1}{M^2} \right) \langle d^\dagger D_0^2 d \rangle - \frac{1}{M^2} \langle d^\dagger g\sigma\mathcal{G}d \rangle \right) . \quad (3.3.21)
\end{aligned}$$

In all the above equations  $\text{Im}\Pi_{per}(s)$  is defined in (3.2.13). These are the desired relations to relate the D meson mass to the QCD condensates. For simplicity, we rewrite (3.3.20) and (3.3.21) as

$$m_+ F_+ e^{-m_+^2/M^2} + m_- F_- e^{-m_-^2/M^2} \equiv f(M, s_0, m_c, \mu) , \quad (3.3.22a)$$

$$F_+ e^{-m_+^2/M^2} - F_- e^{-m_-^2/M^2} \equiv g(M, m_c) , \quad (3.3.22b)$$

where we did not explicitly label the dependence of the functions  $f$  and  $g$  on the condensates.

In order to obtain equations for the D meson mass  $\tilde{m}$  for the vacuum sum rule, we take a derivative of (3.3.19) with respect to  $1/M^2$  and divide by (3.3.19) giving

$$\begin{aligned}
-\tilde{m}^2 &= \left[ -\frac{1}{\pi} \int_{m_c^2}^{s_0} ds s e^{-s/M^2} \text{Im}\Pi_{per}(s) + e^{-m_c^2/M^2} \frac{1}{2} \left( \frac{m_c^3}{M^2} - m_c \right) \langle \bar{d}g\sigma\mathcal{G}d \rangle \right. \\
&- m_c^2 e^{-m_c^2/M^2} \left( -m_c \langle \bar{d}d \rangle + \frac{1}{2} \left( \frac{m_c^3}{2M^4} - \frac{m_c}{M^2} \right) \langle \bar{d}g\sigma\mathcal{G}d \rangle + \frac{1}{12} \langle \frac{\alpha_s}{\pi} G^2 \rangle \right) \Big] \\
&\times \left[ \frac{1}{\pi} \int_{m_c^2}^{s_0} ds e^{-s/M^2} \text{Im}\Pi_{per}(s) + e^{-m_c^2/M^2} \left( -m_c \langle \bar{d}d \rangle + \frac{1}{12} \langle \frac{\alpha_s}{\pi} G^2 \rangle \right. \right. \\
&\left. \left. + \frac{1}{2} \left( \frac{m_c^3}{2M^4} - \frac{m_c}{M^2} \right) \langle \bar{d}g\sigma\mathcal{G}d \rangle \right) \right]^{-1} . \quad (3.3.23)
\end{aligned}$$

In doing so, we have assumed that the resonance mass  $\tilde{m}$ , considered as physical quantity, does not depend on the Borel mass  $M^2$ .

In order to give expressions for the D meson mass  $m_\pm$  for the in-medium sum rules, we derive from (3.3.22)

$$(m_+ + m_-) F_+ e^{-m_+^2/M^2} = f(M, s_0, m_c, \mu) + m_- g(M, m_c) , \quad (3.3.24a)$$

$$(m_+ + m_-) F_- e^{-m_-^2/M^2} = f(M, s_0, m_c, \mu) - m_+ g(M, m_c) . \quad (3.3.24b)$$

Taking a derivative of (3.3.24) with respect to  $1/M^2$ , again assuming that the D meson masses  $m_{\pm}$  do not depend on the Borel mass  $M^2$ , and dividing each resulting equation by the corresponding equation of (3.3.24) yields the following system of coupled, non-linear equations for the masses  $m_{\pm}$  in medium

$$-m_+^2 = \frac{\frac{d}{d(1/M^2)}f(M, s_0, m_c, \mu) + m_- \frac{d}{d(1/M^2)}g(M, m_c)}{f(M, s_0, m_c, \mu) + m_- g(M, m_c)}, \quad (3.3.25a)$$

$$-m_-^2 = \frac{\frac{d}{d(1/M^2)}f(M, s_0, m_c, \mu) - m_+ \frac{d}{d(1/M^2)}g(M, m_c)}{f(M, s_0, m_c, \mu) - m_+ g(M, m_c)}. \quad (3.3.25b)$$

The Borel mass  $M^2$  and the threshold parameter  $s_0$  enter the coefficient functions  $f$  and  $g$  for the in-medium sum rules as well as the vacuum sum rule (3.3.23). They have to be fixed numerically according to appropriate physical requirements.

In the limit of vanishing density, we deduce the vacuum sum rules from (3.3.25). In this case one has  $g = 0$  and  $f$  reduces to the r.h.s. of (3.3.19). Therefore, (3.3.25) reduces to (3.3.23). From (3.3.21) we derive  $F_+ e^{-m_+^2/M^2} = F_- e^{-m_-^2/M^2}$ . Taking one derivative with respect to  $1/M^2$  of this expression, we observe that  $m_-^2 = m_+^2$  and, hence,  $F_- = F_+$ . Inserting these results into the zero density limit of (3.3.20), where the r.h.s. simply reduces to the vacuum OPE, we rediscover the vacuum sum rule (3.3.19).

Rewriting these equations as polynomials in the masses  $m_+$  and  $m_-$

$$0 = -m_+^2 f(M, s_0, m_c, \mu) - m_+^2 m_- g(M, m_c) - \frac{d}{d(1/M^2)}f(M, s_0, m_c, \mu) - m_- \frac{d}{d(1/M^2)}g(M, m_c), \quad (3.3.26a)$$

$$0 = -m_-^2 f(M, s_0, m_c, \mu) + m_-^2 m_+ g(M, m_c) - \frac{d}{d(1/M^2)}f(M, s_0, m_c, \mu) + m_+ \frac{d}{d(1/M^2)}g(M, m_c), \quad (3.3.26b)$$

we can derive equations that are more handsome for calculations than the non-linear system of equations in (3.3.25). The latter ones would require numerical procedures. Subtracting (3.3.26b) from (3.3.26a) on the one hand side and summing the products of (3.3.26a) with  $m_-$  and (3.3.26b) with  $m_+$  on the other side, we derive the following system of linear equations for  $\Delta m$  and  $m_+ m_-$

$$0 = -2\Delta m f(M, s_0, m_c, \mu) - m_+ m_- g(M, m_c) - \frac{d}{d(1/M^2)}g(M, m_c), \quad (3.3.27a)$$

$$0 = -m_+ m_- f(M, s_0, m_c, \mu) + 2\Delta m \frac{d}{d(1/M^2)}g(M, m_c) - \frac{d}{d(1/M^2)}f(M, s_0, m_c, \mu). \quad (3.3.27b)$$

Here we have introduced the following quantities

$$\Delta m = \frac{1}{2}(m_+ - m_-), \quad \bar{m} = \frac{1}{2}(m_+ + m_-). \quad (3.3.28)$$

Therefore, we have

$$m_{\pm} = \bar{m} \pm \Delta m, \quad \bar{m}^2 = \Delta m^2 + m_+ m_- \quad (3.3.29)$$

and the solution of (3.3.27) reads

$$\Delta m = \frac{1}{2} \frac{g(M, m_c) \frac{d}{d(1/M^2)} f(M, s_0, m_c, \mu) - f(M, s_0, m_c, \mu) \frac{d}{d(1/M^2)} g(M, m_c)}{f^2(M, s_0, m_c, \mu) + g(M, m_c) \frac{d}{d(1/M^2)} g(M, m_c)}, \quad (3.3.30)$$

$$m_+ m_- = - \frac{f(M, s_0, m_c, \mu) \frac{d}{d(1/M^2)} f(M, s_0, m_c, \mu) + \left( \frac{d}{d(1/M^2)} g(M, m_c) \right)^2}{f^2(M, s_0, m_c, \mu) + g(M, m_c) \frac{d}{d(1/M^2)} g(M, m_c)}. \quad (3.3.31)$$

Hence, the meson masses are given by

$$\begin{aligned} \bar{m} = & \left[ \frac{1}{4} \left( \frac{g(M, m_c) \frac{d}{d(1/M^2)} f(M, s_0, m_c, \mu) - f(M, s_0, m_c, \mu) \frac{d}{d(1/M^2)} g(M, m_c)}{f^2(M, s_0, m_c, \mu) + g(M, m_c) \frac{d}{d(1/M^2)} g(M, m_c)} \right)^2 \right. \\ & \left. - \frac{f(M, s_0, m_c, \mu) \frac{d}{d(1/M^2)} f(M, s_0, m_c, \mu) + \left( \frac{d}{d(1/M^2)} g(M, m_c) \right)^2}{f^2(M, s_0, m_c, \mu) + g(M, m_c) \frac{d}{d(1/M^2)} g(M, m_c)} \right]^{\frac{1}{2}}, \end{aligned} \quad (3.3.32a)$$

$$\begin{aligned} m_+ = & \left[ \frac{1}{4} \left( \frac{g(M, m_c) \frac{d}{d(1/M^2)} f(M, s_0, m_c, \mu) - f(M, s_0, m_c, \mu) \frac{d}{d(1/M^2)} g(M, m_c)}{f^2(M, s_0, m_c, \mu) + g(M, m_c) \frac{d}{d(1/M^2)} g(M, m_c)} \right)^2 \right. \\ & \left. - \frac{f(M, s_0, m_c, \mu) \frac{d}{d(1/M^2)} f(M, s_0, m_c, \mu) + \left( \frac{d}{d(1/M^2)} g(M, m_c) \right)^2}{f^2(M, s_0, m_c, \mu) + g(M, m_c) \frac{d}{d(1/M^2)} g(M, m_c)} \right]^{\frac{1}{2}} \\ & + \frac{1}{2} \frac{g(M, m_c) \frac{d}{d(1/M^2)} f(M, s_0, m_c, \mu) - f(M, s_0, m_c, \mu) \frac{d}{d(1/M^2)} g(M, m_c)}{f^2(M, s_0, m_c, \mu) + g(M, m_c) \frac{d}{d(1/M^2)} g(M, m_c)}, \end{aligned} \quad (3.3.32b)$$

$$\begin{aligned} m_- = & \left[ \frac{1}{4} \left( \frac{g(M, m_c) \frac{d}{d(1/M^2)} f(M, s_0, m_c, \mu) - f(M, s_0, m_c, \mu) \frac{d}{d(1/M^2)} g(M, m_c)}{f^2(M, s_0, m_c, \mu) + g(M, m_c) \frac{d}{d(1/M^2)} g(M, m_c)} \right)^2 \right. \\ & \left. - \frac{f(M, s_0, m_c, \mu) \frac{d}{d(1/M^2)} f(M, s_0, m_c, \mu) + \left( \frac{d}{d(1/M^2)} g(M, m_c) \right)^2}{f^2(M, s_0, m_c, \mu) + g(M, m_c) \frac{d}{d(1/M^2)} g(M, m_c)} \right]^{\frac{1}{2}} \\ & - \frac{1}{2} \frac{g(M, m_c) \frac{d}{d(1/M^2)} f(M, s_0, m_c, \mu) - f(M, s_0, m_c, \mu) \frac{d}{d(1/M^2)} g(M, m_c)}{f^2(M, s_0, m_c, \mu) + g(M, m_c) \frac{d}{d(1/M^2)} g(M, m_c)}, \end{aligned} \quad (3.3.32c)$$

where the functions  $f(M, s_0, m_c, \mu)$  and  $g(M, m_c)$  are defined in (3.3.20), (3.3.21) and (3.3.22).



### 3.4 Numerical Evaluations

We now turn to the numerical analysis of the sum rules, i.e. equations (3.3.32) and (3.3.31). We will only use the in-medium equations, because, as shown in section 3.3.5, the vacuum case is naturally reproduced by the zero density limit of the in-medium sum rules.

#### 3.4.1 Parameters

We will work in linear density approximation in order to estimate in-medium values for the condensates, i.e.

$$\langle \hat{O} \rangle = \langle \hat{O} \rangle_{vac} + n \langle \hat{O} \rangle_{med}, \quad (3.4.1)$$

where we denoted the medium density by  $n$ . The following parameterizations are used [Ji93]

$$\langle \bar{d}d \rangle = \langle \bar{d}d \rangle_{vac} + \frac{\sigma_N}{2m_q} n, \quad (3.4.2a)$$

$$\langle \frac{\alpha_s}{\pi} G^2 \rangle = \langle \frac{\alpha_s}{\pi} G^2 \rangle_{vac} - \frac{8M_N^0}{9} n, \quad (3.4.2b)$$

$$\langle \bar{d}g\sigma\mathcal{G}d \rangle = \lambda^2 \langle \bar{d}d \rangle, \quad (3.4.2c)$$

$$\langle d^\dagger d \rangle = \frac{3}{2} n, \quad (3.4.2d)$$

$$\langle \frac{\alpha_s}{\pi} \left( \frac{(vG)^2}{v^2} - \frac{G^2}{4} \right) \rangle = -\frac{3}{4} M_N \alpha_s(\mu^2) A_2^g(\mu^2) n, \quad (3.4.2e)$$

$$\langle d^\dagger iD_0 d \rangle = \frac{3}{8} M_N A_2^g(\mu^2) n, \quad (3.4.2f)$$

$$\left[ \langle \bar{d}D_0^2 d \rangle - \frac{1}{8} \langle \bar{d}g\sigma\mathcal{G}d \rangle \right] = \frac{\lambda^2 \sigma_N}{2m_q} n, \quad (3.4.2g)$$

$$\langle d^\dagger g\sigma\mathcal{G}d \rangle = (-0.33 \text{ GeV}^2) n, \quad (3.4.2h)$$

$$\langle d^\dagger D_0^2 d \rangle = -\frac{1}{4} M_N^2 A_3^g(\mu^2) n + \frac{1}{12} \langle d^\dagger g\sigma\mathcal{G}d \rangle. \quad (3.4.2i)$$

We further use the nucleon sigma term  $\sigma_N = 0.045 \text{ GeV}$ , the average light quark mass  $m_q = 0.007 \text{ GeV}$ , the nucleon mass  $M_N = 0.939 \text{ GeV}$ ,  $M_N^0 = 0.77 \text{ GeV}$ ,  $\lambda^2 = 0.8 \text{ GeV}^2$ ,  $\alpha_s(1 \text{ GeV}^2) = 0.5$ ,  $A_2^g(1 \text{ GeV}^2) = 0.5$ ,  $A_2^q(1 \text{ GeV}^2) = 0.5$  and  $A_3^q(1 \text{ GeV}^2) = 0.14$ . Also, we use the standard value for the chiral vacuum condensate  $\langle \bar{d}d \rangle_{vac} = (-0.245 \text{ GeV})^3$ , the gluon condensate  $\langle \frac{\alpha_s}{\pi} G^2 \rangle_{vac} = (0.33 \text{ GeV})^4$  and a charm quark mass of  $m_c = 1.45 \text{ GeV}$ . We work at a renormalization point  $\mu = 1 \text{ GeV}$  and the medium density at nuclear matter saturation density is taken to be  $n = 0.17 \text{ fm}^{-3}$ .

#### 3.4.2 Area of Validity of the Sum Rules

The validity of (3.3.20) and (3.3.21) in the Borel plane is limited. Partly following [Le97, Ha04], we derive conditions which quantify the area of validity of the sum rules. On the one

hand side, we have to ensure that the "pole + continuum" ansatz sufficiently reproduces the features of the hadronic spectrum. This means, the approximation of higher excitations by a continuum, calculated from the perturbative contribution, to the current-current correlator, should not have too much influence to the result. Therefore, the weighting function in the spectral integral plays in our hand because it allows for an exponential suppression of higher excitations and errors caused by the continuum approximation. The maximum Borel mass is determined so that the continuum contribution to the spectral integral is smaller than the pole contribution to the spectral integral. This gives us the following condition for the maximum Borel mass  $M_{max}$

$$1 \geq \frac{\frac{1}{\pi} \int_{s_0}^{\infty} ds \text{Im}\Pi_{per}(s) e^{-s/M_{max}^2}}{m_+ F_+ e^{-m_+^2/M_{max}^2} + m_- F_- e^{-m_-^2/M_{max}^2}}. \quad (3.4.3)$$

Using (3.3.20) this can be written as

$$1 \geq \frac{\frac{1}{\pi} \int_{s_0}^{\infty} ds \text{Im}\Pi_{per}(s) e^{-s/M_{max}^2}}{f(M_{max}, s_0, m_c, \mu)}. \quad (3.4.4)$$

On the other side, we know from section 2.3 that the operator product expansion of the non-local operator product  $A(x)B(y)$  approximates the divergent operator product for  $y \rightarrow x$  best, if the series is truncated at a certain  $N$ . The value of  $N$  depends on the distance  $x - y$ . As we have calculated the OPE up to a certain mass dimension, i.e.  $N = 5$ , we now seek the appropriate distance at which the OPE is a good approximation to the operator product. This translates into a restriction to the validity of (3.3.20) and (3.3.21) within the Borel plane. We demand, that the terms with the highest mass dimension, i.e. mass dimension 5, do not contribute more than 10% to the OPE. This gives us the following two inequalities for the lower bound  $M_{min}$  of the Borel window

$$0.1 \geq \frac{e^{-m_c^2/M_{min}^2} \left( \frac{m_c^3}{4M_{min}^4} \langle \bar{d}g\sigma\mathcal{G}d \rangle + 2\frac{m_c^3}{M_{min}^4} [\langle \bar{d}D_0^2d \rangle - \frac{1}{8} \langle \bar{d}g\sigma\mathcal{G}d \rangle] \right)}{\frac{1}{\pi} \int_{s_0}^{\infty} ds \text{Im}\Pi_{per}(s) e^{-s/M_{min}^2} + f(M_{min}, s_0, m_c, \mu)}, \quad (3.4.5a)$$

$$0.1 \geq \frac{e^{-m_c^2/M_{min}^2} 2\frac{m_c^2}{M_{min}^4} \langle d^+ D_0^2 d \rangle}{g(M_{min}, m_c)}. \quad (3.4.5b)$$

The integral term in the denominator of the first equation has been added in order to cancel the continuum contribution in  $f(M, s_0, m_c, \mu)$ , because it is not part of the OPE. Hence,  $M_{min}$  does not depend on the threshold  $s_0$ .

### 3.4.3 Vacuum Borel Curves

We plot different curves for the D meson mass as a function of the Borel mass  $M$  and vary the threshold (fig. 3.4.1), the charm quark mass (fig. 3.4.2) and the chiral vacuum condensate (fig. 3.4.3) for the purpose of examining their importance and influence on the Borel curves. In each diagram of this and the next section we also indicate the Borel windows by vertical lines.

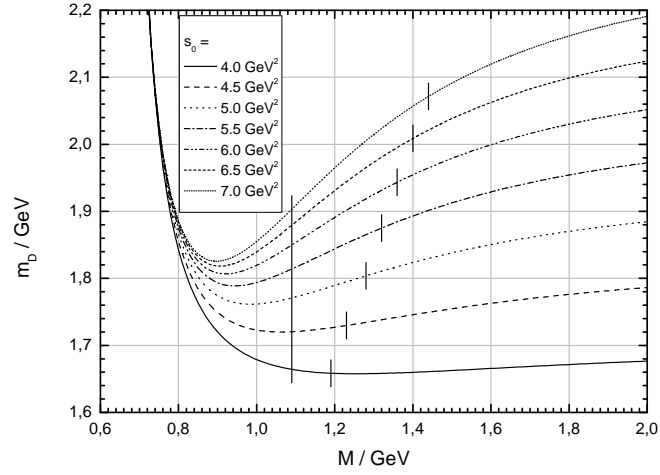


**Figure 3.4.1:** Pole masses  $m_D$  for different thresholds  $s_0$  at  $m_c = 1.45 \text{ GeV}$  and  $\langle \bar{q}q \rangle_{vac} = (-0.245 \text{ GeV})^3$ .

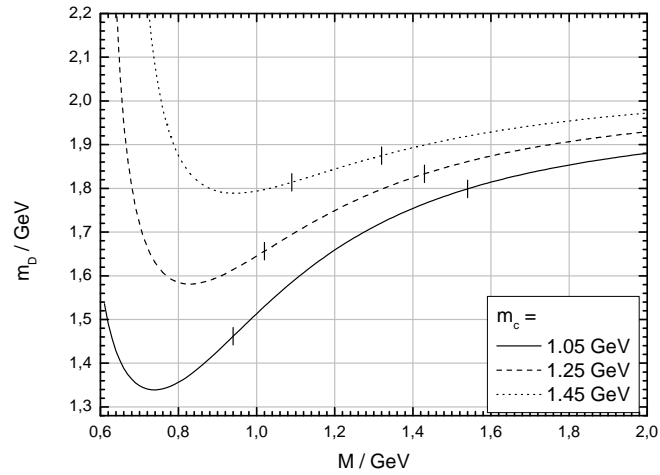


**Figure 3.4.2:** Pole masses  $m_D$  at different charm masses  $m_c$  for  $s_0 = 5.5 \text{ GeV}^2$  and  $\langle \bar{q}q \rangle_{vac} = (-0.245 \text{ GeV})^3$ .

From the graphs in fig. 3.4.1 and 3.4.2 we see the mass parameter  $m_D$  grows with growing thresholds and charm quark masses. The Borel maximum increases with increasing threshold but decreases with increasing charm quark mass. While the Borel minimum does not depend on the threshold, as expected from the equations in section 3.4.2, it increases with increasing charm quark mass. Hence, the validity of (3.3.20) and (3.3.21) is rapidly getting lost with growing charm quark mass. Furthermore, there are plateaus within the Borel windows for smaller thresholds and the minima of the Borel curves are shifted out of the Borel windows for growing thresholds. On the other side, we learn from fig. 3.4.2 that the Borel curves are getting flatter within the Borel window when going to higher charm quark masses. We also expect that the minima of the Borel curves can not be shifted into the Borel windows by varying the charm quark mass.

From fig. 3.4.3 we learn that the mass parameter  $m_D$  grows with decreasing absolute value of the chiral vacuum condensate. Furthermore, a change of the chiral vacuum condensate has only little influence on the width of the Borel window, but results in a shift to higher values for higher absolute values of the vacuum condensate. The minima of the Borel curves are slightly shifted to higher Borel masses and lower pole masses. If we compare with the shift of the Borel window, we see that, varying the chiral condensate, can not shift the minima to Borel masses within the Borel window.

In fig. 3.4.4 we display the D meson mass for different Wilson coefficients switched off in order to determine the importance of the corresponding condensates for the sum rules.

We observe that switching off the chiral condensate has almost no influence to the vacuum pole mass as a function of the Borel mass, but significantly changes the Borel window. The Borel minimum is higher and the Borel maximum much smaller. The branch of reliability is, hence, strongly determined by the chiral condensate while the function itself remains numerically unchanged.<sup>11</sup>

Switching off the gluon condensate, has almost no influence on the Borel window. Within the Borel window  $m_D$  changes less and the curve lies slightly below the curve for the complete sum rule. For Borel masses larger than the above defined Borel maximum the curves are almost equal, and the curve for switched off gluon condensate lies slightly above the curve for the complete sum rule. On the other hand, for Borel masses below the Borel minimum, the curve for switched off gluon condensate has a complete different behavior. It is strictly monotonic increasing, while the curve for the complete sum rule has a minimum at these Borel masses.

Finally, switching off the mixed quark-gluon condensate slightly reduces the Borel window, by increasing the Borel minimum and decreasing the Borel maximum. The curve generally lies far above the curve for the complete sum rule, but, in principle, has the same behavior. Within the Borel window, the curve for switched off mixed quark-gluon condensate is almost flat compared to the curve for the complete sum rule. The latter one increases nearly linearly over the whole Borel window, while the first one even decreases at the lower bound of the Borel window.

<sup>11</sup>This is not in contrast to the conclusions we draw from fig. 3.4.3. The chiral condensate enters via its Wilson coefficient and via the parametrization of the mixed quark-gluon condensate (3.4.2c). Varying the chiral condensate, also changes the mixed quark-gluon condensate. If the Wilson coefficient is switched off, the influence of the chiral condensate can be tested independent of the parametrization.

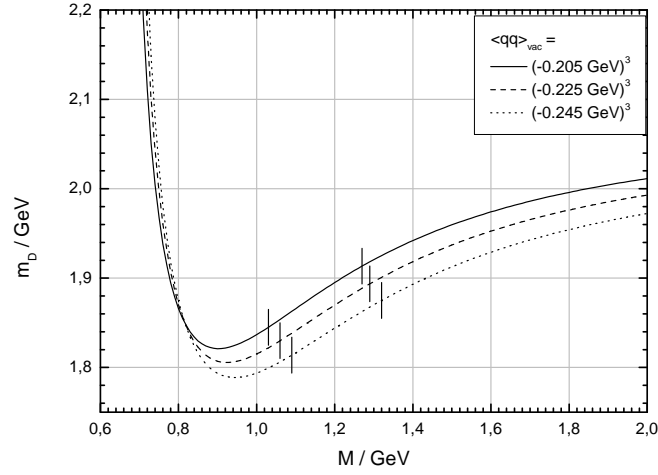


**Figure 3.4.3:** Pole masses  $m_D$  for different chiral vacuum condensates  $\langle \bar{q}q \rangle_{vac}$  at  $s_0 = 5.5 \text{ GeV}^2$  and  $m_c = 1.45 \text{ GeV}$ .

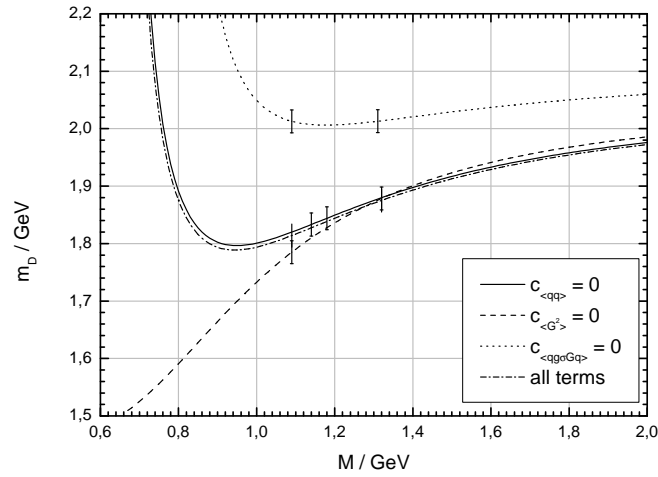


**Figure 3.4.4:** Pole masses  $m_D$  for different Wilson coefficients switched off at  $s_0 = 5.5 \text{ GeV}^2$ ,  $m_c = 1.45 \text{ GeV}$  and  $\langle \bar{q}q \rangle_{vac} = (-0.245 \text{ GeV})^3$ .

For the formation of a minimum of the Borel curve the gluon condensate seems to be most important, while the mixed quark-gluon condensate is of minor importance, and the influence of the chiral condensate to the formation of a minimum is negligible.

We conclude that the chiral vacuum condensate has the biggest influence on the validity of the vacuum sum rule which expresses its role as the next-to-leading order term in the OPE, but is of minor importance for the Borel curve itself, i.e. the mass parameter  $m_D$  as a function of the Borel mass. In contrast, the gluon condensate and the mixed quark-gluon condensate have only little influence on the validity of the sum rule. The gluon condensate is of severe importance for the shape of the Borel curve for small Borel masses, but the mixed quark-gluon condensate has an essential influence on the vertical position of the Borel curve and its shape and numerical values within the Borel window. Hence, it is the most important term for the determination of the vacuum D meson mass, apart from the perturbative one.

From fig. 3.4.1 and 3.4.2 we infer that the D meson mass strongly depends on the choice of the parameters  $s_0$  and  $m_c$ . The dependence on the latter one is not a surprise, but the dependence on the threshold  $s_0$  reveals the dependence of the result, which is obtained for the D meson mass, on the method or arguments which are employed to determine the threshold. This has also been observed in [Mo01].

Let us compare our result to the vacuum sum rule given in [Ha04]. In fig. 3.4.5 we plot a comparison between the results of [Ha04] and calculations we performed using the sum rule in [Ha04] and their parameters. We observe only a small deviation. Because the difference is rather small (increases with decreasing Borel mass) and seems to have a systematic origin, we believe there is a tiny difference in some constant that enters four-quark terms. Switching off the four-quark condensate gives a good agreement.

In fig. 3.4.6 we exhibit the Borel curves obtained from the sum rule given in [Ha04] using the parameters (3.4.2) and (3.3.32) at  $s_0 = 6.0 \text{ GeV}^2$ . We observe a not surprising deviation, due to the different Wilson coefficients for the gluon condensate (see section 3.3.2). But we see, this difference is of minor importance and does not cause large numerical deviations.

#### 3.4.4 In-Medium Borel Curves

The Borel curves for the average D meson mass  $\bar{m}$  at finite density  $n = 0.17 \text{ fm}^{-3}$  for different thresholds, the charm quark mass being  $m_c = 1.45 \text{ GeV}$  and the chiral vacuum condensate being  $\langle \bar{q}q \rangle = (-0.245 \text{ GeV})^{-3}$  are plotted in fig. 3.4.7. Their principle shape is identical to the zero density limit, but we observe there is no plateau or minimum within the Borel window for the plotted thresholds anymore. For  $s_0$  further decreasing the Borel window closes, pointing to some deficit in the definition used.

In order to simplify the comparison between the Borel curves for different densities, we plot the mass centroid parameter  $\bar{m}$  for  $m_c = 1.45 \text{ GeV}$  and  $\langle \bar{q}q \rangle_{vac} = (-0.245 \text{ GeV})^3$  in fig. 3.4.9 at threshold  $s_0 = 5.5 \text{ GeV}^2$  and at  $s_0 = 4.0 \text{ GeV}^2$  in fig. 3.4.8. Note that  $\bar{m}$  actually is the centroid of the D iso-doublet.

For  $s = 5.5 \text{ GeV}^2$  we see the Borel minimum is nearly unaffected by a density change, but the Borel maximum slightly decreases with increasing density. Furthermore, we ob-

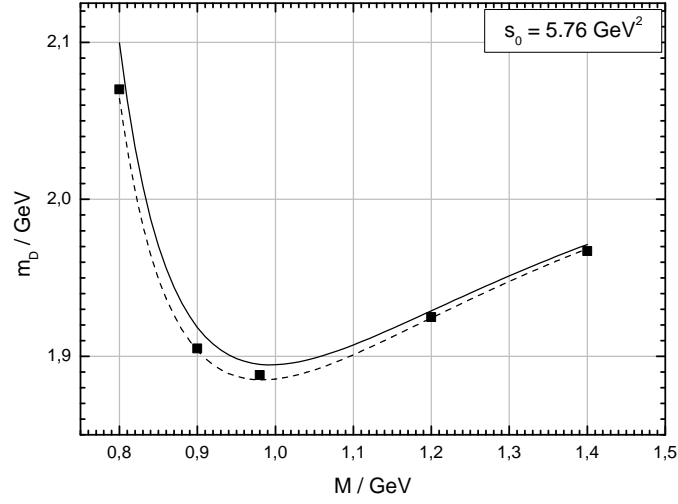


**Figure 3.4.5:** Borel curve obtained from the vacuum sum rule given in [Ha04] (plain line), the same sum rule but with switched-off four-quark condensate (dashed line) and the data which has been taken from diagrams in there (squares) at  $s_0 = 5.76 \text{ GeV}^2$ .

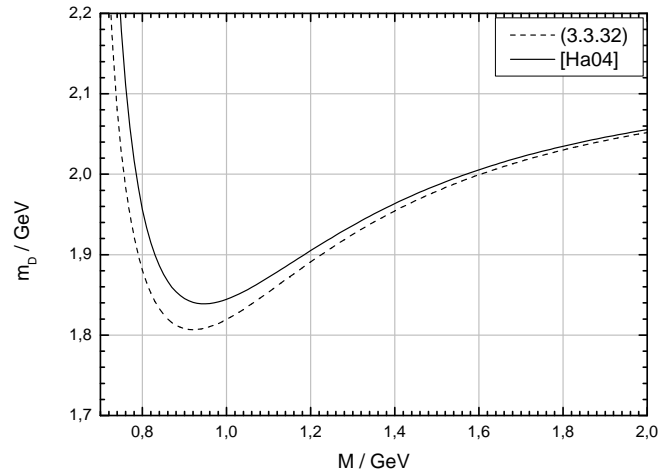


**Figure 3.4.6:** Borel curves obtained from the vacuum sum rule up to mass dimension 5 in [Ha04] and determined from (3.3.32) at  $s_0 = 6.0 \text{ GeV}^2$ .

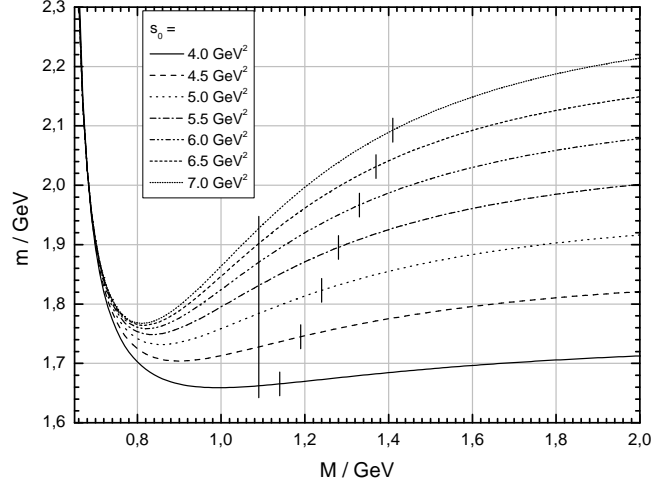


**Figure 3.4.7:** Average in-medium  $D$  meson mass  $\bar{m}$  for different thresholds at  $n = 0.17 \text{ fm}^{-3}$ ,  $m_c = 1.45 \text{ GeV}$  and  $\langle \bar{q}q \rangle_{vac} = (-0.245 \text{ GeV})^3$ .

serve a shift to higher values within and beyond the Borel window, equality for all densities at about  $M = 1 \text{ GeV}$  and a lowering and left-shift of the minima with increasing density. At the intersection point no medium modifications of the mass centroid  $\bar{m}$  are existent, signaling uncertainties for its determination. The minimum of the Borel curve is shifted to lower Borel masses and pole masses.

For the threshold being  $s = 4.0 \text{ GeV}^2$  we observe a similar situation, but with the point of intersection lying within the Borel window. It has been shifted to higher values of the Borel mass while the Borel minimum remains the same, as can be seen from fig. 3.4.7. In contrast to the  $s_0 = 5.5 \text{ GeV}^2$  case, the minimum is indeed still shifted to lower Borel masses, hence, crossing the Borel window and leaving it for higher densities. But despite of this shift, it is numerically almost unaffected by a density change. For completeness we also exhibit the corresponding diagram for  $s_0 = 7.0 \text{ GeV}^2$  in fig. 3.4.10. Qualitatively, the situation is equal to that of fig. 3.4.9.

For even lower values of the threshold than  $s_0 = 4.0 \text{ GeV}^2$ , we expect complementary results. Namely, the interception point lying to the right of the Borel window and, hence, the pole masses being continuously lower for higher densities within the Borel window. But the minima will be shifted to higher pole masses for higher densities.

Different criteria are common to determine the mass centroid  $\bar{m}$ . We will discuss three of them. The first one is to look for the mass centroid  $\bar{m}$  within the above defined Borel window. This would mean, the shift of the mass centroid increases with increasing threshold and is almost zero for the threshold being  $s_0 = 4.0 \text{ GeV}^2$ . Going to lower thresholds even gives a negative mass shift.



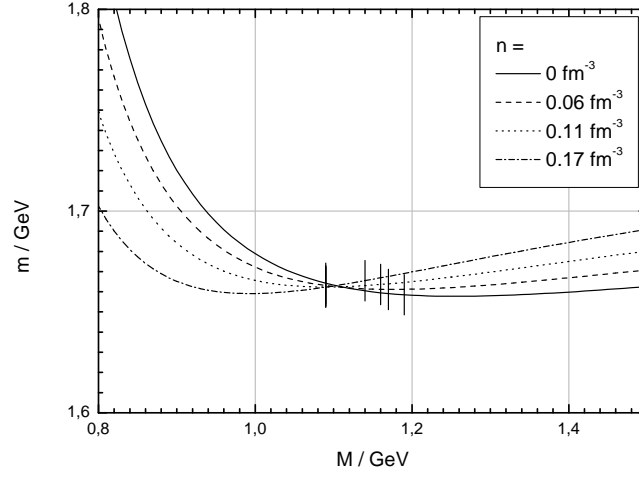


**Figure 3.4.8:** Average in-medium  $D$  meson mass  $\bar{m}$  for different densities at  $s_0 = 4.0 \text{ GeV}^2$ ,  $m_c = 1.45 \text{ GeV}$  and  $\langle \bar{q}q \rangle_{vac} = (-0.245 \text{ GeV})^3$ .

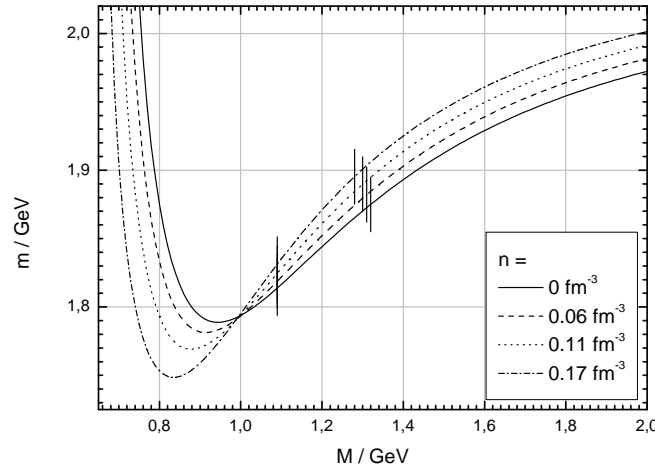


**Figure 3.4.9:** Average in-medium  $D$  meson mass  $\bar{m}$  for different densities at  $s_0 = 5.5 \text{ GeV}^2$ ,  $m_c = 1.45 \text{ GeV}$  and  $\langle \bar{q}q \rangle_{vac} = (-0.245 \text{ GeV})^3$ .

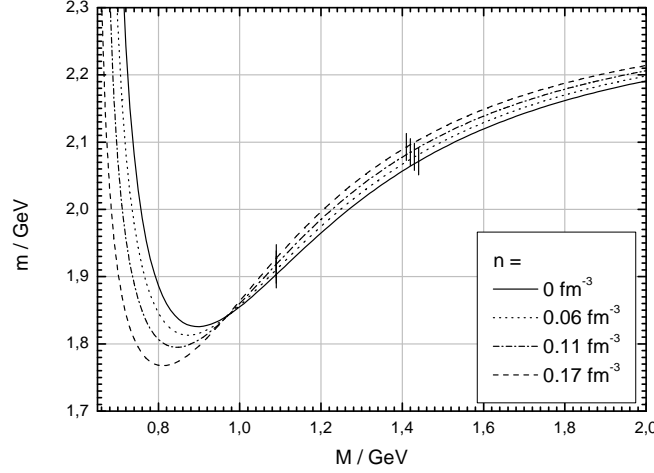


**Figure 3.4.10:** Average in-medium  $D$  meson mass  $\bar{m}$  for different densities at  $s_0 = 7.0 \text{ GeV}^2$ ,  $m_c = 1.45 \text{ GeV}$  and  $\langle \bar{q}q \rangle_{vac} = (-0.245 \text{ GeV})^3$ .

The second criterion is to fix the mass centroid at the minimum of the Borel curve or from a branch around it. In contrast to the first criterion this leads to a decreasing mass centroid for increasing density at larger thresholds, e.g.  $s_0 = 5.5 \text{ GeV}^2$  or  $s_0 = 7.0 \text{ GeV}^2$ . For the threshold being  $s_0 = 4.0 \text{ GeV}^2$ , no mass shift would be observed, although the minimum is shifted to lower Borel masses with increasing density.

The third criterion uses a different Borel window. It is also possible to define the Borel window to cover the plateau of a Borel curve, if there is one. In this case, the Borel window would be shifted to lower Borel masses and becomes smaller with increasing thresholds, as can be seen from fig. 3.4.9. Both, Borel minimum and Borel maximum, then depend on the threshold and decrease with increasing threshold, whereas the Borel maximum decreases much faster than the Borel minimum. This behavior is contrary to the behavior of the Borel window defined in section 3.4.2 and the threshold is automatically limited to lower values. From fig. 3.4.8 a lowering of the threshold for increasing density can be read off. Therefore, a lowering of the mass centroid is predicted in the scope of this criterion, as can be seen from fig. 3.4.7.

Hence, we are forced to conclude that a determination of the average in-medium mass shift can not be performed independent of the method or the arguments we use to determine the threshold  $s_0$  and the stability region of the sum rule. This is clear, insofar as we met the same problems already for the determination of the  $D$  meson vacuum mass in section 3.4.3.

In figs. 3.4.11, 3.4.12 and 3.4.13 we display the mass splitting  $\Delta m = (m_+ - m_-)/2$  as a function of the Borel mass for different densities at  $s_0 = 4.0, 5.5, 7.0 \text{ GeV}^2$ ,  $m_c = 1.45 \text{ GeV}$  and  $\langle \bar{q}q \rangle_{vac} = (-0.245 \text{ GeV})^3$ .

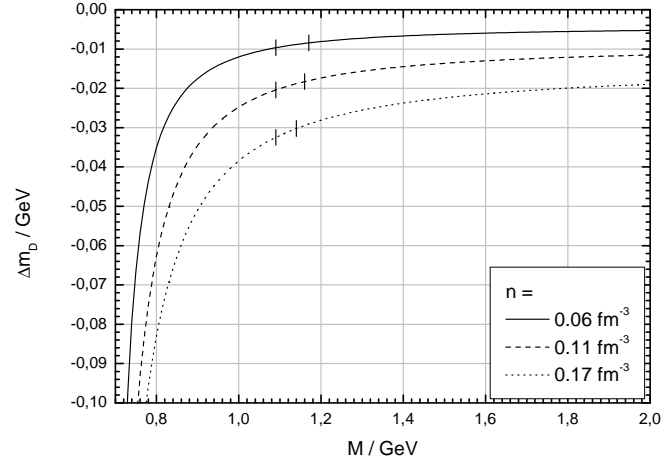


**Figure 3.4.11:** Mass splitting  $\Delta m$  for different densities at  $s_0 = 4.0 \text{ GeV}^2$ ,  $m_c = 1.45 \text{ GeV}$  and  $\langle \bar{q}q \rangle_{vac} = (-0.245 \text{ GeV})^3$ .

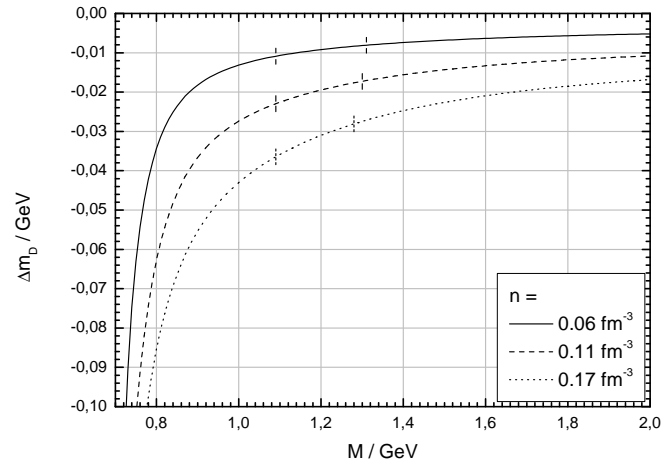


**Figure 3.4.12:** Mass splitting  $\Delta m$  for different densities at  $s_0 = 5.5 \text{ GeV}^2$ ,  $m_c = 1.45 \text{ GeV}$  and  $\langle \bar{q}q \rangle_{vac} = (-0.245 \text{ GeV})^3$ .

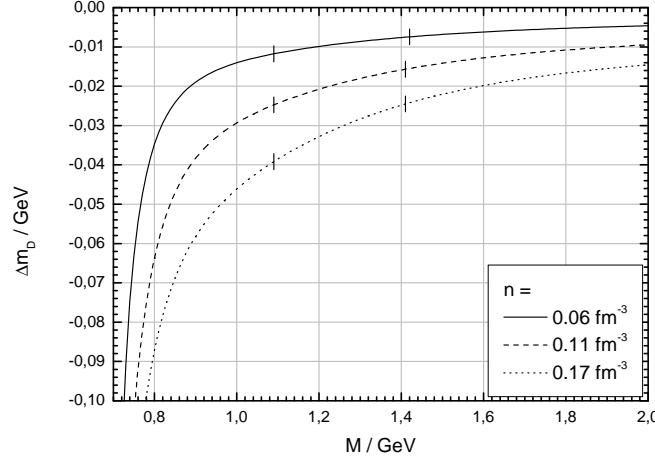


**Figure 3.4.13:** Mass splitting  $\Delta m$  for different densities at  $s_0 = 7.0 \text{ GeV}^2$ ,  $m_c = 1.45 \text{ GeV}$  and  $\langle \bar{q}q \rangle_{vac} = (-0.245 \text{ GeV})^3$ .

From these diagrams we read off that the mass splitting is rather independent of the threshold compared to the shift of the mass centroid. Regardless of which threshold we choose, we observe a mass splitting of  $\Delta m \approx -10 \text{ MeV}$  at  $n = 0.06 \text{ fm}^{-3}$ ,  $\Delta m \approx -20 \text{ MeV}$  at  $n = 0.11 \text{ fm}^{-3}$  and  $\Delta m \approx -30 \text{ MeV}$  at  $n = 0.17 \text{ fm}^{-3}$  within the Borel window defined in section 3.4.2. For all thresholds we observe no minimum within the plotted values. This is not expected to change for higher or lower thresholds.

If we determine the mass splitting according to the second criterion, i.e. we determine the mass splitting at the minima of the Borel curves for the mass centroid parameter  $\bar{m}$ , we immediately read off much larger mass splittings for the considered thresholds. Because the minima are located at Borel masses lower than the Borel minimum and, therefore, in a region where the mass splitting is rather steep, small deviations in the Borel mass cause large changes of the mass splitting, as can be seen in figs. 3.4.11, 3.4.12 and 3.4.13. A determination of the mass splitting is not reliable within this criterion.

On the other side, the mass centroid parameter is not more preferable than the mass splitting. Both are merely sums or differences of the mass parameters  $m_+$  and  $m_-$ . Therefore, it is just as well to fix the mass splitting at its minimum within the Borel plane and determine the mass centroid from the corresponding Borel mass. These minima are located at very large Borel masses, providing much lower mass splittings. The values vary from 10 MeV to 20 MeV at nuclear saturation density according to which threshold is taken. Whereas the average pole mass strongly depends on the threshold, although the curves are rather flat for large Borel masses.

Alternatively, the minima of the Borel curves for the mass parameters  $m_+$  and  $m_-$  could be considered (see figs. 3.4.14, 3.4.15, 3.4.16). The problem of deciding which param-

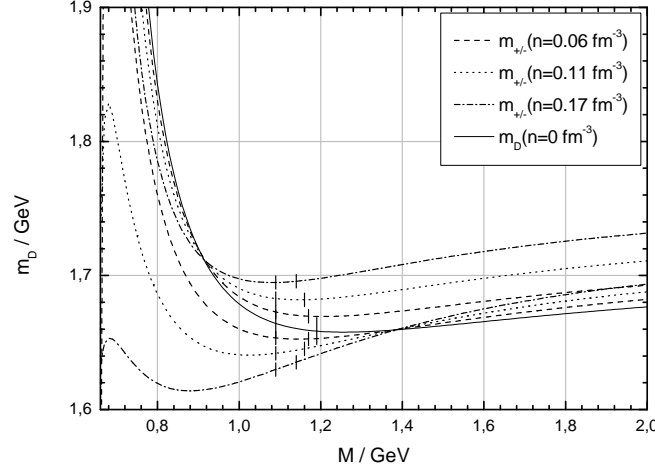


**Figure 3.4.14:** Mass parameters  $m_+$  and  $m_-$  for different densities at  $s_0 = 4.0 \text{ GeV}^2$ ,  $m_c = 1.45 \text{ GeV}$  and  $\langle \bar{q}q \rangle_{vac} = (-0.245 \text{ GeV})^3$ . The upper line of two equal line styles corresponds to the  $m_-$  mass, the lower one to the  $m_+$  mass.

eter,  $\bar{m}$  or  $\Delta m$ , is preferable to fix the minima, could be circumvented. Both quantities,  $m_+$  and  $m_-$ , are physically preferable to sums or differences of them. Different Borel masses would then be derived for the minima. The mass splitting as well as the mass centroid could be obtained directly from  $m_+$  and  $m_-$ .

From these figures we also observe different interception points for the mass parameters. The Borel curve for  $m_+$  is changing its principal shape for increasing density. A local maximum for  $m_+$  has been formed at a Borel mass of about  $M = 0.7 \text{ GeV}$ . It is shifted downwards for increasing density and the minimum of the Borel curve turns into a saddle point. Together with the observations we made in section 3.4.3,<sup>12</sup> this indicates a suppression of the influence of the gluon condensate at higher densities.

In fig. 3.4.17, 3.4.18 and 3.4.19 (Line style coding as in fig. 3.4.14.) we displayed an enlargement of the Borel windows from the above given figures. These diagrams affirm the conclusion we already drew from the previous diagrams. The mass shift is nearly unaffected by a variation of the threshold. In contrast to the shift of the mass centroid parameter, which is almost zero in fig. 3.4.17, but reveals a shift to higher masses in fig. 3.4.18 and 3.4.19.

In fig. 3.4.20 we show the mass splitting  $\Delta m = (m_+ - m_-)/2$  for different Wilson coefficients switched off at  $s_0 = 5.5 \text{ GeV}^2$ ,  $m_c = 1.45 \text{ GeV}$  and  $\langle \bar{q}q \rangle_{vac} = (-0.245 \text{ GeV})^3$  for the purpose of investigating its dependence on the various condensates. We observe that switching off the Wilson coefficient of the chiral condensate not only significantly changes

<sup>12</sup>The gluon condensate is crucial for the formation of a minimum of the mass parameter in the vacuum case.

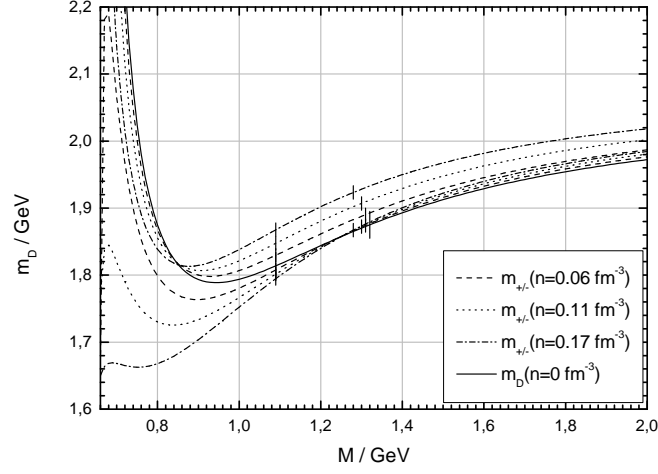


**Figure 3.4.15:** Mass parameters  $m_+$  and  $m_-$  for different densities at  $s_0 = 5.5 \text{ GeV}^2$ ,  $m_c = 1.45 \text{ GeV}$  and  $\langle \bar{q}q \rangle_{vac} = (-0.245 \text{ GeV})^3$ . Line style coding as in fig. 3.4.14.

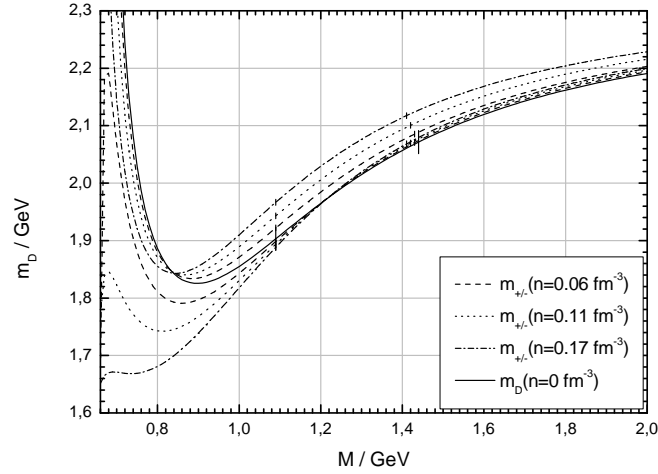


**Figure 3.4.16:** Mass parameters  $m_+$  and  $m_-$  for different densities at  $s_0 = 7.0 \text{ GeV}^2$ ,  $m_c = 1.45 \text{ GeV}$  and  $\langle \bar{q}q \rangle_{vac} = (-0.245 \text{ GeV})^3$ . Line style coding as in fig. 3.4.14.

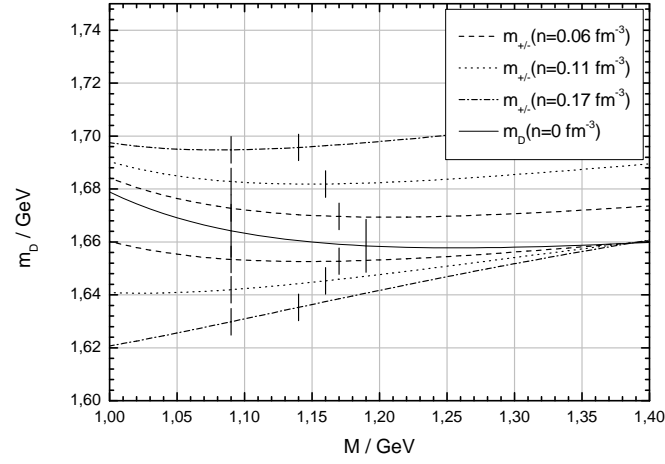


**Figure 3.4.17:** Enlargement of the Borel windows in fig. 3.4.14. ( $s_0 = 4.0 \text{ GeV}^2$ ,  $m_c = 1.45 \text{ GeV}$  and  $\langle \bar{q}q \rangle_{vac} = (-0.245 \text{ GeV})^3$ )

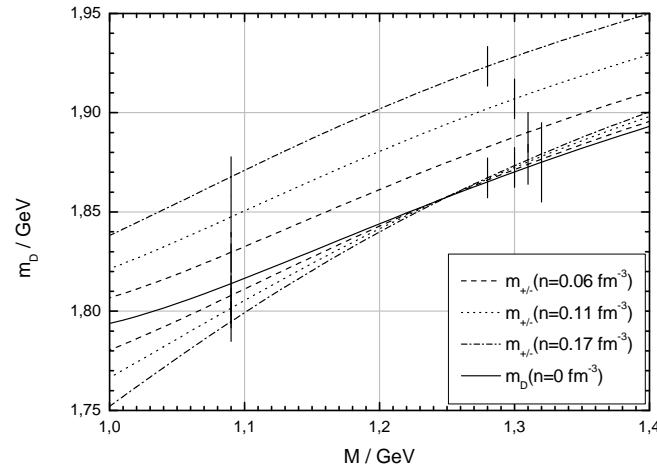


**Figure 3.4.18:** Enlargement of the Borel windows in fig. 3.4.15. ( $s_0 = 5.5 \text{ GeV}^2$ ,  $m_c = 1.45 \text{ GeV}$  and  $\langle \bar{q}q \rangle_{vac} = (-0.245 \text{ GeV})^3$ )

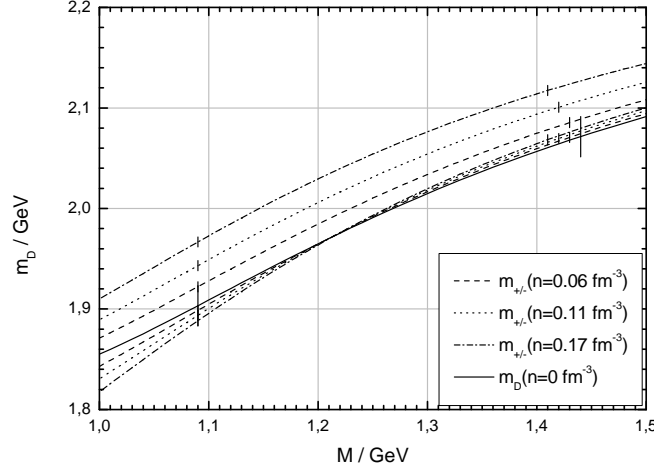


**Figure 3.4.19:** Enlargement of the Borel windows in fig. 3.4.16. ( $s_0 = 7.0 \text{ GeV}^2$ ,  $m_c = 1.45 \text{ GeV}$  and  $\langle \bar{q}q \rangle_{vac} = (-0.245 \text{ GeV})^3$ )

the Borel window, but also results in a much larger mass splitting. Instead, switching off the mixed quark-gluon condensate, changes the Borel curve at Borel masses lower than the Borel minimum; lower absolute mass splittings are found and a minimum outside the Borel window has been formed. No significant change is found for Borel masses larger than the Borel minimum. The gluon condensate is less important for the mass splitting. This is in contrast to the observations we made at the end of the previous section. Indeed, we discovered a strong dependence of the Borel window on the chiral vacuum condensate, but a rather weak dependence of the pole mass on it. Hence, we conclude that the mass splitting strongly depends on the in-medium behavior of the chiral condensate in the whole Borel plane. Contrary to the vacuum case we observe that the mixed quark-gluon condensate now seems responsible for the fact that there is no minimum for the mass splitting.<sup>13</sup>

Regardless which criterion is chosen to determine the mass splitting, the chiral condensate has the biggest influence. The mixed quark-gluon condensate has some influence, if a method is chosen that emphasizes lower Borel masses. Again, the gluon condensate is of minor importance, regardless which criterion is chosen.

Unfortunately, a direct comparison to the in-medium sum rule given in [Ha00] is not possible, because an odd part is not given there.<sup>14</sup>

<sup>13</sup>For the vacuum mass parameter the gluon condensate is responsible for the formation of a minimum, while the mixed quark-gluon condensate is less important in this case.

<sup>14</sup>See section 3.3.2.



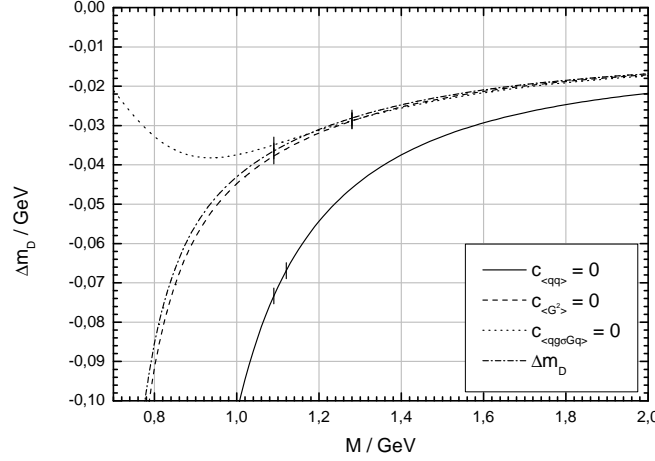


**Figure 3.4.20:** Mass splitting  $\Delta m$  for different Wilson coefficients switched off at  $s_0 = 5.5 \text{ GeV}^2$ ,  $m_c = 1.45 \text{ GeV}$ ,  $\langle \bar{q}q \rangle_{vac} = (-0.245 \text{ GeV})^3$  and  $n = 0.17 \text{ fm}^{-3}$ .

### 3.4.5 Analyzing the Sum Rules

In [Mo01] the authors determined the region of stability as the region where the ratio of power corrections (OPE without the perturbative term) to the perturbative contribution of the OPE and the ratio of the continuum contribution to the perturbative contribution are less than 0.5.<sup>15</sup> The Borel windows obtained in this way are comparable to ours. The pole mass is assumed to vary within the corresponding interval. The threshold parameter is fixed such that the vacuum sum rule reproduces the vacuum pole mass. They obtain a threshold of  $s_0 = 6.76 \text{ GeV}^2$ .

In [Ha00] a threshold of  $s_0 = 6 \text{ GeV}^2$  has been used. It was fixed in [Al83] in order to give a rather broad plateau in the Borel curve for the leptonic decay constant of the D meson. The Borel window for the in-medium sum rule in [Ha00] was determined as the interval where the deviation of the mass centroids shift from its minimum is less than 10%.<sup>16</sup> Hence, the threshold is chosen to maximize the Borel window defined as the plateau region of the Borel curve.<sup>17</sup> Whereas the mass centroids shift is determined by the minimum of the Borel curve.<sup>18</sup>

Against the hitherto appearance, we are not free in our choice of the threshold. Apart from physical arguments that can be employed to fix the threshold, our choice is defined by the derivation of (3.3.32) and (3.3.31). We assumed, that the pole masses do not depend on the Borel mass and therefore its derivative with respect to  $M$  (and thus its derivative with

<sup>15</sup>This criterion is similar to the one defined in section 3.4.2.

<sup>16</sup>They obtain a negative shift of the mass centroid.

<sup>17</sup>See p. 82.

<sup>18</sup>This can be understood as a combination of the second and the third criterion. See p. 80.

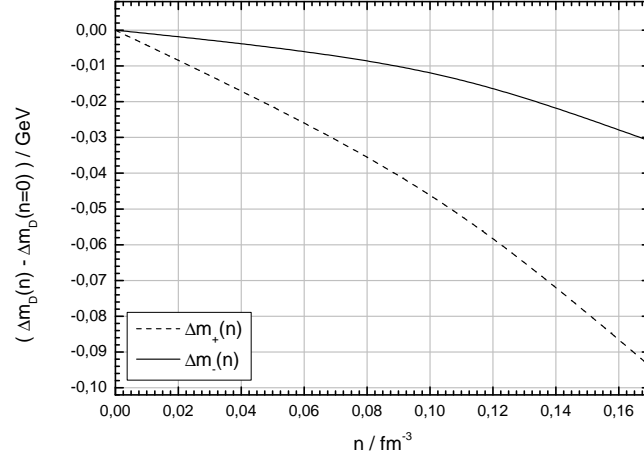


**Figure 3.4.21:** Mass shift as a function of the medium density  $n$ .

respect to  $1/M^2$ ) must vanish. Together with the above defined restrictions (3.4.4) and (3.4.5) to the validity of (3.3.20) and (3.3.21) this gives us a recipe for the determination of the threshold.

We demand that the pole masses must be as flat as possible within the Borel window. Thereby, we assure the best agreement to the requirement for a vanishing derivative of the pole masses within the stability region of the sum rules. Hence, the optimal threshold minimizes the deviations of the pole masses from their average value.

As a result the threshold varies with the density and the pole mass, averaged within the Borel window, is a good approximation for the values that it can adopt; cf. fig. 3.4.21. We determine a mass splitting of about 32 MeV at nuclear saturation density  $n = 0.17 \text{ fm}^{-3}$ .

Another method not to violate the assumptions we made in order to derive (3.3.32) and (3.3.31) is to look for the minimum of a Borel curve, where the derivative with respect to  $M$  naturally vanishes. On the other side, we still can take into account the limited validity of our sum rule. This results in a restriction to lower thresholds, where the minima of the Borel curves lie within the Borel windows. Fixing the Borel window in a way that it covers the plateau region of a Borel curve is also merely a realization of a Borel mass independent pole mass. Of course, we understand that the conditions we have chosen in order to find comprehensible conditions for the validity of the sum rule in section 3.4.2 are somewhat arbitrary in the parameters on the l.h.s. of (3.4.4) and (3.4.5) as well as in the general appearance of these inequalities. Different authors have chosen different conditions in order to find stability regions for their sum rule. The analysis of the sum rule therefore appears somewhat arbitrary and one has to look carefully for results that do not depend too strong on that choice.

Furthermore, we expect larger pole masses if mass dimension 6 condensates are in-

cluded. Their numerical importance is rather small, that is why the Borel curves will not change significantly. But, because of this, they will cause lower Borel minima. By means of section 3.4.2 and the Borel window defined there, they are expected to modify the validity of the sum rule and will give larger pole masses when the mass parameters are averaged within the Borel window.<sup>19</sup>

However, we could abandon the assumption of a Borel mass independent pole mass. In such a case we would get different expressions for the masses  $m_{\pm}$  and  $F_{\pm}$  as functions of the Borel mass and additional expressions for their derivatives. On the other side we would vary the threshold  $s_0$  to fit the pole masses to linear functions with non-vanishing slope within the Borel window, in contrast to fit them to linear functions with vanishing slope, i.e. a constant, as we did in the above case. An abrasive look at the Borel curves tells us that this leads to larger pole masses as well because the curves are rising almost linearly within the Borel window for slightly larger thresholds. It is not clear up to this point if the analysis of the sum rule is improved by such a method.

We note that the problems arising on the choice of the threshold parameter make it difficult to find a unique and successful way of analyzing the sum rule. Thus, it would be natural not to employ a "pole + continuum" ansatz. Alternatively, we could directly investigate the moments of the spectral integral without making too limiting assumptions for the spectral density or employ a finite width ansatz instead of a pole.

---

<sup>19</sup>The employed method to determine the threshold results in values  $s < 5 \text{ GeV}$ . A look in fig. 3.4.1 tells us that the pole mass is increasing with decreasing Borel mass.



## 4 Summary and Outlook

In this thesis the operator product expansion for D mesons has been performed in vacuum and in medium up to mass dimension 5 and up to first order in the strong coupling  $\alpha_s$ . In doing so, we assured a neat separation of scales by introducing physical condensates in vacuum as well as at finite density. As a result, the equations, which are necessary to cancel the mass logarithms, have been reproduced and, hence, an operator product expansion which is free from infrared divergences has been given. Thereby, we gave an exact relation which provides the possibility to perform the replacement of normal ordered condensates by physical ones up to all orders in  $\alpha_s$  generically. Moreover, it provides a consistent extension to finite densities. It has also been shown, introducing physical condensates in a finite density operator product expansion, requires additional equations. Along the way it has been shown, that the heavy-quark mass expansion relies upon the same physical backgrounds and is met within the renormalization of condensates.

A comparison of the operator product expansion with the literature shows unsatisfactory differences [Ha00, Mo01]. In both cases, as far as a comparison was possible, the origin of these differences is unclear. Also, in [Ha00, Mo01] it is not clear whether a consistent separation of scales has been performed in vacuum and in medium or not. The obvious differences of the QCD sum rules reputed in the literature caused the present investigation. Therefore, our focus was on the operator product expansion; a detailed derivation is presented. This is the main result of this thesis.

Our numerical evaluation follows the standard procedure: "pole + continuum" ansatz for the phenomenological hadron spectral function. The numerical analysis of the vacuum sum rules has shown a strong dependence on the method used to determine the threshold. While the influence of the chiral condensate on the Borel curves is rather weak, it is of high importance for the validity of the sum rules in the sense of a reasonable definition of the Borel window. Instead, the mixed quark gluon condensate is important for the Borel curves and, hence, for the numerical value of the D meson masses. Its influence on the validity of the sum rules is negligible. Switching off the gluon condensate, seems to have minor influence on the Borel window and on the Borel curves. The shape of the Borel curve is slightly changed near its lower Borel mass, but the vertical position stays unaffected. It causes a rapid change of the Borel curve for masses lower than the Borel minimum.

The analysis of the in-medium sum rules has shown the same dependences of the Borel curves and the Borel window on the threshold and the condensates. Hence, a firm determination of the shift of the mass centroid is hardly possible within the presented calculations. On the other side, it turned out that the mass splitting is comparatively robust with respect to the choice of the threshold. We determined a mass splitting of about 32 MeV at nuclear saturation density. This is the second result of this thesis.

We found that the mass splitting crucially depends on the in-medium chiral condensate, while it is almost unaffected by the mixed quark-gluon and the gluon condensate. Hence, medium modifications of D mesons seem to be good sensors for the in-medium behavior of the chiral condensate. Of course, all the results obtained in this work hold true for B mesons as well, i.e. mesons consisting of a bottom quark.

Future investigations have to include an estimate of the influence of higher dimensional condensates, e.g. four-quark condensates. Thereby, care has to be taken about possible new in-medium condensates. Also it is conceivable to introduce asymmetric continuum thresholds  $s_0^\pm$  for particle and anti-particle. In addition, testing methods which include Borel mass dependent pole masses should also be subject to future investigations.

The relevance of the "pole + continuum" ansatz and whether a finite-width spectral function provides an improvement of the accuracy have to be clarified. Also, the role of a possible Landau damping term should be investigated. Finally, the problems concerning the threshold parameter introduced by the "pole + continuum" ansatz can be circumvented by investigating moments of the spectral integral. In this way, a possibility to investigate higher excitations is also given.

# Appendix A      Brief Survey on Quantum Chromodynamics

We will briefly review the basics of QCD. We will focus on the essential equations and relations which are needed in this work. For a detailed essay on QCD we recommend [Pa84, Mu87]. The Lagrange density of classical chromodynamics reads

$$\mathcal{L} = \bar{\Psi} \left( i\hat{D} - M \right) \Psi - \frac{1}{4} G_{\mu\nu}^A G_A^{\mu\nu}, \quad (\text{A.1})$$

where we have introduced the following notation

$$D_\mu^{ab}(x) = \partial_\mu \mathbb{1}^{ab} - ig \mathcal{A}_\mu^{ab}(x) : \quad \text{covariant derivative,} \quad (\text{A.2})$$

$$\mathcal{A}_{ab}^\mu = A^{A\mu} t_{ab}^A : \quad \text{Gluon fields,} \quad (\text{A.3})$$

$$\mathcal{G}_{\mu\nu} = G_{\mu\nu}^A t^A = \frac{i}{g} [D_\mu, D_\nu] : \quad \text{Gluon field strength tensor,} \quad (\text{A.4})$$

$$\Psi_i^a : \quad \text{quark field operators,} \quad (\text{A.5})$$

$$t_{ab}^A = \frac{1}{2} \lambda^A : \quad \text{generators of SU}(N_c), \quad (\text{A.6})$$

$$\lambda^A : \quad \text{Gell-Mann matrices.} \quad (\text{A.7})$$

Dirac indices are denoted by latin letters  $i, j, k, \dots$ , Lorentz indices by greek letters  $\mu, \nu, \kappa, \dots$  and color indices by latin letters  $a, b, c, \dots$ . The generators  $t^A$  satisfy

$$[t^A, t^B] = if^{ABC} t^C, \quad \text{tr}(t^A) = 0, \quad \text{tr}(t^A t^B) = \frac{\delta^{AB}}{2}, \quad (\text{A.8})$$

where  $f^{ABC}$  are the structure constants of the  $\text{SU}(N_c)$  algebra. From (A.4) one can show that

$$G_{\mu\nu}^A = \partial_\mu A_\nu^A - \partial_\nu A_\mu^A + gf^{ABC} A_\mu^B A_\nu^C, \quad (\text{A.9})$$

and

$$G_{\mu\nu}^A = -G_{\nu\mu}^A. \quad (\text{A.10})$$

$N_c$  denotes the number of colors, and the index  $A$  refers to the generators of  $\text{SU}(N_c)$ . The quark fields are column vectors where each of the six entries corresponds to one flavor,

$\Psi = (u, d, s, c, b, t)^T$ . The mass matrix  $M$  is diagonal with the following entries [Ya06]

$$m_u = 1.5 \text{ to } 3.0 \text{ MeV} , \quad (\text{A.11})$$

$$m_d = 3 \text{ to } 7 \text{ MeV} , \quad (\text{A.12})$$

$$m_s = 95 \pm 25 \text{ MeV} , \quad (\text{A.13})$$

$$m_c = 1.25 \pm 0.09 \text{ GeV} , \quad (\text{A.14})$$

$$m_b = 4.20 \pm 0.07 \text{ GeV} \quad (\overline{\text{MS}} \text{ mass}) , \quad (\text{A.15})$$

$$\text{or } 4.70 \pm 0.07 \text{ GeV} \quad (1\text{S mass}) , \quad (\text{A.16})$$

$$m_t = 174.2 \pm 3.3 \text{ GeV} \quad (\text{direct observation of top events}) , \quad (\text{A.17})$$

$$\text{or } 172.3^{+10.2}_{-7.6} \text{ GeV} \quad (\text{Standard Model electroweak fit}) . \quad (\text{A.18})$$

Because quarks are confined within hadrons and can not be observed as isolated free particles, the determination of their masses depends on the theoretical framework used for calculations. Therefore, different values for the bottom and top masses are quoted. The difference is of no importance for our calculations as the top quark is not considered here; for the bottom quarks the difference is of minor importance.

The coupling strength of strong interaction, denoted by  $g$ , is defined as

$$g = \sqrt{4\pi\alpha_s} , \quad (\text{A.19})$$

$$\alpha_s(q^2) = \frac{4\pi}{(33 - 2N_f) \ln \left( \frac{-q^2}{\Lambda_{QCD}^2} \right)} , \quad (\text{A.20})$$

with  $N_f$  being the number of active quark flavors and  $\Lambda_{QCD}^2$  the renormalization scale parameter of QCD, usually determined to reproduce  $\alpha_s(M_Z) \approx 0.19$  with  $M_Z = 91.1876 \pm 0.0021 \text{ GeV}$  being the Z boson mass.

The Lagrange density (A.1) emerges from the requirement of invariance under the local gauge color transformation

$$\Psi_i^a(x) \rightarrow \Psi_i'^a(x) = \left[ e^{-igt^A \Theta_A(x)} \right]^{ab} \Psi_i^b(x) . \quad (\text{A.21})$$

By this one obtains the following transformation laws for color transformations

$$D_\mu \Psi_i(x) \rightarrow D'_\mu \Psi_i'(x) = e^{-igt^A \Theta_A(x)} D_\mu \Psi_i(x) , \quad (\text{A.22})$$

$$D_\mu \rightarrow D'_\mu = e^{-igt^A \Theta_A(x)} D_\mu e^{igt^A \Theta_A(x)} , \quad (\text{A.23})$$

$$\mathcal{A}_\mu \rightarrow \mathcal{A}'_\mu = e^{-igt^A \Theta_A} \mathcal{A}_\mu e^{igt^A \Theta_A(x)} + \left[ \partial_\mu e^{-igt^A \Theta_A(x)} \right] e^{igt^A \Theta_A(x)} , \quad (\text{A.24})$$

$$\mathcal{G}_{\mu\nu}(x) \rightarrow \mathcal{G}'_{\mu\nu} = e^{-igt^A \Theta_A} \mathcal{G}_{\mu\nu}(x) e^{igt^A \Theta_A(x)} . \quad (\text{A.25})$$

The equations of motion for the quark and gluon fields follow from (A.1) as

$$\hat{D}q = -im_q q , \quad (\text{A.26})$$

$$\overleftarrow{\hat{D}}\bar{q} = im_q \bar{q} , \quad (\text{A.27})$$

$$[D^\mu, \mathcal{G}_{\mu\nu}](x) = -gt^A \sum_{n=u,d,s,c} \bar{n}(x) t^A \gamma_\nu n(x) , \quad (\text{A.28})$$



where summation over  $A$  is understood and we have defined

$$\gamma^\mu D_\mu = \hat{D} , \quad (\text{A.29})$$

$$\sigma^{\mu\nu} \mathcal{G}_{\mu\nu} = \sigma \mathcal{G} \quad (\text{A.30})$$

with spin matrices

$$\sigma_{\mu\nu} = \frac{1}{2} [\gamma_\mu, \gamma_\nu] = i(\gamma_\mu \gamma_\nu - g_{\mu\nu}) . \quad (\text{A.31})$$

Exploiting these relations, one can show that the gluon field strength tensor fulfills the following useful relations

$$D^2 = \hat{D} \hat{D} + \frac{1}{2} g \sigma \mathcal{G} , \quad (\text{A.32a})$$

$$D^2 \Psi = \left( \frac{1}{2} g \sigma \mathcal{G} - m^2 \right) \Psi , \quad (\text{A.32b})$$

where we have defined

$$D^2 = g^{\mu\nu} D_\mu D_\nu . \quad (\text{A.33})$$

Splitting up the Lagrange density into a free part  $\mathcal{L}_0$  and a part containing the interaction, we define the interaction Lagrange density as

$$\mathcal{L}_{int} = \mathcal{L} - \mathcal{L}_0 . \quad (\text{A.34})$$

The free Lagrange density reads

$$\mathcal{L}_0 = \bar{\Psi} \left( i \hat{\partial} - M \right) \Psi - \frac{1}{4} G_{\mu\nu}^A G_A^{\mu\nu} . \quad (\text{A.35})$$



# Appendix B      Bethe-Salpeter Approach

In the preceding sections we have used the method of QCD sum rules to determine the mass of a bound state consisting of two quarks. The method introduces universal phenomenological parameters which enable an understanding of non-perturbative hadronic properties in intimate contact to QCD.

Alternatively, for a system consisting of two quarks, another method is given by the Bethe-Salpeter equation (BSE). It is an integral equation for the relativistic two-particle problem and can be applied to both, bound states and scattering problems.

The Bethe-Salpeter equation is the only exact integral equation for the relativistic two-particle problem in a quantum field theory. Unfortunately, there are no exact solutions for realistic interaction kernels and, due to the high dimensionality, it can not directly be solved numerically. Hence, one has to apply approximations to the exact Bethe-Salpeter equation. Often the so called ladder approximation is employed. This means, only a certain kind of interaction procedures, which can be characterized by their diagrammatic representation, are taken into account. But even for the ladder approximation there is only one model that can be solved exactly, the so called Cutkosky model [Cu54]. It is often referred to as a toy model, because it entails unphysical states and gives the wrong limit for the ratio of the masses tending to infinity, i.e. one mass being much heavier than the other.

Apart from the problems that can not be solved by it, the ladder approximation enables one to solve the Bethe-Salpeter equation numerically. Usually, one has to make additional assumptions and approximations. Recently, in [Do07] the authors have given a closed numerical solution to the Bethe-Salpeter equation in ladder approximation for the deuteron, without employing additional approximations or assumptions and, hence, providing the possibility to give suitable numerical solutions to the Bethe-Salpeter equation within the ladder approximation.

In the next sections we will give a brief introduction to the Bethe-Salpeter equation and describe the method developed in [Do07] for the deuteron.

## B.1 Introduction

The Bethe-Salpeter equation is a 16-dimensional integral equation for the Bethe-Salpeter amplitude. Its derivation can be found in many textbooks about quantum field theory, e.g. [Lu68, Ro69, Gr84]. It starts with an analysis of the two-particle propagator defined as the four-point function

$$K_{\alpha\beta\mu\nu}(x_1, x_2; y_1, y_2) := -\langle \Omega | T \left[ \psi_{\alpha}^A(x_1) \psi_{\beta}^B(x_2) \bar{\psi}_{\mu}^A(y_1) \bar{\psi}_{\nu}^B(y_2) \right] | \Omega \rangle, \quad (\text{B.1.1})$$

where the sign is just convention. Different particles are denoted by A and B respectively and greek letters denote the spinor indices. Close to the QSR part of this thesis we are working with Heisenberg field operators. Following [Ge51] one can give a perturbative expansion for the two-particle propagator similar to (2.1.4). The diagrammatic representation is given in fig. B.1.1.

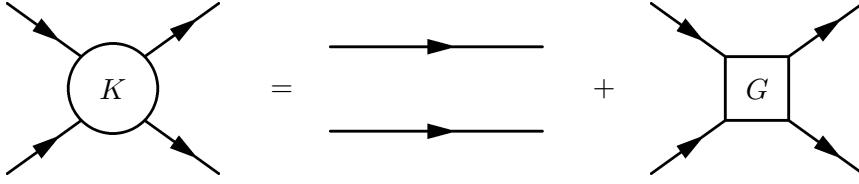


**Figure B.1.1:** The exact four-point function is split into a part without interaction and a part which contains interaction between the two particles. All lines represent exact propagators.

The diagram, which is labeled by  $G$  contains all diagrams where an interaction between the particles took place. Some examples of this infinite sum are depicted in fig. B.1.2. We also noted one diagram which describes a rather complicated process and includes self-interactions.

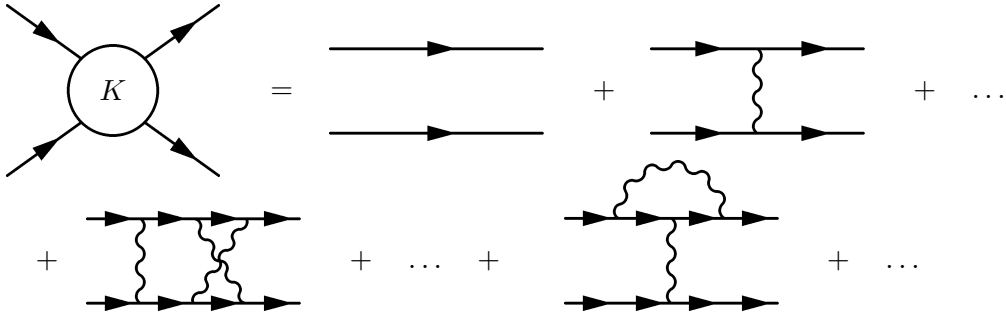


**Figure B.1.2:** Perturbative expansion of the two-particle propagator (B.1.1). All the lines stand for free propagators.

The corresponding equation reads

$$\begin{aligned}
 K_{\alpha\beta\mu\nu}(x_1, x_2; y_1, y_2) &= iS_{\alpha\mu}^A(x_1, y_1)iS_{\beta\nu}^B(x_2, y_2) \\
 &+ \int d^4y_3 d^4y_4 d^4y_5 d^4y_6 iS_{\alpha\alpha'}^A(x_1, y_3)iS_{\beta\beta'}^B(x_2, y_4) \\
 &\times G_{\alpha'\beta'\mu'\nu'}(y_3, y_4; y_5, y_6)iS_{\mu'\nu'}^A(y_5, y_6)iS_{\mu\nu}^B(y_1, y_2) . \quad (\text{B.1.2})
 \end{aligned}$$

The important observation now is, that the diagrams occurring at the r.h.s. of the equation given in fig. B.1.2, i.e. in  $G$ , can be categorized according to whether they are reducible or

not. A reducible diagram is defined as a graph, that can be separated into two diagrams by cutting two internal fermion lines, where each diagram has got two incoming and two outgoing fermion lines (see fig. B.1.3).

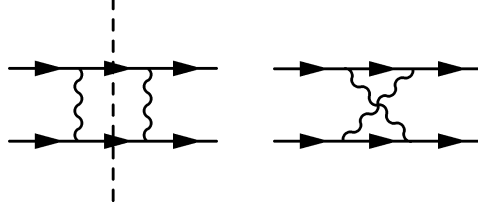


**Figure B.1.3:** Left panel: reducible diagram. Right panel: irreducible diagram.

Hence, each reducible diagram can be expressed by a combination of appropriate irreducible ones. If we define the sum of all irreducible diagrams as  $\overline{G}$ , we are able to express the exact four-point function  $K$  by the infinite sum of all irreducible diagrams only. One obtains the equation of diagrams depicted in fig. B.1.4.

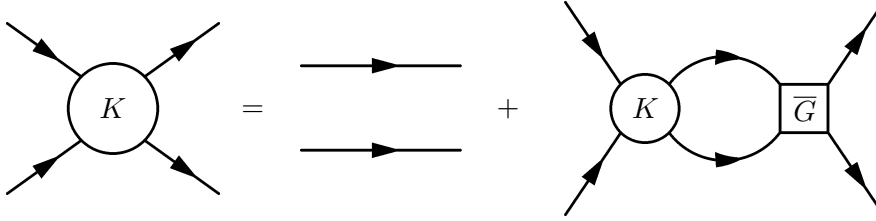


**Figure B.1.4:** The exact four-point function  $K$  in terms of irreducible interactions encoded in the infinite sum  $\overline{G}$ . All lines stand for the exact propagators.

The integral equation which corresponds to fig. B.1.4 reads

$$\begin{aligned}
 K_{\alpha\beta\mu\nu}(x_1, x_2; y_1, y_2) &= -S_{\alpha\mu}^A(x_1, y_1)S_{\beta\nu}^B(x_2, y_2) \\
 &\quad - \int d^4y_3 d^4y_4 d^4y_5 d^4y_6 S_{\alpha\alpha'}^A(x_1, y_3)S_{\beta\beta'}^B(x_2, y_4) \\
 &\quad \times \overline{G}_{\alpha'\beta'\mu'\nu'}(y_3, y_4; y_5, y_6)K_{\mu'\nu'\mu\nu}(y_5, y_6; y_1, y_2) .
 \end{aligned} \tag{B.1.3}$$

In coordinate space, it is an inhomogeneous 16-dimensional integral equation. In order to verify that this equation indeed reproduces the equation depicted in fig. B.1.1 and fig. B.1.2 one has to investigate the iterated solution of (B.1.3) or fig. B.1.4, which is depicted in fig. B.1.5. Clearly, every irreducible interaction is included in  $\overline{G}$ , while every reducible interaction is reproduced by an appropriate combination of irreducible diagrams appearing somewhere in the second line of fig. B.1.5. The integration kernel  $\overline{G}$  can be calculated in perturbation theory.

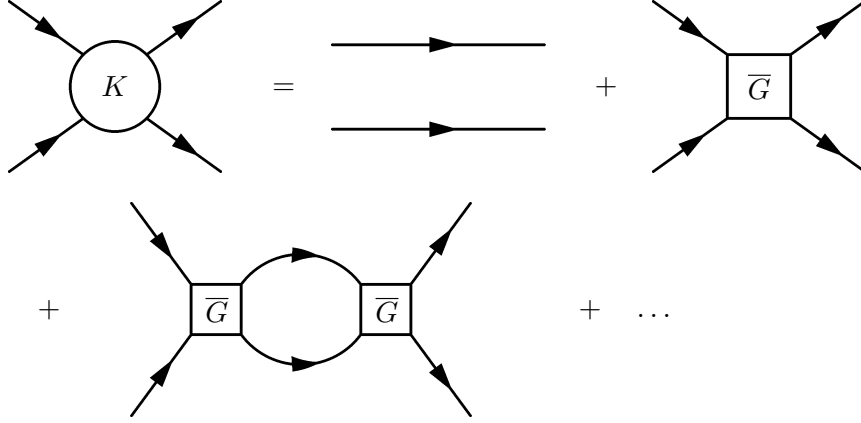


**Figure B.1.5:** Iterated solution of (B.1.3) and fig. B.1.4.

Apart from this rather artificial looking diagrammatic construction, the integral equation (B.1.3) can also be derived from a generalized form of the Dyson-Schwinger equation for four-point functions.

The Bethe-Salpeter amplitude (BSA) and the adjoint Bethe-Salpeter amplitude are defined as

$$\chi_{K,\alpha\beta}(x_1, x_2) := \langle \Omega | T [\psi_\alpha^A(x_1) \psi_\beta^B(x_2)] | K \rangle \quad (\text{B.1.4a})$$

$$\bar{\chi}_{K,\mu\nu}(y_1, y_2) := \langle K | T [\bar{\psi}_\mu^A(y_1) \bar{\psi}_\nu^B(y_2)] | \Omega \rangle, \quad (\text{B.1.4b})$$

where  $|K\rangle$  is an arbitrary physical eigenstate of the momentum operator, carrying the momentum  $K$ . It can be a scattering state as well as a bound state. Both quantities have 16 components. Often they are defined as matrices by transposing the second spinor, but as long as one is using indices there is no need to care about this. Unfortunately, the connection between them is not as simple as one might think at the first sight. By adjoining the BSA one gets the anti time-ordered product of the adjoint spinors. Accordingly, the connection is not simply given by adjoining and multiplying (B.1.4) by  $\gamma_0$  from both sides. An analytic relation between both quantities is given in [Ma55].

With these definitions one can introduce a complete set of physical eigenstates of the momentum operator in (B.1.1) and derive the homogeneous BSE for the BSA and the adjoint BSA from (B.1.3) as

$$\begin{aligned} \chi_{K,\alpha\beta}(x_1, x_2) = & - \int d^4 y_1 d^4 y_2 d^4 y_3 d^4 y_4 S_{\alpha\alpha'}^A(x_1, y_1) S_{\beta\beta'}^B(x_2, y_2) \\ & \times \bar{G}_{\alpha'\beta'\mu'\nu'}(y_1, y_2; y_3, y_4) \chi_{K,\mu'\nu'}(y_3, y_4). \end{aligned} \quad (\text{B.1.5})$$

We note here, that the inhomogeneity in (B.1.3) corresponds to interactions where the two particles stop interacting at some time and the particles become free, i.e. to scattering states. To restrict ourselves to bound states only, we had to neglect the first term in

(B.1.3). This restriction to the propagator function represents the claim that two particles which are bounded never stop interacting. By this we also see, that a finite number of diagrams in fig. B.1.2 and, hence, in (B.1.2) would never be sufficient to describe bound states. Although the expansion of the four-point function (B.1.1) by means of perturbation theory and the integral equation (B.1.3) are equivalent, the latter one is more powerful, providing a broader range of physical applications.<sup>1</sup>

## B.2 Ladder Approximation

Sometimes it is sufficient to include only a certain kind of interactions between the two particles. The so-called ladder approximation only takes the lowest-order perturbative contributions to the fermion propagators  $S^{A,B}$ , i.e. one uses the free propagators, and the lowest-order term of the interaction kernel  $\overline{G}$ . The latter one means that there is only one interaction at a time between the two particles. The result is that the included interactions have a characteristic look. In fig. B.2.1 some examples for interactions included in ladder approximation are given. From fig. B.2.1 it should become clear why this approximation is called ladder approximation. Strictly speaking, when one considers the homogeneous BSE, i.e. bound states, in each of these diagrams an infinite number of interactions take place and the "ladder" is endless.

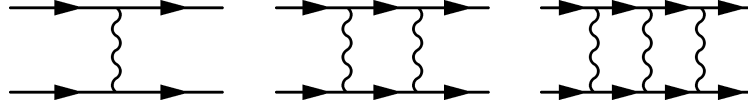


**Figure B.2.1:** Typical contributions to the homogeneous BSE in ladder approximation. All lines stand for free propagators.

In fig. B.2.2 we give an example for a diagram that is not included by the ladder approximation. It has, however, to be taken into account, e.g. for positronium bound states.

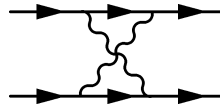


**Figure B.2.2:** A diagram beyond the ladder approximation.

The free fermion propagators are given in (2.4.15) and for a scalar interaction the lowest-order contribution to the irreducible interaction kernel in momentum space reads

$$\overline{G}^{(0)}(p, p', K)_{\alpha\beta\alpha'\beta'} = (2\pi)^4 g^2 \Gamma_{\alpha\alpha'}^1 \Gamma_{\beta\beta'}^2 \Delta(p - p'), \quad (\text{B.2.1})$$

<sup>1</sup>In fact, comparing the power expansion of the four-point function (B.1.1) and its integral equation (B.1.3), the differences according to divergence or convergence of the one or the other are even more fundamental [Ge51].

where the propagator for a scalar particle is defined as

$$\Delta(p) = \frac{1}{p^2 - \mu^2} . \quad (\text{B.2.2})$$

The mass of the interaction particle is denoted by  $\mu$  while  $\Gamma \in \{\mathbb{1}, \gamma_\mu, \sigma_{\mu<\nu}, i\gamma_5\gamma_\mu, \gamma_5\}$  represents the coupling of the interaction particles to the fermions. In fig. B.2.3 we give the diagrammatic representation of the integral equation for the four-point function in ladder approximation.

The homogeneous BSE for the BSA in ladder approximation and momentum space reads

$$\begin{aligned} & \left[ S^A \left( \frac{K}{2} + p \right) \right]_{\alpha\alpha'}^{-1} \left[ S^B \left( \frac{K}{2} - p \right) \right]_{\beta\beta'}^{-1} \chi_{K,\alpha'\beta'}(p) \\ &= - \int \frac{d^4 p'}{(2\pi)^4} g^2 \Delta(p-p') \Gamma_{\alpha\alpha'}^1 \Gamma_{\beta\beta'}^2 \chi_{K,\alpha'\beta'}(p') . \end{aligned} \quad (\text{B.2.3})$$

It is a four dimensional integral equation for the 16 components of the BSA. Whether a solution exists or not depends, beside other requirements, on the four-momentum  $K$  of the bound state. Considered as an eigenvalue problem, (B.2.3) has solutions only for discrete values of the bound state four-momentum. Unfortunately, the BSA does not have direct physical meaning and calculating observables from it requires knowledge of the adjoint BSA. Hence, in general, if no further restrictions to the time ordering are made and a simple algebraic relation between the BSA and its adjoint counterpart is provided, one also has to solve the BSE for the adjoint BSA. Nevertheless, solving the BSE for the BSA alone is a problem of finding eigenvalues  $K$  and eigenstates  $\chi_K$  to the operator defined in (B.2.3). Thus, a solution at least provides us the determination of the bound state mass  $K_0$ , if we work in the bound states rest frame. Because the BSE is Lorentz invariant and the BSA transforms covariantly, one is free to choose any frame that is convenient to simplify calculations. Choosing the center of mass system does not mean any loss of generality, but enables a direct determination of the bound state mass by solving the eigenvalue problem defined in (B.2.3).

If one desires to calculate observables, e.g. the electromagnetic form factor, both are essential, the BSA in the rest frame of the bound state and in other frames. The latter one can be obtained as Lorentz transform of the first one.

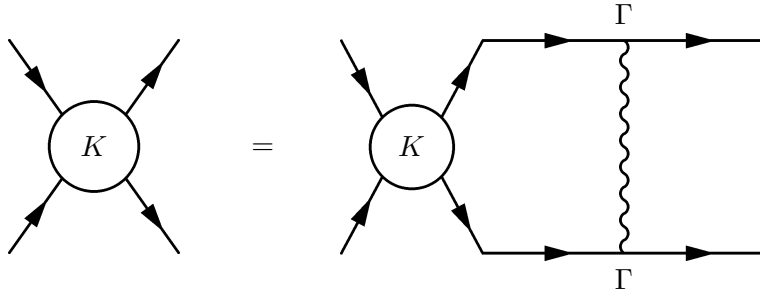


**Figure B.2.3:** Diagrammatic representation of (B.1.3) and fig. B.1.4 in ladder approximation. All lines depict free propagators.



### B.3 Solving the Bethe-Salpeter Equation in Ladder Approximation

In order to simplify notations, in what follows, we will use the matrix notation and introduce a redefined BSA as

$$\Psi_K(p) := -\chi_K(p)C, \quad (\text{B.3.1})$$

with  $C = i\gamma_0\gamma_2$  being the charge conjugation matrix. Furthermore, we introduce the Bethe-Salpeter vertex function  $g_K(p)$  as

$$\Psi_K(p) = S\left(\frac{K}{2} + p\right) g_K(p) \tilde{S}\left(\frac{K}{2} - p\right), \quad (\text{B.3.2})$$

where we have implicitly introduced

$$\tilde{S}(p) = CS^TC = \frac{\hat{p} - m}{p^2 - m^2} \quad (\text{B.3.3})$$

and assumed equal masses  $m_A = m_B = m$ , omitting the superscripts  $A, B$  for the propagators. For the BSA these definitions translate to

$$\chi_K(p) = S\left(\frac{K}{2} + p\right) \tilde{g}_K(p) S^T\left(\frac{K}{2} - p\right) \quad (\text{B.3.4})$$

and

$$g_K(p) := \tilde{g}_K(p)C. \quad (\text{B.3.5})$$

Transforming into the bound states rest frame, the BSE for the vertex-function of a bound-state in ladder approximation then reads

$$\begin{aligned} g_K(p) &= i \int \frac{d^4 p'}{(2\pi)^4} V(p-p') \Gamma_1 S\left(\frac{K}{2} + p'\right) g_K(p') \tilde{S}\left(\frac{K}{2} - p'\right) \tilde{\Gamma}_2 \\ &= i \int \frac{d^4 p'}{(2\pi)^4} V(p-p') s(p') \Gamma_1 \left(\frac{\hat{K}}{2} + \hat{p}' + m\right) g_K(p') \left(\frac{\hat{K}}{2} - \hat{p}' - m\right) \tilde{\Gamma}_2, \end{aligned} \quad (\text{B.3.6})$$

with  $\tilde{\Gamma} = C\Gamma^TC$  and

$$V(p-p') = \frac{g^2}{(p-p')^2 - \mu^2}, \quad (\text{B.3.7a})$$

$$s(p') = \frac{1}{(p'^2 - \kappa^2)^2 - p_0'^2 M^2}, \quad \kappa^2 = m^2 - \frac{M^2}{4}. \quad (\text{B.3.7b})$$

$M$  denotes the mass of the bound state in its rest frame  $K = (M, \vec{0})$ . In the following sections the amplitudes and vertex functions will be expanded in suitable bases to reduce the high dimensionality of the BSE. Therefore, symmetry properties of the bound state

imposed in the expansions play an important role. We will demonstrate all calculations for the example of the  $^1S_0$  channel, where we employ the spectroscopic notation  $\alpha = \alpha_0 M$ .  $M$  is the projection of the total angular momentum  $L$  and  $\alpha_0 = {}^{2S+1}L_J^{\rho_1 \rho_2}$ ,  $S$  being the total spin of the two nucleons,  $J$  the total angular momentum  $J = L + S$  and  $\rho_{1,2}$  denoting particle and anti-particle.

The following presentation is for the example of the deuteron, where the treatment in [Do07] was developed for and accordingly tested. Our presentation here is aimed at recollecting the technique which is essentially ready for an application to the  $J/\Psi$  as  $c\bar{c}$  bound state. The application to D mesons as  $u\bar{c}$ ,  $d\bar{c}$ ,  $c\bar{u}$  and  $c\bar{d}$  bound states requires further special developments. In the course of this thesis it was decided to employ the QCD sum rules as main tool for dealing with D mesons. Therefore, this appendix summarizes preparatory work for future and separate applications.

Restricting to  $^1S_0$  states means that only a simplified model of the deuteron is considered because the deuteron is a superposition of  $^3S_1$  and  $^3D_1$  states. However, the presented method for the  $^1S_0$  state can also be performed for the  $^3S_1$  and  $^3D_1$  or other states. Likewise, we will only consider a scalar coupling of the interaction particle with the nucleons, i.e.  $\Gamma = 1$ . Other couplings can easily be considered as well. As the extensiveness of the required calculations is the smallest for the  $^1S_0$  state with scalar coupling, we restrict ourselves to this case.

## B.4 Decomposition into Spin-Angular Matrices

The vertex function will now be expanded in a complete set of  $4 \times 4$  matrices. As one is dealing with states of certain symmetry properties choosing a base which reflects these properties is convenient. For definite spin, angular momentum and total momentum such a base is given by the spin-angular harmonics and the expansion reads

$$\chi_K(p) = \Psi_K(p)C = \sum_{\alpha} \Phi_{\alpha}(p_0, |\vec{p}|) \Gamma_{\alpha}(\vec{p})C. \quad (\text{B.4.1})$$

The sum goes over all quantum numbers  $\alpha$ . The partial amplitudes  $\Phi_{\alpha}(p_0, |\vec{p}|)$  do not depend on  $\Omega_{\vec{p}}$ , where

$$\Omega_{\vec{p}} = \sin \theta d\phi d\theta \quad (\text{B.4.2})$$

denotes the infinitesimal solid angle. The spin angular harmonics  $\Gamma_{\alpha}$  are defined as

$$\begin{aligned} \Gamma_{\alpha}(\vec{p})C &= (-1)^{\rho_1 + \rho_2} i^L \sum_{\substack{\mu_1 \mu_2 \\ m_L m_S}} \langle L m_L S m_S | J M \rangle \langle \frac{1}{2} \mu_1 \frac{1}{2} \mu_2 | S m_S \rangle \\ &\times Y_{L m_L}(\Omega_{\vec{p}}) U_{\mu_1}^{\rho_1}(\vec{p}) U_{\mu_2}^{\rho_2 T}(-\vec{p}). \end{aligned} \quad (\text{B.4.3})$$

The spherical harmonics are denoted by  $Y_{L m_L}(\Omega_{\vec{p}})$  and the Dirac unity spinors read

$$U_{\mu}^{+}(\vec{p}) = u_{\mu}(\vec{p}) = \frac{m + \hat{p}_1}{\sqrt{2E(E+m)}} \begin{pmatrix} \chi_{\mu} \\ 0 \end{pmatrix} = \frac{m + \hat{p}_1 \gamma_0}{\sqrt{2E(E+m)}} \begin{pmatrix} \chi_{\mu} \\ 0 \end{pmatrix}, \quad (\text{B.4.4a})$$

$$U_{\mu}^{-}(\vec{p}) = v_{\mu}(-\vec{p}) = \frac{m - \hat{p}_2}{\sqrt{2E(E+m)}} \begin{pmatrix} 0 \\ \chi_{\mu} \end{pmatrix} = \frac{m + \hat{p}_2 \gamma_0}{\sqrt{2E(E+m)}} \begin{pmatrix} 0 \\ \chi_{\mu} \end{pmatrix}, \quad (\text{B.4.4b})$$

where we have used

$$\chi_{+\frac{1}{2}} = \begin{pmatrix} 1 \\ 0 \end{pmatrix}, \quad \chi_{-\frac{1}{2}} = \begin{pmatrix} 0 \\ 1 \end{pmatrix}, \quad (\text{B.4.5a})$$

$$p_1 = (p_0, \vec{p}), \quad p_2 = (p_0, -\vec{p}), \quad \gamma_0 \hat{p}_1 \gamma_0 = \hat{p}_2. \quad (\text{B.4.5b})$$

In order to ensure the correct symmetry properties for the  $^1S_0$  channel, the following harmonics have to be taken into account

$$\alpha_0 = {}^1S_0^{++}, {}^1S_0^{--}, {}^3P_0^{+-}, {}^3P_0^{-+} \quad (\text{B.4.6})$$

and the following four 4×4 matrices form a complete set in the subspace of the  $^1S_0$  ( $M = 0$ ) channel

$$\alpha_0 = {}^1S_0^{++} : \Gamma_+ = \frac{1}{\sqrt{8\pi}} \frac{m + \hat{p}_1}{\sqrt{2E(E+m)}} \frac{1 + \gamma_0}{2} \gamma_5 \frac{m - \hat{p}_2}{\sqrt{2E(E+m)}}, \quad (\text{B.4.7a})$$

$$\alpha_0 = {}^1S_0^{--} : \Gamma_- = \frac{1}{\sqrt{8\pi}} \frac{\hat{p}_2 - m}{\sqrt{2E(E+m)}} \frac{1 - \gamma_0}{2} \gamma_5 \frac{m + \hat{p}_1}{\sqrt{2E(E+m)}}, \quad (\text{B.4.7b})$$

$$\alpha_0 = {}^3P_0^{+-} : \Gamma_{+-} = \frac{1}{\sqrt{8\pi}} \frac{m + \hat{p}_1}{\sqrt{2E(E+m)}} \frac{1 + \gamma_0}{2} \frac{1}{2} \frac{\hat{p}_1 - \hat{p}_2}{|\vec{p}|} \gamma_5 \frac{m + \hat{p}_1}{\sqrt{2E(E+m)}}, \quad (\text{B.4.7c})$$

$$\alpha_0 = {}^3P_0^{-+} : \Gamma_{-+} = \frac{1}{\sqrt{8\pi}} \frac{m - \hat{p}_2}{\sqrt{2E(E+m)}} \frac{\gamma_0 - 1}{2} \frac{1}{2} \frac{\hat{p}_1 - \hat{p}_2}{|\vec{p}|} \gamma_5 \frac{\hat{p}_2 - m}{\sqrt{2E(E+m)}}. \quad (\text{B.4.7d})$$

They fulfill the orthogonality condition

$$\int d\Omega_{\vec{p}} \text{Tr}_D \left[ \Gamma_{\alpha}^{\dagger}(\vec{p}) \Gamma_{\alpha'}(\vec{p}) \right] = 4\pi \delta_{\alpha\alpha'}. \quad (\text{B.4.8})$$

In the subsequent sections we will expand the partial amplitudes into hyperspherical harmonics using Gegenbauer polynomials which leads to a further reduction of the dimensionality of the BSE. Unfortunately, this decomposition can not be performed analytically if spin-angular harmonics are used and further approximations have to be employed in order to solve the BSE. Therefore, in [Do07] the authors developed a basis that enables one to perform analytically the decomposition into Gegenbauer polynomials.

The new base for the  $^1S_0$  state is given by the following set of four 4×4 matrices

$$T_1(\vec{p}) = \frac{\gamma_5}{2} = T_1^{\dagger}(\vec{p}) = -\bar{T}_1(\vec{p}) = -\tilde{T}_1(\vec{p}), \quad (\text{B.4.9a})$$

$$T_2(\vec{p}) = \frac{\gamma_0 \gamma_5}{2} = -T_2^{\dagger}(\vec{p}) = \bar{T}_2(\vec{p}) = -\tilde{T}_2(\vec{p}), \quad (\text{B.4.9b})$$

$$T_3(\vec{p}) = -\frac{\vec{p} \cdot \vec{\gamma}}{2|\vec{p}|} \gamma_5 = T_3^{\dagger}(\vec{p}) = \bar{T}_3(\vec{p}) = \tilde{T}_3(\vec{p}), \quad (\text{B.4.9c})$$

$$T_4(\vec{p}) = -\frac{\vec{p} \cdot \vec{\gamma}}{2|\vec{p}|} \gamma_0 \gamma_5 = T_4^{\dagger}(\vec{p}) = \bar{T}_4(\vec{p}) = -\tilde{T}_4(\vec{p}), \quad (\text{B.4.9d})$$

with

$$\bar{T} = \gamma_0 T^{\dagger}(\vec{p}) \gamma_0, \quad \tilde{T} = C T^T C. \quad (\text{B.4.10})$$

They obey the following orthogonality condition

$$\int \frac{d\Omega_{\vec{p}}}{4\pi} \text{Tr}_D (T_i T_j^\dagger) = \delta_{ij} \quad (\text{B.4.11})$$

and are a suitable choice for expanding the vertex function. The connection between the spin-angular harmonics for the  $^1S_0$  state and the base defined in (B.4.9) is given by

$$\begin{pmatrix} T_1 \\ T_2 \\ T_3 \\ T_4 \end{pmatrix} = \begin{pmatrix} \frac{1}{\sqrt{8\pi}} & -\frac{1}{\sqrt{8\pi}} & 0 & 0 \\ \frac{1}{\sqrt{8\pi}} \frac{m}{E} & \frac{1}{\sqrt{8\pi}} \frac{m}{E} & \frac{1}{2\sqrt{\pi}} \frac{|\vec{p}|}{E} & 0 \\ \frac{1}{\sqrt{8\pi}} \frac{|\vec{p}|}{E} & \frac{1}{\sqrt{8\pi}} \frac{|\vec{p}|}{E} & -\frac{1}{2\sqrt{\pi}} \frac{m}{E} & 0 \\ 0 & 0 & 0 & \frac{1}{\sqrt{4\pi}} \end{pmatrix} \begin{pmatrix} \Gamma_+ \\ \Gamma_- \\ \Gamma_o \\ \Gamma_e \end{pmatrix}. \quad (\text{B.4.12})$$

Here, we have defined the even and odd spin-angular harmonics as

$$\Gamma_o = \frac{1}{\sqrt{2}} (\Gamma_{+-} + \Gamma_{-+}), \quad \Gamma_e = \frac{1}{\sqrt{2}} (\Gamma_{+-} - \Gamma_{-+}). \quad (\text{B.4.13})$$

The vertex-function expanded in terms of the basis above reads

$$g_K(p_0, \vec{p}) = \sum_i g_K^i(p_0, |\vec{p}|) T_i(\vec{p}) \quad (\text{B.4.14})$$

and the coefficients are given by virtue of the orthogonality condition (B.4.11)

$$\begin{aligned} g_K^i(p_0, |\vec{p}|) &= \int \frac{d\Omega_{\vec{p}}}{4\pi} \text{Tr}_D [g_K(p_0, \vec{p}) T_i(\vec{p})] \\ &= i \int \frac{d\Omega_{\vec{p}}}{4\pi} \int \frac{d^4 p'}{(2\pi)^4} V(p - p') s(p') \sum_j g_K^j(p'_0, |\vec{p}'|) \\ &\quad \times \text{Tr}_D \left[ \Gamma_1 \left( \frac{\hat{K}}{2} + \hat{p}' + m \right) T_j(\vec{p}') \left( \frac{\hat{K}}{2} - \hat{p}' - m \right) \tilde{\Gamma}_2 T_i^\dagger(\vec{p}) \right]. \end{aligned} \quad (\text{B.4.15})$$

In the last step we have used the BSE for the vertex function (B.3.6) and reinserted the above expansion. For a scalar coupling of the interaction particle to the nucleons one has  $\Gamma_1 = I$ ,  $\tilde{\Gamma}_2 = -I$  and the trace reduces to

$$\begin{aligned} g_K^i(p_0, |\vec{p}|) &= -i \int \frac{d\Omega_{\vec{p}}}{4\pi} \int \frac{d^4 p'}{(2\pi)^4} V(p - p') S(p') \\ &\quad \times \sum_j g_K^j(p'_0, |\vec{p}'|) \text{Tr}_D \left[ T_i^\dagger(\vec{p}) \left( \frac{\hat{K}}{2} + \hat{p}' + m \right) T_j(\vec{p}') \left( \frac{\hat{K}}{2} - \hat{p}' - m \right) \right]. \end{aligned} \quad (\text{B.4.16})$$

The result is a set of four coupled seven-dimensional integral equations for the vertex coefficient functions  $g_K^i$ :

$$\begin{aligned} g_K^1(p_0, |\vec{p}|) &= -i \int \frac{d^4 p'}{(2\pi)^4} \int \frac{d\Omega_{\vec{p}}}{4\pi} s(p') V(p - p') \\ &\quad \times \left\{ \left( -\frac{M^2}{4} + p'^2 - m^2 \right) g_K^1 - M m g_K^2 + M |\vec{p}'| g_K^3 \right\}, \end{aligned} \quad (\text{B.4.17a})$$

$$g_K^2(p_0, |\vec{p}|) = -i \int \frac{d^4 p'}{(2\pi)^4} \int \frac{d\Omega_{\vec{p}}}{4\pi} s(p') V(p-p') \left\{ -M m g_K^1 \right. \\ \left. + \left( -\frac{M^2}{4} + p_0'^2 + \vec{p}'^2 - m^2 \right) g_K^2 + 2m |\vec{p}'| g_K^3 - 2p_0' |\vec{p}'| g_K^4 \right\}, \quad (\text{B.4.17b})$$

$$g_K^3(p_0, |\vec{p}|) = -i \int \frac{d^4 p'}{(2\pi)^4} \int \frac{d\Omega_{\vec{p}}}{4\pi} s(p') V(p-p') \frac{\vec{p}' \cdot \vec{p}}{|\vec{p}'| |\vec{p}|} \left\{ -M |\vec{p}'| g_K^1 \right. \\ \left. - 2m |\vec{p}'| g_K^2 + \left( \frac{M^2}{4} - p'^2 - m^2 \right) g_K^3 + 2m p_0' g_K^4 \right\}, \quad (\text{B.4.17c})$$

$$g_K^4(p_0, |\vec{p}|) = -i \int \frac{d^4 p'}{(2\pi)^4} \int \frac{d\Omega_{\vec{p}}}{4\pi} s(p') V(p-p') \frac{\vec{p}' \cdot \vec{p}}{|\vec{p}'| |\vec{p}|} \left\{ 2 |\vec{p}'| p_0' g_K^2 + 2m p_0' g_K^3 \right. \\ \left. + \left( \frac{M^2}{4} - p_0'^2 - \vec{p}'^2 - m^2 \right) g_K^4 \right\}, \quad (\text{B.4.17d})$$

where the coefficients inside the integral are taken at  $p' = (p_0', |\vec{p}'|)$ . Before expanding these coefficient functions in hyperspherical harmonics, it is necessary to perform a Wick rotation in order to continue (B.4.16) to Euclidean momenta  $p \rightarrow p_E = (ip_4, \vec{p})$ . The results read

$$g_K^1(ip_4, |\vec{p}|) = \int \frac{d^4 p'_E}{(2\pi)^4} \int \frac{d\Omega_{\vec{p}}}{4\pi} s(ip_4', \vec{p}') \tilde{V}(p_E - p'_E) \\ \times \left\{ \left( \frac{M^2}{4} + p_E'^2 + m^2 \right) g_K^1 + M m g_K^2 - M |\vec{p}'| g_K^3 \right\}, \quad (\text{B.4.18a})$$

$$g_K^2(ip_4, |\vec{p}|) = \int \frac{d^4 p'_E}{(2\pi)^4} \int \frac{d\Omega_{\vec{p}}}{4\pi} s(ip_4', \vec{p}') \tilde{V}(p_E - p'_E) \left\{ M m g_K^1 \right. \\ \left. + \left( \frac{M^2}{4} + p_4'^2 - \vec{p}'^2 + m^2 \right) g_K^2 - 2m |\vec{p}'| g_K^3 - 2p_4' |\vec{p}'| g_K^4 \right\}, \quad (\text{B.4.18b})$$

$$g_K^3(ip_4, |\vec{p}|) = \int \frac{d^4 p'_E}{(2\pi)^4} \int \frac{d\Omega_{\vec{p}}}{4\pi} s(ip_4', \vec{p}') \tilde{V}(p_E - p'_E) \frac{\vec{p}' \cdot \vec{p}}{|\vec{p}'| |\vec{p}|} \left\{ M |\vec{p}'| g_K^1 \right. \\ \left. + 2m |\vec{p}'| g_K^2 + \left( -\frac{M^2}{4} - p_E'^2 + m^2 \right) g_K^3 + 2m p_4' g_K^4 \right\}, \quad (\text{B.4.18c})$$

$$g_K^4(ip_4, |\vec{p}|) = \int \frac{d^4 p'_E}{(2\pi)^4} \int \frac{d\Omega_{\vec{p}}}{4\pi} s(ip_4', \vec{p}') \tilde{V}(p_E - p'_E) \frac{\vec{p}' \cdot \vec{p}}{|\vec{p}'| |\vec{p}|} \left\{ -2 |\vec{p}'| p_4' g_K^2 \right. \\ \left. - 2m p_4' g_K^3 + \left( -\frac{M^2}{4} - p_4'^2 + \vec{p}'^2 + m^2 \right) g_K^4 \right\}, \quad (\text{B.4.18d})$$

with

$$\tilde{V}(p_E - p'_E) = \frac{g^2}{(p_E - p'_E)^2 + \mu^2}. \quad (\text{B.4.19})$$

## B.5 Symmetry properties of the partial amplitudes

For bound states with isospin zero the BS amplitude and the redefined BS amplitude behave under an inversion of all coordinates as follows

$$\chi_{\alpha\beta}(p) = \chi_{\beta\alpha}(-p), \quad \Psi(p) = C\Psi^T(-p)C. \quad (\text{B.5.1})$$

This can be verified by introducing the isospin operator into the definition of the BSA (B.1.4). For the vertex function this relation translates to

$$g(p) = Cg^T(-p)C. \quad (\text{B.5.2})$$

The corresponding transformation properties for the matrix base are given in (B.4.9). Together with (B.4.14) these relations translate into the following symmetry properties for the coefficient functions of the vertex function

$$g_k^i(-p_0, |\vec{p}|) = g_k^i(p_0, |\vec{p}|) \quad i = 1, 2, 3, \quad (\text{B.5.3a})$$

$$g_k^4(-p_0, |\vec{p}|) = -g_k^4(p_0, |\vec{p}|). \quad (\text{B.5.3b})$$

Of course the same properties are also valid in Euclidean space.

## B.6 Decomposition into Hyperspherical Harmonics

The next step in this calculation consists of the expansion of the 4 partial amplitudes  $g_K^i(ip_4, |\vec{p}|)$  into hyperspherical harmonics. Thus, a change of variables into spherical coordinates is necessarily accomplished by

$$p_1 = p \sin \chi \sin \theta \sin \phi, \quad (\text{B.6.1a})$$

$$p_2 = p \sin \chi \sin \theta \cos \phi, \quad (\text{B.6.1b})$$

$$p_3 = p \sin \chi \cos \theta, \quad (\text{B.6.1c})$$

$$p_4 = p \cos \chi, \quad (\text{B.6.1d})$$

$$p = \sqrt{p_4^2 + \vec{p}^2} = \sqrt{p_E^2} \quad (\text{B.6.1e})$$

denoting the Euclidean norm from now on. The 4-dimensional infinitesimal volume reads

$$d^4 p'_E = dp'_4 |\vec{p}'|^2 d|\vec{p}'| d\Omega_{\vec{p}'} \quad (\text{B.6.2})$$

where  $d\Omega_{\vec{p}'}$  is defined in (B.4.2). Furthermore, the hyperspherical harmonics in four-dimensional Euclidean space read

$$Z_{klm}(\chi, \theta, \phi) = X_{kl}(\chi) Y_{lm}(\theta, \phi), \quad (\text{B.6.3})$$

$$X_{kl}(\chi) = 2^l l! \sqrt{\frac{2}{\pi}} \sqrt{\frac{(k+1)(k-l)!}{(k+l+1)!}} \sin^l \chi C_{k-l}^{l+1}(\cos \chi), \quad (\text{B.6.4})$$

with  $C_m^n$  being the Gegenbauer polynomials and  $Y_{lm}$  being the ordinary spherical harmonics. The Gegenbauer polynomials are a solution to the Gegenbauer differential equation [Er55a]. Because the Gegenbauer polynomials  $C_m^n(x)$  contain either even or odd powers of  $x$ , i.e. they are an even polynomial for  $m$  being even and odd for  $m$  being odd, they obey definite parity; namely even parity for  $m$  being even and odd parity for  $m$  being odd. Hence, considering the transformation  $\chi \rightarrow \chi'$  with  $\cos \chi = -\cos \chi'$ , the functions  $X_{kl}(\chi)$  behave as

$$X_{kl}(\chi') = \begin{cases} X_{kl}(\chi) & : k-l \text{ even} \\ -X_{kl}(\chi) & : k-l \text{ odd} \end{cases}, \quad (\text{B.6.5})$$

where we used that  $\sin^l \chi = (1 - \cos^2 \chi)^{l/2}$  remains unaffected by the transformation given above. For  $l = 0, 1, 2$  the  $X_{kl}$  are given by

$$X_{k0} = \sqrt{\frac{2}{\pi}} C_k^1(\cos \chi), \quad (\text{B.6.6})$$

$$X_{k1} = 2\sqrt{\frac{2}{\pi}} \frac{1}{\sqrt{k(k+2)}} \sin \chi C_{k-1}^2(\cos \chi), \quad (\text{B.6.7})$$

$$X_{k2} = 8\sqrt{\frac{2}{\pi}} \frac{1}{\sqrt{(k-1)k(k+2)(k+3)}} \sin^2 \chi C_{k-2}^3(\cos \chi). \quad (\text{B.6.8})$$

It is important to notice that appropriate indices must fulfill  $k \geq l \geq m \geq 0$ , otherwise the above equations are not well defined. The hyperspherical harmonics satisfy the orthonormality condition

$$\int_0^{2\pi} d\phi \int_0^\pi d\theta \sin \theta \int_0^\pi d\chi \sin^2 \chi Z_{klm}(\chi, \theta, \phi) Z_{k'l'm'}^*(\chi, \theta, \phi) = \delta_{kk'} \delta_{ll'} \delta_{mm'} \quad (\text{B.6.9})$$

and by using the corresponding condition for the spherical harmonics, namely

$$\int d\Omega Y_{lm}^*(\Omega) Y_{l'm'}(\Omega) = \int_0^\pi \int_0^{2\pi} \sin \theta d\phi d\theta Y_{lm}^*(\theta, \phi) Y_{l'm'}(\theta, \phi) = \delta_{ll'} \delta_{mm'}, \quad (\text{B.6.10})$$

one derives the orthonormality condition for the  $X_{kl}(\chi)$

$$\int_0^\pi \sin^2 \chi X_{kl}(\chi) X_{k'l}^*(\chi) = \delta_{kk'}. \quad (\text{B.6.11})$$

This condition only holds for the second index being equal. Writing the  $X_{kl}$  in terms of the Gegenbauer polynomials (B.6.4), one obtains the following useful relation

$$\int_{-1}^1 (1-x^2)^{\alpha-\frac{1}{2}} C_n^\alpha(x) C_m^\alpha(x) = \delta_{mn} \frac{\pi}{2^{2\alpha-1}} \frac{\Gamma(n+2\alpha)}{\Gamma(n+1)(n+\alpha)\Gamma^2(\alpha)}. \quad (\text{B.6.12})$$

Further relations, which become evident later on, are given by one of the numerous generating functions of the Gegenbauer polynomials [Er55a]

$$\frac{1}{(1-2xz+z^2)^\alpha} = \sum_{n=0}^{\infty} z^n C_n^\alpha(x) \quad |z| < 1, \alpha \neq 0 \quad (\text{B.6.13})$$

and

$$C_n^1(\cos(1, 2)) = \frac{2\pi^2}{n+1} \sum_{lm} Z_{nlm}(\chi_1, \theta_1, \phi_1) Z_{nlm}^*(\chi_2, \theta_2, \phi_2), \quad (\text{B.6.14})$$

where  $\cos(1, 2)$  denotes the angle between the two Euclidean four-vectors.

We now proceed with the expansion of (B.4.18) into the hyperspherical harmonics introduced above. We remark that the only terms which depend on the spatial angle  $\vec{p}_E$  in (B.4.18) are contained in  $\tilde{V}(p_E - p'_E)$  for the first two partial vertex functions and an additional dependence of the form  $\vec{p}'\vec{p}/|\vec{p}'||\vec{p}|$  for the last two partial vertex functions. This is the result of the special choice for the matrix base.

Furthermore, the function  $s(ip'_4, \vec{p}')$  does not depend on spatial angles ( $p, p'$  are Euclidean vectors now)

$$\begin{aligned} s(ip'_4, \vec{p}') &= \frac{1}{(-p'^2 - \kappa^2)^2 + p_4'^2 M^2} = \frac{1}{(p'^2 + \kappa^2)^2 + p_4'^2 M^2} \\ &= \frac{1}{(p'^2 + \kappa^2)^2 + M^2 p'^2 \cos^2 \chi} = s(p'^2, \chi). \end{aligned} \quad (\text{B.6.15})$$

The expansion of the meson propagator in terms of hyperspherical harmonics is then given by

$$\frac{G_0^2}{(p-q)^2 + \mu^2} = 2\pi^2 \sum_{klm} \frac{1}{k+1} V_k(|p|, |q|) Z_{klm}(\chi, \theta, \phi) Z_{klm}^*(\chi, \theta, \phi), \quad (\text{B.6.16})$$

where we have defined

$$V_k(a, b) = \frac{4G_0^2}{(\Lambda_+ + \Lambda_-)^2} \left( \frac{\Lambda_+ - \Lambda_-}{\Lambda_+ + \Lambda_-} \right)^k, \quad (\text{B.6.17})$$

$$\Lambda_{\pm} = \sqrt{(a \pm b)^2 + \mu^2}. \quad (\text{B.6.18})$$

This result can be derived by rewriting the meson propagator and assuming the following expansion

$$\frac{1}{(p-q)^2 + \mu^2} = \frac{1}{2pq} \frac{1}{z-t} \stackrel{!}{=} \sum_n V_n(p, q) C_n^1(t), \quad (\text{B.6.19})$$

with

$$z = \frac{p^2 + q^2 + \mu^2}{2pq}, \quad t = \cos(p, q) \quad (\text{B.6.20})$$

where  $\cos(p, q)$  denotes the cosine of the angle between the four-vectors  $p$  and  $q$ . These definitions obey the following properties

$$z+1 = \frac{(p+q)^2 + \mu^2}{2pq}, \quad z-1 = \frac{(p-q)^2 + \mu^2}{2pq}. \quad (\text{B.6.21})$$



Applying the orthogonality condition (B.6.12) for the Gegenbauer polynomials to (B.6.19) and making use of

$$\int_{-1}^1 \sqrt{1-t^2} \frac{C_n^1(t)}{z-t} dt = \pi(z - \sqrt{z^2-1})^{n+1}, \quad (\text{B.6.22})$$

one obtains

$$V_n(p, q) = \frac{1}{pq} (z - \sqrt{z^2-1})^{n+1}. \quad (\text{B.6.23})$$

From the definitions of  $\Lambda_{\pm}$  in (B.6.18) we deduce

$$\Lambda_+^2 + \Lambda_-^2 = 2(p^2 + q^2 + \mu^2), \quad \Lambda_+^2 - \Lambda_-^2 = 4pq, \quad (\text{B.6.24})$$

as well as

$$z = \frac{1}{2pq} \frac{\Lambda_+^2 + \Lambda_-^2}{2}, \quad \sqrt{(z+1)(z-1)} = \frac{\Lambda_+ \Lambda_-}{2pq}. \quad (\text{B.6.25})$$

Thus, inserting these relations into (B.6.23), one finally arrives at

$$V_n(p, q) = \frac{4}{(\Lambda_+^2 + \Lambda_-^2)^2} \left( \frac{\Lambda_+ - \Lambda_-}{\Lambda_+ + \Lambda_-} \right)^n, \quad (\text{B.6.26})$$

verifying (B.6.18).

Alternatively and more directly, one can rewrite the meson propagator in terms of  $\Lambda_{\pm}$  defined in (B.6.18) giving

$$\frac{1}{(p-q)^2 + \mu^2} = \frac{2}{(\Lambda_+^2 + \Lambda_-^2)^2} \frac{2}{1 + \left( \frac{\Lambda_+ - \Lambda_-}{\Lambda_+ + \Lambda_-} \right)^2 - 2 \left( \frac{\Lambda_+ - \Lambda_-}{\Lambda_+ + \Lambda_-} \right)^2 t}, \quad (\text{B.6.27})$$

where  $t$  is defined in (B.6.20). Using (B.6.13) for  $\alpha = 1$  and  $x = t$ , we recover the desired expansion (B.6.16).

Furthermore, the scalar product of three-vectors in terms of four-dimensional polar coordinates is given by

$$\vec{p} \vec{q} = \frac{4\pi}{3} |p| |q| \sin \chi_p \sin \chi_q \sum_{m=0, \pm 1} Y_{1m}^*(\theta_p, \phi_p) Y_{1m}(\theta_q, \phi_q), \quad (\text{B.6.28})$$

which can be verified from the corresponding expression for the spherical harmonics  $Y_{lm}$ .

We now insert these expansions into the 4 coupled integral equations (B.4.18) and perform the integration over space angles, giving

$$\begin{aligned} g_K^1(ip_4, |\vec{p}|) = & 2\pi^2 \sum_{k=0} \int \frac{dq_4 |\vec{q}|^2 d|\vec{q}|}{(2\pi)^4} s(q^2, \chi) \frac{V_k(p, q)}{k+1} \left\{ \left( \frac{M^2}{4} + q^2 + m^2 \right) g_k^1 \right. \\ & \left. + M m g_k^2 - M |\vec{q}| g_k^3 \right\} X_{k,0}(\chi_p) X_{k,0}(\chi_q), \end{aligned} \quad (\text{B.6.29a})$$

$$\begin{aligned}
g_K^2(ip_4, |\vec{p}|) &= 2\pi^2 \sum_{k=0} \int \frac{dq_4 |\vec{q}|^2 d|\vec{q}|}{(2\pi)^4} s(q^2, \chi) \frac{V_k(p, q)}{k+1} \left\{ M m g_k^1 \right. \\
&\quad + \left( \frac{M^2}{4} + q_4^2 - \vec{q}^2 + m^2 \right) g_k^2 - 2m |\vec{q}| g_k^3 \\
&\quad \left. - 2q_4 |\vec{q}| g_k^4 \right\} X_{k,0}(\chi_p) X_{k,0}(\chi_q), \tag{B.6.29b}
\end{aligned}$$

$$\begin{aligned}
g_K^3(ip_4, |\vec{p}|) &= 2\pi^2 \sum_{k=1} \int \frac{dq_4 |\vec{q}|^2 d|\vec{q}|}{(2\pi)^4} s(q^2, \chi) \frac{V_k(p, q)}{k+1} \left\{ M |\vec{q}| g_k^1 + 2m |\vec{q}| g_k^2 \right. \\
&\quad + \left( -\frac{M^2}{4} - q_4^2 + m^2 \right) g_k^3 + 2mq_4 g_k^4 \left. \right\} X_{k,1}(\chi_p) X_{k,1}(\chi_q), \tag{B.6.29c}
\end{aligned}$$

$$\begin{aligned}
g_K^4(ip_4, |\vec{p}|) &= 2\pi^2 \sum_{k=1} \int \frac{dq_4 |\vec{q}|^2 d|\vec{q}|}{(2\pi)^4} s(q^2, \chi) \frac{V_k(p, q)}{k+1} \left\{ -2 |\vec{q}| q_4 g_k^2 - 2mq_4 g_k^3 \right. \\
&\quad + \left( -\frac{M^2}{4} - q_4^2 + \vec{q}^2 + m^2 \right) g_k^4 \left. \right\} X_{k,1}(\chi_p) X_{k,1}(\chi_q). \tag{B.6.29d}
\end{aligned}$$

Only two integrations remain. From these expressions one observes that the only dependence of the angle  $\chi$  of the relative momentum  $p$  is contained in  $X_{k,0}(\chi_p)$  and  $X_{k,1}(\chi_p)$  respectively. Therefore, the partial vertex functions  $g_K^i(ip_4, |\vec{p}|)$  can be written as an infinite sum over Gegenbauer polynomials

$$g_M^\alpha(ip_4, |\vec{p}|) = \sum_{k=0}^{\infty} g_M^{\alpha,k}(p) X_{k,0}(\chi) \quad \alpha = 1, 2, \tag{B.6.30a}$$

$$g_M^\alpha(ip_4, |\vec{p}|) = \sum_{k=1}^{\infty} g_M^{\alpha,k}(p) X_{k,1}(\chi) \quad \alpha = 3, 4. \tag{B.6.30b}$$

Time inversion  $p_4 \rightarrow -p_4$  translated into spherical coordinates corresponds to a transformation  $\chi \rightarrow \chi'$  with  $\cos \chi' = -\cos \chi$ . In order to ensure the correct behavior of the  $g_M^\alpha(ip_4, |\vec{p}|)$  under this transformation it is sufficient that certain Gegenbauer polynomials do not appear in the sum depending on which partial vertex function is considered. From the symmetry properties given in (B.6.5) and the symmetry properties of the partial vertex functions given in (B.5.3) we see that the sums in (B.6.30) do only cover even  $k$  or odd  $k$ , according to which partial vertex function is considered. One obtains the following expressions

$$g_M^\alpha(ip_4, |\vec{p}|) = \sum_{k=0}^{\infty} g_M^{\alpha,2k}(p) X_{2k,0}(\chi) \quad \alpha = 1, 2, \tag{B.6.31a}$$

$$g_M^3(ip_4, |\vec{p}|) = \sum_{k=1}^{\infty} g_M^{\alpha,2k+1}(p) X_{2k+1,1}(\chi), \tag{B.6.31b}$$

$$g_M^4(ip_4, |\vec{p}|) = \sum_{k=1}^{\infty} g_M^{\alpha,2k+2}(p) X_{2k+2,1}(\chi). \tag{B.6.31c}$$

Inserting these expansions into the 4 coupled integral equations (B.6.29), multiplying with  $X_{k,0}(\chi_p)$ ,  $X_{k,1}(\chi_p)$  respectively, integrating both sides of the resulting equation over  $\int_0^\pi d\chi_p \sin^2 \chi_p$  and using the orthonormality condition (B.6.11), one obtains the following infinite system of coupled integral equations for the coefficient functions  $g_M^{\alpha,n}(p)$ :

$$g_M^{1,2n}(p) = \int \frac{dq \cdot q^3}{8\pi^2} \frac{V_{2n}(p, q)}{2n+1} \sum_{l=0}^{\infty} \left\{ A_{2n,2l}^{1,1}(q) g_M^{1,2l}(q) + A_{2n,2l}^{1,2}(q) g_M^{2,2l}(q) \right. \\ \left. + A_{2n,2l+1}^{1,3}(q) g_M^{3,2l+1}(q) + A_{2n,2l+2}^{1,4}(q) g_M^{4,2l+2}(q) \right\}, \quad (\text{B.6.32a})$$

$$g_M^{2,2n}(p) = \int \frac{dq \cdot q^3}{8\pi^2} \frac{V_{2n}(p, q)}{2n+1} \sum_{l=0}^{\infty} \left\{ A_{2n,2l}^{2,1}(q) g_M^{1,2l}(q) + A_{2n,2l}^{2,2}(q) g_M^{2,2l}(q) \right. \\ \left. + A_{2n,2l+1}^{2,3}(q) g_M^{3,2l+1}(q) + A_{2n,2l+2}^{2,4}(q) g_M^{4,2l+2}(q) \right\}, \quad (\text{B.6.32b})$$

$$g_M^{3,2n+1}(p) = \int \frac{dq \cdot q^3}{8\pi^2} \frac{V_{2n+1}(p, q)}{2n+2} \sum_{l=0}^{\infty} \left\{ A_{2n+1,2l}^{3,1}(q) g_M^{1,2l}(q) + A_{2n+1,2l}^{3,2}(q) g_M^{2,2l}(q) \right. \\ \left. + A_{2n+1,2l+1}^{3,3}(q) g_M^{3,2l+1}(q) + A_{2n+1,2l+2}^{3,4}(q) g_M^{4,2l+2}(q) \right\}, \quad (\text{B.6.32c})$$

$$g_M^{4,2n+2}(p) = \int \frac{dq \cdot q^3}{8\pi^2} \frac{V_{2n+2}(p, q)}{2n+3} \sum_{l=0}^{\infty} \left\{ A_{2n+2,2l}^{4,1}(q) g_M^{1,2l}(q) + A_{2n+2,2l}^{4,2}(q) g_M^{2,2l}(q) \right. \\ \left. + A_{2n+2,2l+1}^{4,3}(q) g_M^{3,2l+1}(q) + A_{2n+2,2l+2}^{4,4}(q) g_M^{4,2l+2}(q) \right\}, \quad (\text{B.6.32d})$$

where  $n = 0, 1, 2, 3, \dots$  and the coefficients  $A_{nl}^{\alpha\beta}(q)$  are given by the following integrals

$$A_{nl}^{1,1}(q) = \int_0^\pi d\chi \sin^2 \chi S(q, \chi) X_{n0}(\chi) X_{l0}(\chi) \left( \frac{M^2}{4} + q^2 + m^2 \right), \quad (\text{B.6.33a})$$

$$A_{nl}^{1,2}(q) = \int_0^\pi d\chi \sin^2 \chi s(q^2, \chi) X_{n0}(\chi) X_{l0}(\chi) (mM), \quad (\text{B.6.33b})$$

$$A_{nl}^{1,3}(q) = \int_0^\pi d\chi \sin^2 \chi s(q^2, \chi) X_{n0}(\chi) X_{l1}(\chi) (-Mq \sin \chi), \quad (\text{B.6.33c})$$

$$A_{nl}^{1,4}(q) = 0, \quad (\text{B.6.33d})$$

$$A_{nl}^{2,1}(q) = \int_0^\pi d\chi \sin^2 \chi s(q^2, \chi) X_{n0}(\chi) X_{l0}(\chi) (mM), \quad (\text{B.6.33e})$$

$$A_{nl}^{2,2}(q) = \int_0^\pi d\chi \sin^2 \chi s(q^2, \chi) X_{n0}(\chi) X_{l0}(\chi) \left( q^2 (2 \cos^2 \chi - 1) + \frac{M^2}{4} + m^2 \right), \quad (\text{B.6.33f})$$

$$A_{nl}^{2,3}(q) = \int_0^\pi d\chi \sin^2 \chi s(q^2, \chi) X_{n0}(\chi) X_{l1}(\chi) (-2mq \sin \chi), \quad (\text{B.6.33g})$$

$$A_{nl}^{2,4}(q) = \int_0^\pi d\chi \sin^2 \chi s(q^2, \chi) X_{n0}(\chi) X_{l1}(\chi) (-2q^2 \sin \chi \cos \chi), \quad (\text{B.6.33h})$$

$$A_{nl}^{3,1}(q) = \int_0^\pi d\chi \sin^2 \chi s(q^2, \chi) X_{n1}(\chi) X_{l0}(\chi) (Mq \sin \chi) , \quad (\text{B.6.33i})$$

$$A_{nl}^{3,2}(q) = \int_0^\pi d\chi \sin^2 \chi s(q^2, \chi) X_{n1}(\chi) X_{l0}(\chi) (2mq \sin \chi) , \quad (\text{B.6.33j})$$

$$A_{nl}^{3,3}(q) = \int_0^\pi d\chi \sin^2 \chi s(q^2, \chi) X_{n1}(\chi) X_{l1}(\chi) \left( m^2 - \frac{M^2}{4} - q^2 \right) , \quad (\text{B.6.33k})$$

$$A_{nl}^{3,4}(q) = \int_0^\pi d\chi \sin^2 \chi s(q^2, \chi) X_{n1}(\chi) X_{l1}(\chi) (2mq \cos \chi) , \quad (\text{B.6.33l})$$

$$A_{nl}^{4,1}(q) = 0 \quad (\text{B.6.33m})$$

$$A_{nl}^{4,2}(q) = \int_0^\pi d\chi \sin^2 \chi s(q^2, \chi) X_{n1}(\chi) X_{l0}(\chi) (-2q^2 \sin \chi \cos \chi) , \quad (\text{B.6.33n})$$

$$A_{nl}^{4,3}(q) = \int_0^\pi d\chi \sin^2 \chi s(q^2, \chi) X_{n1}(\chi) X_{l1}(\chi) (-2mq \cos \chi) , \quad (\text{B.6.33o})$$

$$A_{nl}^{4,4}(q) = \int_0^\pi d\chi \sin^2 \chi s(q^2, \chi) X_{n1}(\chi) X_{l1}(\chi) \left( m^2 - \frac{M^2}{4} - q^2 (2 \cos^2 \chi - 1) \right) . \quad (\text{B.6.33p})$$

From these equations one can read off the following relations among the integrals

$$A_{nl}^{1,2}(q) = A_{nl}^{2,1}(q) , \quad A_{nl}^{1,3}(q) = -A_{nl}^{3,1}(q) , \quad A_{nl}^{1,4}(q) = A_{nl}^{4,1}(q) , \quad (\text{B.6.34a})$$

$$A_{nl}^{2,3}(q) = -A_{nl}^{3,2}(q) , \quad A_{nl}^{2,4}(q) = A_{nl}^{4,2}(q) , \quad A_{nl}^{3,4}(q) = -A_{nl}^{4,3}(q) , \quad (\text{B.6.34b})$$

which means that the integrals  $A_{nl}^{\alpha,\beta}(q)$  are symmetric in the upper indices if both functions  $X_{kl}$ , which occur in the integrals, have the same parity, i.e. either both  $k$  are only covering even values or both are only covering odd values, and antisymmetric if they have different parity.

To calculate these integrals one can use basic recursion formulas for the Gegenbauer polynomials, i.e.

$$2\alpha(1-x^2)C_{n-1}^{\alpha+1}(x) = (2\alpha+n-1)C_{n-1}^\alpha - nx C_n^\alpha(x) , \quad (\text{B.6.35})$$

$$(n+1)C_{n+1}^\alpha(x) = 2(n+\alpha)xC_n^\alpha - (n+2\alpha-1)C_{n-1}^\alpha(x) . \quad (\text{B.6.36})$$

For  $\alpha = 1, 2$  (B.6.35) reads

$$2(1-x^2)C_{n-1}^2(x) = (n+1)C_{n-1}^1(x) - nx C_n^1(x) , \quad (\text{B.6.37})$$

$$4(1-x^2)C_{n-1}^3(x) = (n+3)C_{n-1}^2(x) - nx C_n^2(x) \quad (\text{B.6.38})$$

and (B.6.36) for  $\alpha = 2$  becomes

$$xC_n^2(x) = \frac{n+1}{2(n+2)}C_{n+1}^2(x) + \frac{n+3}{2(n+2)}C_{n-1}^2(x) . \quad (\text{B.6.39})$$

Combining these equations, gives

$$(1-x^2)C_{n-1}^3(x) = \frac{(n+3)(n+4)}{8(n+2)}C_{n-1}^2(x) - \frac{n(n+1)}{8(n+2)}C_{n+1}^2(x) . \quad (\text{B.6.40})$$

From (B.6.36) one also derives

$$xC_n^1(x) = \frac{1}{2}(C_{n+1}^1(x) + C_{n-1}^1(x)) , \quad (\text{B.6.41})$$

$$xC_n^2(x) = \frac{n+1}{2(n+2)}C_{n+1}^2(x) + \frac{n+3}{2(n+2)}C_{n-1}^2(x) , \quad (\text{B.6.42})$$

$$xC_n^3(x) = \frac{n+1}{2(n+3)}C_{n+1}^3(x) + \frac{n+5}{2(n+3)}C_{n-1}^3(x) . \quad (\text{B.6.43})$$

Using these recursion formulas, one can express products of  $X_{kl}(\chi)$  and  $\sin \chi$ , or  $\cos \chi$  respectively, by sums of  $X_{kl}(\chi)$ . We list the most important expressions:

$$X_{j1}(\chi) \sin \chi = \frac{1}{2} \left( \sqrt{\frac{j+2}{j}} X_{j-1,0}(\chi) - \sqrt{\frac{j}{j+2}} X_{j+1,0}(\chi) \right) , \quad (\text{B.6.44a})$$

$$X_{j2}(\chi) \sin \chi = \frac{1}{2} \left( \sqrt{\frac{(j+2)(j+3)}{j(j+1)}} X_{j-1,1}(\chi) - \sqrt{\frac{(j-1)j}{(j+1)(j+2)}} X_{j+1,1}(\chi) \right) , \quad (\text{B.6.44b})$$

$$\begin{aligned} X_{j2}(\chi) \sin^2 \chi = & \frac{1}{4} \left( \sqrt{\frac{(j+2)(j+3)}{(j-1)j}} X_{j-2,0}(\chi) + \sqrt{\frac{(j-1)j}{(j+2)(j+3)}} X_{j+2,0}(\chi) \right) \\ & - \frac{1}{4} \frac{\sqrt{(j-1)(j+3)}}{j+1} \left( \sqrt{\frac{j+2}{j}} + \sqrt{\frac{j}{j+2}} \right) X_{j0}(\chi) , \end{aligned} \quad (\text{B.6.44c})$$

$$X_{j0}(\chi) \cos \chi = \frac{1}{2} (X_{j+1,0}(\chi) + X_{j-1,0}(\chi)) , \quad (\text{B.6.44d})$$

$$X_{j1}(\chi) \cos \chi = \frac{1}{2} \left( \sqrt{\frac{j(j+3)}{(j+1)(j+2)}} X_{j+1,1}(\chi) + \sqrt{\frac{(j-1)(j+2)}{j(j+1)}} X_{j-1,1}(\chi) \right) , \quad (\text{B.6.44e})$$

$$X_{j2}(\chi) \cos \chi = \frac{1}{2} \left( \sqrt{\frac{(j-1)(j+4)}{(j+1)(j+2)}} X_{j+1,2}(\chi) + \sqrt{\frac{(j-2)(j+3)}{j(j+1)}} X_{j-1,2}(\chi) \right) . \quad (\text{B.6.44f})$$

In particular this is useful, because these recursion formulas can be applied to (B.6.33) so that the second index is equal in all products  $X_{ni}X_{lj} \rightarrow X_{ni}X_{li}$  and  $n, l$  are both even or both odd.

Basically, one has to solve the following type of integrals

$$S_{k'k}^l(q) = \int_0^\pi d\chi \sin^2 \chi \frac{X_{k'l}(\chi) X_{kl}(\chi)}{A^2 + B^2 \cos^2 \chi} \quad A = q^2 + \kappa^2 , \quad B = Mq . \quad (\text{B.6.45})$$

To calculate this integral we make use of the identity [Pr83]

$$\begin{aligned} & \int_{-1}^1 dx (1-x^2)^{\lambda-\frac{1}{2}} C_m^\lambda(x) C_n^\lambda(x) \frac{1}{x-iz} \\ &= -\frac{2\sqrt{\pi}}{\Gamma(\lambda)} \left(\frac{1}{2}\right)^{\lambda-\frac{1}{2}} e^{(\frac{1}{2}-\lambda)i\pi} (-z^2-1)^{\frac{2\lambda-1}{4}} C_{min}^\lambda(iz) Q_{max+\lambda-\frac{1}{2}}^{\lambda-\frac{1}{2}}(iz), \end{aligned} \quad (\text{B.6.46})$$

where  $Q_m^\lambda(x)$  are the Legendre functions of the second kind and  $min = \min(m, n)$ ,  $max = \max(m, n)$ . The integral (B.6.45) then becomes

$$\begin{aligned} S_{k'k}^l(q) &= (-1)^l \sqrt{\frac{2}{\pi}} \frac{2^{l+1}}{AB} \sqrt{\frac{(k'+1)(k'-l)!}{(k'+l+1)!} \frac{(k+1)(k-l)!}{(k+l+1)!}} \\ & C_{min-l}^{l+1}(iz) (-z^2-1)^{\frac{2l+1}{4}} Q_{max+\frac{1}{2}}^{l+\frac{1}{2}}(iz), \end{aligned} \quad (\text{B.6.47})$$

where  $max$  ( $min$ ) denotes the maximal (minimal) index of  $k, k'$  and  $z = \frac{A}{B}$ . We give a short list of the Legendre functions of the second kind that will be needed

$$Q_{n+\frac{1}{2}}^{\frac{1}{2}}(z) = i \sqrt{\frac{\pi}{2}} (z^2-1)^{-\frac{1}{4}} \left(z - \sqrt{z^2-1}\right)^{n+1}, \quad (\text{B.6.48a})$$

$$Q_{n+\frac{3}{2}}^{\frac{3}{2}}(z) = \left((n+1)zQ_{n+\frac{3}{2}}^{\frac{1}{2}}(z) - (n+2)Q_{n+\frac{1}{2}}^{\frac{1}{2}}(z)\right) \frac{1}{\sqrt{z^2-1}}, \quad (\text{B.6.48b})$$

$$Q_{n+\frac{5}{2}}^{\frac{5}{2}}(z) = \left((n+1)zQ_{n+\frac{5}{2}}^{\frac{3}{2}}(z) - (n+4)Q_{n+\frac{3}{2}}^{\frac{3}{2}}(z)\right) \frac{1}{\sqrt{z^2-1}} \quad (\text{B.6.48c})$$

and some useful relations among them

$$Q_{n+1/2}^{1/2}(iz) (-z^2-1)^{1/4} = -i^n \sqrt{\frac{\pi}{2}} Z^{n+1}, \quad (\text{B.6.49a})$$

$$Q_{n+1/2}^{3/2}(iz) (-z^2-1)^{3/4} = -i^{n+1} \sqrt{\frac{\pi}{2}} (nZ^{n+1} + (n+1)Z^n), \quad (\text{B.6.49b})$$

$$Q_{n-1/2}^{3/2}(iz) (-z^2-1)^{3/4} = -i^n \sqrt{\frac{\pi}{2}} ((n-1)Z^n + nZ^{n-1}), \quad (\text{B.6.49c})$$

$$Q_{n+1/2}^{5/2}(iz) (-z^2-1)^{5/4} = i^n \sqrt{\frac{\pi}{2}} \left(n(n-1)Z^{n+1} + (n-1)(2n+3)Z^n \right. \quad (\text{B.6.49d})$$

$$\left. + n(n+2)Z^{n-1}\right), \quad (\text{B.6.49e})$$

where we introduced  $Z = \left(z - \sqrt{z^2+1}\right) = -1/\left(z + \sqrt{z^2+1}\right)$ . Only a small number of the integrals defined in (B.6.45) are interesting for our purpose. For  $S_{k'k}^0(q)$  and  $S_{k'k}^1(q)$  one obtains

$$S_{k'k}^0(q) = \frac{2}{AB} (-i)^{max} C_{min}^1(iz) R_{k'k}^0(z), \quad (\text{B.6.50a})$$

$$R_{k'k}^0(z) = \left(z + \sqrt{z^2 + 1}\right)^{-max-1},$$

$$S_{k'k}^1(q) = \frac{4}{AB}(-1)^{max} \frac{C_{min-1}^2(iz)R_{k'k}^1}{\sqrt{k(k+2)k'(k'+2)}}, \quad (\text{B.6.50b})$$

$$R_{k'k}^1(z) = \left(-maxz \left(z + \sqrt{z^2 + 1}\right)^{-max-1} + (max+1) \left(z + \sqrt{z^2 + 1}\right)^{-max}\right),$$

$$S_{k'k}^2(q) = \frac{16}{AB}(-i)^{max} \frac{C_{min-2}^3(iz)R_{k'k}^2}{\sqrt{(k-1)k(k+2)(k+3)(k'-1)k'(k'+2)(k'+3)}}, \quad (\text{B.6.50c})$$

$$R_{k'k}^2(z) = \left( -\frac{max(max-1)z^2}{\left(z + \sqrt{z^2 + 1}\right)^{max+1}} + \frac{(max-1)(2max+3)z}{\left(z + \sqrt{z^2 + 1}\right)^{max}} \right. \\ \left. - \frac{max(max+2)}{\left(z + \sqrt{z^2 + 1}\right)^{max-1}} \right). \quad (\text{B.6.50d})$$

Using the recursion formulas (B.6.44) for the  $A_{nl}^{\alpha\beta}(q)$  coefficients, one recognizes that they can be brought into a form where only even or odd indices appear and the results for the integrals (B.6.50) read:

for even  $k, k'$

$$S_{k'k}^0(q) = \frac{2}{AB}C_{min}^1(iz)(-1)^{\frac{max}{2}}R_{k'k}^0, \quad (\text{B.6.51a})$$

$$S_{k'k}^1(q) = \frac{-4}{AB}(-1)^{\frac{max}{2}} \frac{(-iC_{min-1}^2(iz))R_{k'k}^1}{\sqrt{k(k+2)k'(k'+2)}}, \quad (\text{B.6.51b})$$

$$S_{k'k}^2(q) = \frac{16}{AB}(-1)^{\frac{max}{2}} \frac{C_{min-2}^3(iz)R_{k'k}^2}{\sqrt{(k-1)k(k+2)(k+3)(k'-1)k'(k'+2)(k'+3)}}, \quad (\text{B.6.51c})$$

for odd  $k, k'$

$$S_{k'k}^0(q) = \frac{2}{AB}(iC_{min}^1(iz))(-1)^{\frac{max+1}{2}}R_{k'k}^0, \quad (\text{B.6.52a})$$

$$S_{k'k}^1(q) = \frac{-4}{AB}(-1)^{\frac{max+1}{2}} \frac{C_{min-1}^2(iz)R_{k'k}^1}{\sqrt{k(k+2)k'(k'+2)}}, \quad (\text{B.6.52b})$$

$$S_{k'k}^2(q) = \frac{16}{AB}(-1)^{\frac{max+1}{2}} \frac{(iC_{min-2}^3(iz))R_{k'k}^2}{\sqrt{(k-1)k(k+2)(k+3)(k'-1)k'(k'+2)(k'+3)}}. \quad (\text{B.6.52c})$$

From these expressions one can see, that all integrals are real. We give a list of all the integrals that are needed to calculate the coefficient functions defined in (B.6.33)

$$\int d\chi \sin^2 \chi \frac{X_{k0}(\chi)X_{j1}(\chi)}{A^2 + B^2 \cos^2 \chi} \sin \chi = \frac{1}{2} \sqrt{\frac{j+2}{j}} S_{k,j-1}^0 - \frac{1}{2} \sqrt{\frac{j}{j+2}} S_{k,j+1}^0, \quad (\text{B.6.53a})$$

$$\begin{aligned} \int d\chi \sin^2 \chi \frac{X_{k1}(\chi)X_{j2}(\chi)}{A^2 + B^2 \cos^2 \chi} \sin \chi &= \frac{1}{2} \sqrt{\frac{(j+2)(j+3)}{j(j+1)}} S_{k,j-1}^1 \\ &- \frac{1}{2} \sqrt{\frac{(j-1)j}{(j+1)(j+2)}} S_{k,j+1}^1, \end{aligned} \quad (\text{B.6.53b})$$

$$\begin{aligned} \int d\chi \sin^2 \chi \frac{X_{k0}(\chi)X_{j2}(\chi)}{A^2 + B^2 \cos^2 \chi} \sin^2 \chi &= \frac{1}{4} \sqrt{\frac{(j+2)(j+3)}{(j-1)j}} S_{k,j-2}^0 \\ &- \frac{1}{4} \frac{\sqrt{(j-1)(j+3)}}{(j+1)} \left( \sqrt{\frac{j+2}{j}} + \sqrt{\frac{j}{j+2}} \right) S_{k,j}^0 + \frac{1}{4} \sqrt{\frac{(j-1)j}{(j+2)(j+3)}} S_{k,j+2}^0, \end{aligned} \quad (\text{B.6.53c})$$

$$\begin{aligned} \int d\chi \sin^2 \chi \frac{X_{k0}(\chi)X_{j0}(\chi)}{A^2 + B^2 \cos^2 \chi} \cos^2 \chi &= \frac{1}{4} (S_{k-1,j-1}^0 + S_{k-1,j+1}^0 + S_{k+1,j-1}^0 \\ &+ S_{k+1,j+1}^0), \end{aligned} \quad (\text{B.6.53d})$$

$$\begin{aligned} \int d\chi \sin^2 \chi \frac{X_{k1}(\chi)X_{j1}(\chi)}{A^2 + B^2 \cos^2 \chi} \cos^2 \chi &= \frac{1}{4} (c_1(k)c_1(j)S_{k+1,j+1}^1 \\ &+ c_1(k)c_2(j)S_{k+1,j-1}^1 + c_2(k)c_1(j)S_{k-1,j+1}^1 + c_2(k)c_2(j)S_{k-1,j-1}^1), \end{aligned} \quad (\text{B.6.53e})$$

$$c_1(k) = \sqrt{\frac{k(k+3)}{(k+1)(k+2)}}, \quad c_2(k) = \sqrt{\frac{(k-1)(k+2)}{k(k+1)}},$$

$$\begin{aligned} \int d\chi \sin^2 \chi \frac{X_{k2}(\chi)X_{j2}(\chi)}{A^2 + B^2 \cos^2 \chi} \cos^2 \chi &= \frac{1}{4} (d_1(k)d_1(j)S_{k+1,j+1}^2 \\ &+ d_1(k)d_2(j)S_{k+1,j-1}^2 + d_2(k)d_1(j)S_{k-1,j+1}^2 + d_2(k)d_2(j)S_{k-1,j-1}^2), \end{aligned} \quad (\text{B.6.53f})$$

$$d_1(k) = \sqrt{\frac{(k-1)(k+4)}{(k+1)(k+2)}}, \quad d_2(k) = \sqrt{\frac{(k-2)(k+3)}{k(k+1)}},$$

$$\begin{aligned} \int d\chi \sin^2 \chi \frac{X_{k1}(\chi)X_{j0}(\chi)}{A^2 + B^2 \cos^2 \chi} \cos \chi \sin \chi &= \frac{1}{4} \left( \sqrt{\frac{k+2}{k}} S_{k-1,j+1}^0 \right. \\ &\left. - \sqrt{\frac{k}{k+2}} S_{k+1,j+1}^0 + \sqrt{\frac{k+2}{k}} S_{k-1,j-1}^0 - \sqrt{\frac{k}{k+2}} S_{k+1,j-1}^0 \right), \end{aligned} \quad (\text{B.6.53g})$$

$$\begin{aligned} \int d\chi \sin^2 \chi \frac{X_{k1}(\chi)X_{j2}(\chi)}{A^2 + B^2 \cos^2 \chi} \cos \chi \sin \chi &= \\ \frac{1}{4} c_1(k) \left( \sqrt{\frac{(j+2)(j+3)}{j(j+1)}} S_{k+1,j-1}^1 - \sqrt{\frac{(j-1)j}{(j+1)(j+2)}} S_{k+1,j+1}^1 \right) \\ &+ \frac{1}{4} c_2(k) \left( \sqrt{\frac{(j+2)(j+3)}{j(j+1)}} S_{k-1,j-1}^1 - \sqrt{\frac{(j-1)j}{(j+1)(j+2)}} S_{k-1,j+1}^1 \right), \end{aligned} \quad (\text{B.6.53h})$$

$$\int d\chi \sin^2 \chi \frac{X_{k1}(\chi)X_{j1}(\chi)}{A^2 + B^2 \cos^2 \chi} \cos \chi = \frac{1}{2} (c_1(k)S_{k+1,j}^1 + c_2(k)S_{k-1,j}^1). \quad (\text{B.6.53i})$$



Inserting these relations into (B.6.33), we obtain exact expressions for the coefficient functions  $A_{nl}^{\alpha,\beta}(q)$  for all  $n, l$ . Hence, the infinite system of coupled one-dimensional integral equations (B.6.32) is completely determined and known and can be solved, in principle, up to arbitrary order in the expansions (B.6.31).

## B.7 Numerical Evaluations

Before solving the infinite system of one-dimensional coupled integral equations (B.6.32), we substitute

$$q = c_0 \frac{1+x}{1-x}, \quad dq = c_0 \frac{2}{(1-x)^2} dx, \quad (\text{B.7.1})$$

which results in new integration bounds  $a = -1$  and  $b = 1$ . The constant  $c_0$  is arbitrary. We map the variable  $p$  in the same way. The reason for this mapping will become evident later on.

In order to solve (B.6.32) the authors in [Do07] developed a method that enables us to rewrite the system of integral equations as one matrix multiplication and, hence, to reduce the problem to an eigenvalue problem of a matrix.

The appropriate tool to perform the first step is to rewrite the integrations using Gauß' numerical integration method. Following Gauß, a good approximation for the integration of a function  $f(x)$  is given by

$$\int_{-1}^1 f(x) dx \approx \sum_{i=1}^n \omega_i f(x_i), \quad (\text{B.7.2})$$

where  $x_i$  are the roots of the  $n$ th Legendre polynomial,  $P_n(x_i) = 0$  and

$$\omega_i = \int_{-1}^1 \prod_{m=1}^{i-1} \left( \frac{x - x_m}{x_i - x_m} \right) \prod_{j=i+1}^n \left( \frac{x - x_j}{x_i - x_j} \right) dx \quad (\text{B.7.3})$$

are the corresponding weights. Hence, weights and roots are always symmetric and do not directly depend on the function  $f(x)$ . (B.7.2) is a good approximation if the function  $f(x)$  can be approximated well enough by a polynomial of the order  $2n - 1$ . For arbitrary integration bounds a mapping can be performed. Therefore, the mapping defined in (B.7.1) is a good choice. Of course, any simpler mapping would be as good, but the constant  $c_0$  enables us to concentrate the poles  $x_i$ , when transformed back to momenta  $q_i$ , at lower values and thereby emphasizing the scan of lower momenta. In particular, for functions that tend to zero very fast, this is necessary to obtain a good approximation by the Gauß method.

If we denote the integration kernels in (B.6.32) as  $F_{kl}^{\alpha\beta}(p, q; M) \rightarrow F_{kl}^{\alpha\beta}(y, x; M)$ , choose a fixed order in the expansion (B.6.31), say  $N = 4$ , and an appropriate order for the Gauß integration, say  $n = 96$ , the system of integral equations (B.6.32) reads

$$g_M^{\alpha k}(y_i) = F_{kl}^{\alpha\beta}(y_i, x_j; M) g_M^{\beta l}(x_j), \quad (\text{B.7.4})$$

where summation over doubled indices is understood and

$$F_{kl}^{\alpha\beta}(y_i, x_j; M) = \omega_j \frac{c_0^4}{4\pi^2(1-x_j)^2} \left( \frac{1+x_j}{1-x_j} \right)^3 \frac{V_k \left( c_0 \frac{1+y_i}{1-y_i}, c_0 \frac{1+x_j}{1-x_j} \right)}{k+1} A_{kl}^{\alpha\beta} \left( c_0 \frac{1+x_j}{1-x_j} \right). \quad (\text{B.7.5})$$

The dependence on  $M$  is encoded in the functions  $V_k$  and  $A_{kl}^{\alpha\beta}$ . Rewritten in matrix form

$$\vec{g}_M = \mathcal{F}(M) \vec{g}_M, \quad (\text{B.7.6})$$

where we have defined

$$\vec{g}_M = (g_M^{1,0}(y_1) \quad \dots \quad g_M^{1,0}(y_n) \quad \dots \quad g_M^{1,6}(y_1) \quad \dots \quad g_M^{1,6}(y_n) \quad \dots \quad g_M^{4,8}(y_n))^T \quad (\text{B.7.7})$$

and

$$\mathcal{F} = \begin{pmatrix} F_{0,0}^{1,1}(y_1, x_1) \dots & F_{0,0}^{1,1}(y_1, x_n) \dots & F_{0,6}^{1,1}(y_1, x_1) \dots & F_{0,6}^{1,1}(y_1, x_n) \dots & F_{0,8}^{1,4}(y_1, x_n) \\ \vdots & & & & \\ F_{0,0}^{1,1}(y_n, x_1) \dots & F_{0,0}^{1,1}(y_n, x_n) \dots & F_{0,6}^{1,1}(y_n, x_1) \dots & F_{0,6}^{1,1}(y_n, x_n) \dots & F_{0,8}^{1,4}(y_n, x_n) \\ \vdots & & & & \\ F_{6,0}^{1,1}(y_1, x_1) \dots & F_{6,0}^{1,1}(y_1, x_n) \dots & F_{6,6}^{1,1}(y_1, x_1) \dots & F_{6,6}^{1,1}(y_1, x_n) \dots & F_{6,8}^{1,4}(y_1, x_n) \\ \vdots & & & & \\ F_{6,0}^{1,1}(y_n, x_1) \dots & F_{6,0}^{1,1}(y_n, x_n) \dots & F_{6,6}^{1,1}(y_n, x_1) \dots & F_{6,6}^{1,1}(y_n, x_n) \dots & F_{6,8}^{1,4}(y_n, x_n) \\ \vdots & & & & \\ F_{8,0}^{4,1}(y_n, x_1) \dots & F_{8,0}^{4,1}(y_n, x_n) \dots & F_{8,6}^{4,1}(y_n, x_1) \dots & F_{8,6}^{4,1}(y_n, x_n) \dots & F_{8,8}^{4,4}(y_n, x_n) \end{pmatrix}. \quad (\text{B.7.8})$$

We abstained from indicating the dependence on  $M$  here.

If one is just interested in determining the bound state mass  $M$ , it is sufficient to solve the equation

$$\det(\mathcal{F}(M) - 1) = 0. \quad (\text{B.7.9})$$

For the mass of the interaction particle being  $\mu = 0.15 \text{ GeV}$ , a nucleon mass of  $m = 1 \text{ GeV}$ , a coupling strength of  $G_0^2 = 10 \text{ GeV}$  and the constant  $c_0 = 1$ , we determine the bound state mass to be  $M = 1.974 \text{ GeV}$ .<sup>2</sup> The convergence of the expansion (B.6.31) is very good and only a few terms have to be taken into account. If only the first two terms are taken into account, a mass of  $M = 1.975 \text{ GeV}$  is derived. This can also be seen from figs. B.7.1, B.7.2, B.7.3 and B.7.4. The dominant contributions are  $g_M^{1,n}(p)$  and  $g_M^{2,n}(p)$ , whereas  $g_M^{3,n}(p)$  and  $g_M^{4,n}(p)$  are comparatively small.

However, the complete eigenvalue problem can easily be solved if the bound state mass  $M$  is determined. In the following figures we display all vertex coefficient functions.

<sup>2</sup>The Deuteron mass is  $1.876 \text{ GeV}$ . The difference is no surprise, as we only considered the  $^1S_0$  channel and a scalar coupling.

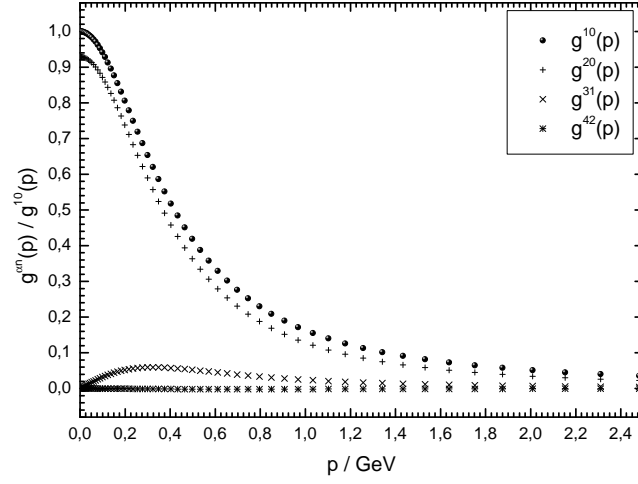


**Figure B.7.1:** Coefficient functions  $g_M^{1,0}(p)$ ,  $g_M^{2,0}(p)$ ,  $g_M^{3,1}(p)$  and  $g_M^{4,2}(p)$ .

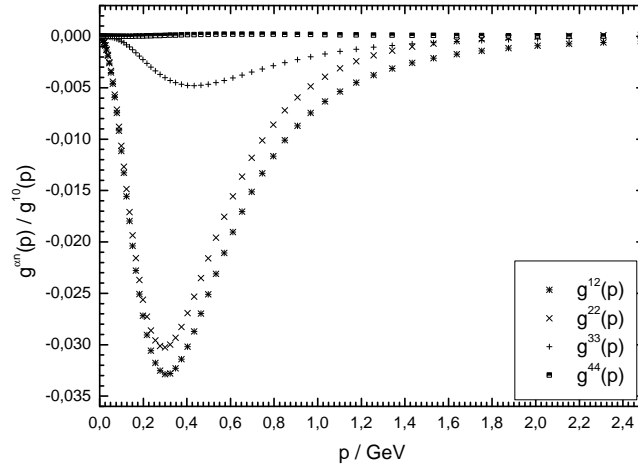


**Figure B.7.2:** Coefficient functions  $g_M^{1,2}(p)$ ,  $g_M^{2,2}(p)$ ,  $g_M^{3,3}(p)$  and  $g_M^{4,4}(p)$ .

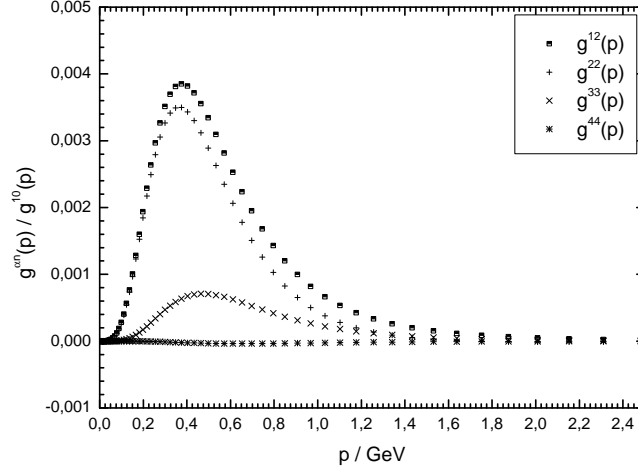


**Figure B.7.3:** Coefficient functions  $g_M^{1,4}(p)$ ,  $g_M^{2,4}(p)$ ,  $g_M^{3,5}(p)$  and  $g_M^{4,6}(p)$ .

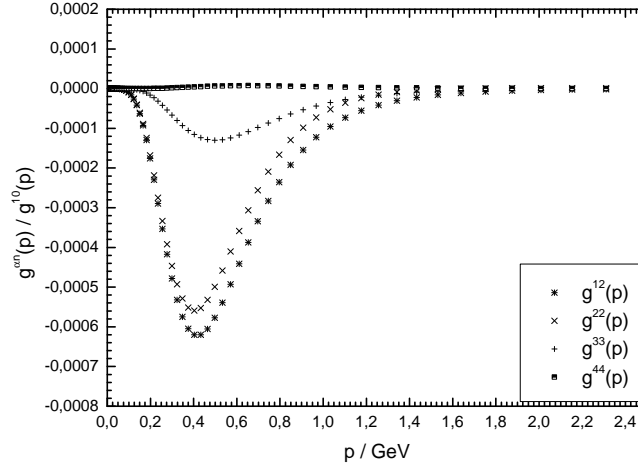


**Figure B.7.4:** Coefficient functions  $g_M^{1,6}(p)$ ,  $g_M^{2,6}(p)$ ,  $g_M^{3,7}(p)$  and  $g_M^{4,8}(p)$ .

As stressed above, this appendix is a recollection of a useful method for treating relativistic two-body bound states. Following [Do07] the essential formulae are listed, however, for the special case of the deuteron  $^1S_0$  state. Further developments are envisaged to deal with the  $J/\Psi$  or  $\Upsilon$ , using this method, and, after extending this approach, with D mesons,

---

too. The basic idea is to employ interactions calculated within lattice QCD at finite temperature, thus having an alternative approach to medium modifications of hadrons composed of heavy quarks.



# Bibliography

- [Al83] T. M. Aliev, V. L. Eletsky, *Sov. J. Nucl. Phys.* **38**, 936 (1983).
- [Br01] I. N. Bronstein, K. A. Semendjajew, *Taschenbuch der Mathematik* (Harri Deutsch, 2001).
- [Ch82] K. G. Chetyrkin, F. V. Tkachov, S. G. Gorishnii, *Phys. Lett.* **B119**, 407 (1982).
- [Cu54] R. E. Cutkosky, *Phys. Rev.* **96**, 1135 (1954).
- [Ra81] E. de Rafael (1981), talk given at NSF-CNRS Joint Seminar on Recent Developments in Quantum Chromodynamics, June 1981.
- [Do07] S. M. Dorkin, M. Beyer, S. S. Semikh, L. P. Kaptari, *Two-fermion bound states within the bethe-salpeter approach*. arXiv:0708.2146 [nucl-th] (2007).
- [Er55a] A. Erdelyi, *Higher Transcendental functions Volume II* (McGraw-Hill, 1955).
- [Er55b] A. Erdelyi, *Higher Transcendental functions Volume III* (McGraw-Hill, 1955).
- [Fe71] A. L. Fetter, J. D. Walecka, *Quantum Theory of Many Particle Systems* (McGraw-Hill, 1971).
- [Fr95] E. Freitag, R. Busam, *Funktionentheorie* (Springer, Berlin, 1995).
- [Fu92] R. J. Furnstahl, D. K. Griegel, T. D. Cohen, *Phys. Rev.* **C46**, 1507 (1992).
- [Ge51] M. Gell-Mann, F. Low, *Phys. Rev.* **84**, 350 (1951).
- [Ge83] S. C. Generalis, D. J. Broadhurst, *Phys. Lett.* **B139**, 85 (1984).
- [Gr84] W. Greiner, J. Reinhardt, *Quantelektrodynamik*, vol. 7 of *Theoretische Physik - Ein Lehr- und Übungsbuch* (Verlag Harri Deutsch, 1984), 1st ed.
- [Gr94] A. G. Grozin, *Int. J. Mod. Phys.* **A10**, 3497 (1995).
- [Ha00] A. Hayashigaki, *Phys. Lett.* **B487**, 96 (2000).
- [Ha04] A. Hayashigaki, K. Terasaki, *Charmed-meson spectroscopy in qcd sum rule*. hep-ph/0411285 (2004).
- [It80] C. Itzykson, J.-B. Zuber, *Quantum Field Theory* (McGraw-Hill, 1980).
- [Ja92] M. Jamin, M. Münz, *Z. Phys.* **C60**, 569 (1993).

- [Ji93] X.-m. Jin, T. D. Cohen, R. J. Furnstahl, D. K. Griegel, Phys. Rev. **C47**, 2882 (1993).
- [Ja96] K. Jänich, *Funktionentheorie* (Springer, Berlin, 1996).
- [Le97] S. Leupold, W. Peters, U. Mosel, Nucl. Phys. **A628**, 311 (1998).
- [Lu68] D. Lurie, *Particles and Fields* (Interscience Publishers, 1968).
- [Ma55] S. Mandelstam, Proc. Roy. Soc. Lond. **A233**, 248 (1955).
- [Mo01] P. Morath, *Schwere Quarks in dichter Materie*. Ph.D. thesis, Technische Universität München (2001).
- [Mu87] T. Muta, *Foundations of Quantum Chromodynamics* (World Scientific Publishing Co., 1987).
- [Na04] S. Narison, *QCD as a Theory of Hadrons - From Partons to Confinement* (Cambridge University Press, 2004).
- [No83] V. A. Novikov, M. A. Shifman, A. I. Vainshtein, V. I. Zakharov, Fortschr. Phys. **32**, 585 (1984).
- [Pa84] P. Pascual, R. Tarrach, *QCD: Renormalization for Practitioner* (Springer-Verlag, 1984).
- [Pr83] A. P. Prudnikov, J. A. Brychkov, O. I. Marichev, *Integraly i Ryady - Specialnye Funkcii* (Moscow "Nauka", 1983).
- [Ro69] P. Roman, *Introduction to Quantum Field Theory* (1969).
- [Sh78] M. A. Shifman, A. I. Vainshtein, V. I. Zakharov, Nucl. Phys. **B147**, 385 (1979).
- [Sp88] V. P. Spiridonov, K. G. Chetyrkin, Sov. J. Nucl. Phys. **47**, 522 (1988).
- [Su61] M. Sugawara, A. Kanazawa, Phys. Rev. **123**, 1895 (1961).
- [Tk83] F. V. Tkachov, Phys. Lett. **B125**, 85 (1983).
- [Wi46] D. V. Widder, *The Laplace Transform* (Princeton Mathematical Series, 1946).
- [Wi69] K. G. Wilson, Phys. Rev. **179**, 1499 (1969).
- [Ya06] W. M. Yao, *et al.*, J. Phys. **G33**, 1 (2006).
- [Zi72] W. Zimmermann, Ann. Phys. **77**, 570 (1973).
- [Zs06] S. Zschocke, *Open charm mesons in nuclear matter within qcd sum rule approach* (2006), unpublished manuscript.



## Danksagung

An erster Stelle bedanke ich mich bei Herrn Prof. Dr. R. Schmidt für die Aufnahme in das Institut für Theoretische Physik und die damit verbundene Möglichkeit das Studium der Physik entsprechend meiner zu Beginn des Studiums gesetzten Ziele abzuschließen.

Desweiteren bedanke ich mich bei Herrn Prof. Dr. B. Kämpfer für das interessante und facettenreich Thema meiner Diplomarbeit, die fortwährende fachliche Unterstützung und Diskussionsbereitschaft und die Möglichkeit an den hervorragenden Arbeitsbedingungen des Forschungszentrums Dresden-Rossendorf teilzuhaben. Mein Dank ist in besonderem Maße auch den intensiven und gründlichen Vorbereitungen im Vorfeld zu Vorträgen und Präsentationen geschuldet. Die zahlreichen aufbauenden und ermutigenden Worte in schwierigen Abschnitten meiner Diplomarbeit sind dabei keineswegs zu vernachlässigen.

Ich danke Dr. Sven Zschocke dafür, dass er mir seine Aufzeichnungen zur Verfügung gestellt hat.

Ganz besonderer Dank gilt auch den Doktoren Leonid Kaptari, Sergej Dorkin und Sergej Semikh, die mich sehr freundlich im Bogoljubow Institut aufgenommen haben und von denen ich sehr viel lernen konnte.

Auch danke ich Dipl. Phys. Ronny Thomas für die vorangegangene Einführung in die Methode der QCD Summenregeln im Rahmen meiner Tätigkeit als studentische Hilfskraft und für die unzähligen, endlosen Diskussionen während meiner Diplomarbeit.

Außerdem danke ich Ronny, Marcus, Henry, Daniel und Robert für ihre Hilfe und Unterstützung sowohl rundum als auch fern ab physikalischer Probleme.

Ich möchte auch meinen Eltern für die jahrelange finanzielle Unterstützung danken. Schließlich danke ich Nadine, meinen Eltern und meinem Bruder für das entgegengebrachte Vertrauen und den moralischen Beistand.

## **Erklärung**

Hiermit erkläre ich, dass ich diese Arbeit im Rahmen der Betreuung im Institut für Theoretische Physik ohne unzulässige Hilfe Dritter verfasst und alle Quellen als solche gekennzeichnet habe. Die Diplomarbeit wurde bisher weder im Inland noch im Ausland in gleicher oder ähnlicher Form bei einer anderen Prüfungsbehörde eingereicht.

Thomas Hilger

Dresden, den 18. März 2008